Chaoticity Versus Stochasticity in Financial Markets: Are Daily S&P 500 Return Dynamics Chaotic?

Abstract

In this study, we present a combinatory chaos analysis of daily wavelet-filtered (denoised) S&P 500 returns (2000–2020) compared with respective surrogate datasets, Brownian motion returns and a Lorenz system realisation. We show that the dynamics of the S&P 500 return series consist of an almost equally divided combination of stochastic and deterministic chaos. The strange attractor of the S&P 500 return system is graphically displayed via Takens' embedding and by spectral embedding in combination with Laplacian Eigenmaps. For the field of nonlinear and financial chaos research, we present a bibliometric analysis paired with citation network analysis. We critically discuss implications and future prospects.

Keywords: nonlinear dynamics, chaos, financial chaos, recurrence analysis, financial predictions, financial markets

Classification Codes (JEL): G1, C01, C02, C22, C18

Highlights [separate page in final version]

- A combinatory methodological analysis framework for financial data is applied to cascadic level 12 Haar wavelet-filtered (denoised) S&P 500 daily returns (2000–2020) compared with respective surrogate datasets (ft, aaft and iaaft), a Brownian motion return realisation and a Lorenz system realisation.
- The dynamics of the daily (denoised) S&P 500 return series are shown to be an almost equally divided combination of stochastic and deterministic chaos.
- The strange (chaotic) attractor of the S&P 500 daily return system is graphically displayed via Takens' delay-time embedding and via spectral embedding in combination with Laplacian Eigenmaps.
- For the field of nonlinear dynamics and financial chaos research, a bibliometric analysis paired with a citation network analysis is presented and relevant publications are shown in order to bridge the diverged research streams of the same research topics and related questions, which occur due to 'over-specialisations'.
- Encompassing theoretical and empirical implications of the financial chaotic dynamics are conducted and a critical discussion of financial forecasting capabilities and future prospects is presented.

1. Introduction

In our digitalised, fully connected and global economy of financial systems, the concepts of financial and risk modelling are a major area of interest within the field of quantitative modelling (Aguilar-Rivera et al., 2015). Central to the entirety of this discipline is the concept of forecasting of financial markets and crises (Beltratti & Stulz, 2019; Gong & Xu, 2018). Nevertheless, market actors and researchers alike are challenged in their forecasting endeavours by the existence of stylised facts, which mimic the underlying properties of markets, shown via empirical experiments (Poon & Granger, 2003; Vogl & Rötzel, 2021).

These stylised facts are evident in a large variety of studies and describe the dynamics of financial time series (e.g., Bodnar & Hautsch, 2016), asymmetries (e.g., Dzieliński et al., 2018) as well as structural breaks (e.g., Jung & Maderitsch, 2014). Moreover, clustering and shocks (e.g., Charfeddine, 2014), regime switches (e.g., Ma et al., 2017) and the trend-inducing momentum effect (e.g., Berghorn, 2015), which is used in factor investments, can be mentioned. Furthermore, elaborating on stylised facts requires the stating of the additional existence of heterogeneity of actors (e.g., Ramiah et al., 2015), leading to multifractal time scales, behavioural patterns (e.g., Celeste et al., 2019) as well as microstructure noise (e.g., Lee & Seo, 2017), among many non-stated others. All of the above-mentioned properties occur at different time scales simultaneously, featuring the emergence of nonlinearities (e.g., De Luca et al., 2019) within the system of financial markets. In recent years, there has been a substantial increase in nonlinear testing and modelling of economic and financial time series, facilitating a better understanding of the behaviour of markets, the price risks and the formation of actors' expectations therein (Kyrtsou et al., 2004).

When contemplating real-life confrontations, similar scenarios tend to evolve in a similar manner and occur repeatedly, leading to the association of a predefined level of determinism in real-life systems (e.g., financial markets) due to the development of memory and experience effects (Marwan et al., 2007). Thus, modelling via deterministic differential equations reveals itself as suitable for these kinds of systems since their entirety can be characterised by equivalent mathematical differential equations (Marwan et al., 2007). Under the premise that the initial conditions of the system are noted exactly, these differential equations enable the prediction of the system states to an indefinite level of precision and time span due to the deterministic behaviour of the system (Marwan et al., 2007). In terms of attempts to forecast systems, considering a deterministic scenario would illustrate the prerequisite of the future development of the system to be completely explicable via the current state, principally indicating a plainness in terms of the predictability of such a system (Song et al., 2016; Guégan & Leroux, 2009).

Nevertheless, scrutinizing a financial market as an example of such a real-world system can also be viewed as highly complex feedback system driven by the aforementioned empirical properties (e.g., asymmetries), resulting in a contrastingly challenging effort in terms of predictability and modelling in comparison to the previously assumed plainness of deterministic forecasts (Marwan et al., 2007; Fernández-Rodríguez et al., 2005).

Furthermore, these seemingly conceptual differences lay grounds for the discussion about the underlying nature and the essential functioning of the emerging dynamics of financial markets or other defined economic systems (Marwan et al., 2007). Elaborating on a deeper understanding of such assumed underlying laws of dynamical motions reveal chaotic dynamical analysis to be thoroughly applied at length in financial systems (Barkoulas et al., 2012). Substantial literature about testing for nonlinear dynamics and chaos in financial markets provides strong evidence of nonlinearity and a special class of models, namely chaos models, that have emerged (Fernández-Rodríguez et al., 2005; Matilla-García et al., 2004).

Chaos constitutes a deeper reasoning about the above-mentioned essential characteristics (stylised facts) and the underlying nature of the evolutionary processes driving a (financial) system, which is affected by nonlinearities (Song et al., 2016). The first property, or one of the distinctive feature of chaotic dynamical systems, is that even though deterministic, these systems characterise themselves via sensitivity on initial conditions. This means that slight fluctuations, or even marginal perturbations of the initial conditions[1], can render precise predictions on a long time scale meaningless (Guégan & Leroux, 2009; Barkoulas et al., 2012). In addition, data measurement limitations[2] with regard to the current initial conditions specify an upper bound for the predictability, even if the model is completely disclosed (Barkoulas et al., 2012). The second is the recurrence property, reflecting upon the dynamical behaviour of such systems (Marwan et al., 2007).

Recent trends within chaotic dynamical analysis have led to a proliferation of studies that state structural nonlinear models capable of displaying financial market instabilities and chaos being able to mimic the empirical properties of time series (Barkoulas et al., 2012). Therefore, a central pillar in nonlinear forecasting for over 40 years is the revelation of whether the considered (financial) data sets are generated via deterministic or stochastic[3] dynamical systems, since their respective mathematical operations differ noticeably (Çoban & Büyüklü, 2009; Matilla-García & Marín, 2010; Sandubete & Escot, 2020). This leads to vast disseminations of literature about deterministic chaotic behaviour and the design of economic models in the regime of chaotic behaviour from a theoretical view (Sandubete & Escot, 2020). A variety of studies imply the cause of structural nonlinear financial models to output chaotic dynamics is due to the previously mentioned heterogeneity in actors' expectations (Fernández-Rodríguez et al., 2005; Sandubete & Escot, 2020).

[1] Deviations from a trajectory of the system's phase (state) space
[2] In terms of measurement errors, sampling frequency and data accuracy, among others
[3] Originating from pure randomness

Speaking in a mathematical sense, a chaotic dynamical system has a dense collection of points with periodic orbits, sensitivity to initial conditions and topological transitivity, which are discussed in Eckmann and Ruelle (1985) and Devaney (1989) (BenSaïda & Litimi, 2013).

Chaos further refers to bounded steady-state behaviour, which neither represents an equilibrium point, a quasi-periodic point or a periodic point nor indicates that nearby points separate exponentially in finite time, resulting in those chaotic systems to manifest very complex and seemingly random evolutions out of the view of standard statistical tests (Barkoulas et al., 2012). In financial systems, hyperchaotic[4] phenomena potentially evolve into a crisis, denying any form of system control (Jahanshahi et al., 2019a). Regarding the academic literature, first tests[5] of chaotic behaviour for financial systems were executed following the BDS (Brock, Dechert and Scheinkman) test of Brock et al. (1996), but also revealed its omnipotence since it cannot differentiate between whether the discovered nonlinearities originate from stochastic or chaotic dynamics (BenSaïda, 2014). Unfortunately, comparisons between even the most powerful tests (e.g., close-return test, BDS-test and Lyapunov exponent[6]) do not result in conclusive findings (BenSaïda, 2014). Actually, several propositions[7] towards a more conclusive solution in the academic literature was brought to light, with no further positive indications (BenSaïda, 2014).

Following BenSaïda and Litimi (2013), the results indicate for six stock indices as well as for six exchange rate series that chaos cannot be confirmed via hypothesis. McKenzie (2001), among many others, states the same result, namely, the denial of chaotic behaviour in favour for stochasticity. On the other hand, following Park & Whang (2012) and Mishra et al. (2011), among many others[8], reveal chaotic dynamics in their respective data samples. As a by-product of this ongoing discussion, Altan et al. (2019) state that the existence of a small correlation dimension[9] in a time series implies a non-zero deterministic part of the 'world decomposition', thereby proofing for a time series with a finite correlation dimension its deterministic part mandatorily to be of non-zero nature. The former statement is an allegory for the vast dilemma concerning the determination of the true, mostly unknown, nature of (financial) dynamical systems, whether it be stochasticity or chaoticity. These systems are almost graphically similar and cannot be differentiated by respective tests (BenSaïda & Litimi, 2013; Aguirre & Billings, 1995).

[4] Hyperchaos is considered if more than two positive Lyapunov exponents exist (e.g., Rössler, 1979; Ma & Wang, 2012; Gao & Ma, 2009). If a discrete nonlinear system is dissipative (spontaneously symmetry-breaking), a positive Lyapunov exponent is an indication of chaotic dynamics within the system under regard (Dechert & Gençay, 1996).
[5] See Hsieh (1991), Takala & Virén (1996) or Opong et al. (1999) as early references.
[6] Applied to financial time series, a positive Lyapunov exponent can occur even in non-chaotic series due to inadequate use on noisy datasets (BenSaïda, 2014).
[7] See fractal dimension estimates of Smith (1992); nonlinear forecasting of Casdagli (1992); estimations of entropy by Eckmann & Ruelle (1985); dominant Lyapunov exponent estimates by Wolf et al. (1985) and Hsieh (1991).
[8] We will provide a sophisticated overview of relevant empirical results in the main part of this study (see 2.3).
[9] An alternative to the fractal (Hausdorff) dimension of a system.

Following Aguirre and Billings (1995), a verification of strong noise influence on the identifiability of chaotic dynamics is provided, leading to misspecifications of chaotic dynamics as stochastic dynamics due to noise disturbance, rendering the discovery of chaotic processes very demanding (Kyrtsou et al., 2004).

Empirical financial data is often small and noisy in comparison to its "physics' data counterparts", suggesting a preclusion of dynamical identification if the noise levels are greater than a predefined critical threshold value (Kostelich, 1997; Aguirre & Billings, 1995; Song et al., 2016). Therefore, the great controversy of the nonlinear financial literature is whether a financial system is characterisable via low-dimensional deterministic chaos or can be generated via stochastic dynamics as well as if those chaotic systems are controllable[10] (Song et al., 2016; Kostelich, 1997). This draws major implications in terms of financial forecasting, since when under the assumption of chaos, predictability is only further possible on short time scales, which still face all the above-mentioned empirical properties (e.g., asymmetries) (Barkoulas et al., 2012). A huge variety of newly developed chaos models tends to explicate the chaotic structures in asset prices due to heterogeneity of traders' expectations (Kyrtsou et al., 2004). Another faction tries to analyse the chaos regime by applying neural network solutions, assuming the phase space of the system to be finite and high-dimensional (Boullé et al., 2020). Further, the quantification of the recurrence property seems promising in terms of distinguishing the nature of the dynamical systems (Holyst & Urbanowicz, 2001).

We contribute to this ongoing debate by (1) deducing a bibliometric and citation network analysis of the whole field of nonlinear dynamics as well as of nonlinear financial analysis in order to bridge diverged research streams of the same research topics and related questions, which occur due to 'over-specialisations', (2) calculating a novel combination of several major chaotic tests (e.g., Bask-Gençay test) for financial datasets in particular, which are only applied scattered within the academic literature so far, in order to provide a sufficient financial analysis framework for nonlinear dynamics to avoid future inconclusive results, (3) analyse financial chaotic dynamics via classical phase space reconstruction[11] using the embedding approach of Takens (1981) as well as by following Song et al. (2016) in applying a spectral embedding for nonlinear dimensionality reduction, which consists of a combination of principal component analysis based on a k-nearest neighbours algorithm and the calculation of eigenvalues via Laplacian Eigenmaps and (4) validating the results via a full recurrence quantification analysis.

We use wavelet-filtered (denoised) daily S&P 500 returns (2000–2020), respective surrogate datasets, a Brownian motion return realisation and a Lorenz system for the points (2)–(4). Lastly, we elucidate the implications of chaos on financial forecasting attempts as well as the possibility of chaos control, before critically discussing financial forecasting under chaotic dynamics and this first-time combinatory framework approach.

[10] Chaos control can be induced via a periodic, dynamically unstable state variable (e.g., Ott et al., 1990) (Kostelich, 1997).
[11] This approach can be executed to show potential (strange) attractors of dynamical systems visually applying a single time series.

2. Bibliometric and Citation Network Analysis

2.1. Bibliometric Analysis and Snowball Sampling

Within this study, we employ a bibliometric analysis to identify relevant publications, conduct a subsequent snowball sampling as well as execute a citation analysis that investigates authors, journals and respective sources (Biernacki & Waldorf, 1981; Rötzel, 2019; Vogl & Rötzel, 2021). The citation analysis is based on the assumption that references provide a valid indication of the scientific interaction between scholars and research organisations. Further, we assume that interconnections between researchers reflect upon the latter interactions, making conjunctions and scientific conceptions visible (Garfield, 1979; Small, 1978; Vogl & Rötzel, 2021). Following Kitchenham and Brereton (2013), we execute a literature search in the database "Science Direct", querying the respective keywords and their combinations as stated in Table 1. The resulting literature is required to be written in English, be blind peer-reviewed and be either review article, research article, data article, mini-review article or practice guideline. Other document types are neglected. The non-duplicate, relevant results are gathered accordingly (Vogl & Rötzel, 2021). The keywords focus on special terms taken out of the field of nonlinear dynamics and financial chaos analysis (e.g., chaotic attractor, financial chaos and nonlinear dynamics).

The initially resulting dataset encompasses 80,651 unique[12] publications. In order to secure the quality of the gathered literature, we apply two journal ranking lists, namely, the Harzing's journal ranking list and the SCImago journal ranking and country ranking list. Harzing's journal ranking list consists of 12 different and independent journal rankings (e.g., VHB-JQ3, EJL2016 and EJIS2007), which additionally need to comply with our following criteria: blind-peer review, more than two rankings in Harzing's list and a rank that is not the lowest in more than 50% of all given ranks on average (Vogl & Rötzel, 2021; Harzing, 2019). Further, the SCImago journal and country rank is developed from information in the Scopus® database by Elsevier B.V. and consists of 27 major thematic areas and 313 specific subject categories, which need to comply with the following criterion for the selected categories stated in Table 2: must belong to the top 25% of the Q1 ranking (SCImago Lab, 2021). After filtering, the stored data executing these frameworks result in a list of literature further used by this paper and results in a sum of 17,413 publications. Furthermore, we rate these publications using a framework stated in Briner and Deyner (2012), which ranks a paper in accordance with four qualitative criteria (namely, contribution, theory, methodology and data analysis). For each criterion, it is possible to evaluate the content of a given paper from low (zero) to high (three) or "not applicable". Further, we enforce studied papers to result in a Deyner rating of greater than two on average over all criteria, leaving 1,674 publications (Briner & Deyner, 2012; Vogl & Rötzel, 2021). Additionally, these 1,674 publications act as input for a snowball-sampling procedure (Biernacki & Waldorf, 1981).

[12] Total results are 148,431 publications for all keywords, including duplicates.

We conclude the snowball sampling with 54,217 additional unique publications. We then select again following the before mentioned process and update the findings accordingly (Vogl & Rötzel, 2021). After applying the two journal rankings, 6,393 papers remain, which results in an addition of 280 Deyner-rated publications, concluding in a complete sample-size of 1,954 publications.

Table 1: Overview of keywords used to search the Science Direct database and the respective counts (#)

Keywords		#	Keywords		#
adiabatic chaos	-	61	embedding dimension	chaotic system	133
	time series analysis	2	financial chaos	technology	5
	diffusion	3		neural networks	8
attractor	financial system	208		algorithms	10
	reconstruction space	105		-	139
bifurcation	Lyapunov exponents	767		nonlinear dynamics	17
	chaotic system	1,704		noise	10
	financial markets	48		topological structure	46
	time series analysis	196		fractals	17
chaos	finance	33	chaos control	-	2,499
	financial system	76	Hamiltonian chaos	-	363
	attractor	1,446	Lyapunov	finance	16
	-	12,536		financial modelling	21
	time series analysis	535	Lyapunov diagrams	financial system	5
	financial markets	67	manifold	dynamical system	1,259
	Lyapunov time	642	manifold	chaotic system	299
	forecasting	229	nonlinear dependence	Hurst	7
	trading	73	nonlinear dynamic system	-	15,946
	economical system	11		wavelets	160
	stochastic processes	371		multiresolution analysis	10
chaotic attractor	financial markets	8		frequency analysis	1,195
	stocks	2	nonlinear dynamics	-	20,452
chaotic dynamical system	-	3,470	nonlinear noise	wavelets	174
chaotic system	-	9,758	nonlinear resonance	financial system	2
	statistical test	122	nonlinear system	-	67,761
	noise	751	Poincaré sections	chaotic system	203
	autocorrelation	80	radial chaotic migration	-	2
	machine learning	60	recurrence quantification analysis	finance	1
	artificial intelligence	25		chaotic system	27
	wavelets	119	sensitive dependence	Initial conditions	214
	diffusion	427	space time separation	time series	111
	time scales	410	spectral embedding	chaotic system	8
	separatrix matrix	1		attractor	23

Keywords		#	Keywords		#
chaotic system	fractals	473	spectral embedding	financial time series	59
correlation dimension	financial system	23	state space	financial system	70
deterministic chaos	-	1,014	stochastic chaos	-	1,214
deterministic system	financial markets	41	surrogates	chaotic system	48
Total Counts for all Keywords					**148,431**
Total Unique Counts for all Keywords					**80,651**

Table 2: SCImago journal and country rank selection of categories and subcategories

Journal Category	Journal Subcategory
Physics and Astronomy	Statistical and Nonlinear Physics General and Miscellaneous
Mathematics	Mathematical Physics Modelling and Simulation Statistics and Probability General and Miscellaneous
Computer Science	Artificial Intelligence Computational Theory and Mathematics Signal Processing

2.2. Citation Network Analysis

Before we present the structure of the analysis, we select 448 publications as financial subsample (FS) of the previously mentioned 1,954 total paper sample (TS), whose content is based on a relation with econometrical and financial topics. We do so to elaborate not only the complete field of nonlinear dynamics, which encompasses many different scientific regimes, but also to display the interconnections of the financial disciplines separately and in more detail. Therefore, we will state these two samples parallel to each other in this section. The structure of the analysis is as follows: First, we determine metrics and other test parameters for each of the samples (Vogl & Rötzel, 2021). Second, we graphically deduce the citation networks using the Force Atlas algorithm provided by the software package Gephi. Third, we modify the plots using filters, size as well as colour changes, which present given metrics (Vogl & Rötzel, 2021). Lastly, we provide a sufficient explication. In order to prepare the input data for Gephi, we include the publications of the two referring samples as "mother-nodes", whilst using their respective references of papers as "daughter-nodes"[13] (Vogl & Rötzel, 2021). For TS, we obtain 56,104 results and for FS 17,156 data points, respectively. Once uploaded, we calculate the HITS-metrics (Hubs distribution and authority measurement), randomised modularity, Eigenvector Centrality with 100 iterations and the average path length as displayed in Table 3 (Vogl & Rötzel, 2021).

[13] This process uses PDF files of the sample literature, extracts references and creates json files, which we then convert into Gephi-readable-formats using self-written Python code.

Table 3: Overview of citation network analysis metrics, analogue to Vogl and Rötzel (2021)

Metric	Description	Explanation	Value (TS)	Value (FS)
HITS	calculates the Hubs-distribution and authority measures	hyperlink-based topic search (~ page authority in surface web)	$1.0 * 10^{-4}$	
Eigenvector Centrality	determines the directed sum of change in terms of Eigenvector centrality with 100 iterations	[0,1] provides the influence between nodes	0.2384	0.2662
Average Path Length (avp)	calculates the directed path length and diameter of the network	diameter ($diam$) is the maximal distance between two nodes	$diam$: 17; avp: 5.6184	$diam$: 4; avp: 1.4044
Modularity	randomised, edge-weighted community creation	[-1,1] gives the structure of networks; density of connections	0.902	0.904

In terms of HITS, we concur for both samples, that not many research papers provide hyperlinks and are not dominant within the visible surface web, since the values of the respective papers tend to be zero[14] (Kleinberg, 1999). Regarding Eigenvector Centrality, which represents the influence of a node within a network, we see weak influence between the respective research papers in each sample, while FS scores a little higher (Vogl & Rötzel, 2021). Further, regarding diameters ($diam$), the sample TS with a $diam$ of 17 exceeds FS with a $diam$ of four. Additionally, the TS sample yields 5.6184 as average path length (avp) in contrast to FS, which states an avp of 1.4044, suggesting that the nodes of FS tend to be closer together (Newman, 2010; Vogl & Rötzel, 2021).

Regarding modularity, which represents the weights of the edges, we state strong (almost identical) values for both samples (Blondel et al., 2008). After the creation of 285 communities for TS and 114 communities for FS, in terms of modularity, we apply three different node sizes and colour manipulations and one filtration each (Vogl & Rötzel, 2021). First, we change the node sizes from small to large as well as their colour with regards to the Betweenness Centrality, which measures how often a node appears on the shortest paths between nodes in the respective networks, with red tones indicating significance (Vogl & Rötzel, 2021). Following this, we apply a filter, which only shows nodes that correspond to a degree greater than three for TS and greater than two for FS accordingly, as stated in Figure 2 for TS and Figure 3 for FS (Vogl & Rötzel, 2021). In our second attempt, we set the colours in terms of the authority measure and the sizes to equal the Eigenvector Centrality of each node. The aggregate of important publications as well as their measure values taken out of both attempts are shown in Table 4 (Vogl & Rötzel, 2021).

[14] Each parameter starts with the value of one and will be normalised into $[0, 1]$, which can be interpreted as probability.

Table 4: Leading publications for the samples TS and FS: $\text{Degree}\,TS > 3$ and $\text{Degree}\,FS > 2$; significant markings in terms of Eigenvector Centrality (EC), Authority and Betweenness Centrality (BC) with stated degree and citation counts; if one publication belongs to FS, TS or both is indicated, the FS value is given in (·) if a reference applies to both samples. The marking "-" indicates a zero value. Results are sorted in ascending order of citations.

FS	TS	Publication	Cited	Degree	BC	Authority	EC
	x	Kennedy & Eberhart (1995)	62,815	85	119,075.848	0.0025	0.0841
	x	Black & Scholes (1973)	41,260	134	52,731.0833	-	0.1598
	x	Lorenz (1963)	23,266	31	38,343.6638	0.0047	0.0465
	x	Guckenheimer & Holmes (1983)	20,657	34	62,338.6425	0.0055	0.0732
	x	Strogatz (2014)	13,478	58	421,022.3169	0.012	0.26472
	x	Pecora & Carroll (1990)	13,311	580	702,138.8041	0.9329	1
	x	Ott et al. (1990)	8,645	447	536,785.0031	0.3247	0.8005
	x	Grassberger & Procaccia (1983)	7,944	90	200,285.2014	-	0.0786
	x	May (1976)	7,879	32	114,217.8468	-	0.0471
	x	Kantz & Schreiber (2003)	7,544	114	228,113.258	0.0017	0.1919
	x	Ott (2002)	6,909	42	230,086.1269	0.0109	0.1455
x		Barberis et al. (1998)	6,502	45	759	-	0.1637
	x	Grassberger & Procaccia (1983)	6,328	105	270,431.7703	0.0109	0.1925
	x	Packard et al. (1980)	5,259	105	115,441.5979	0.0032	0.1967
	x	Andrews (1991)	4,494	227	20,034.8524	0.0039	0.3618
	x	Theiler et al. (1992)	4,212	56	130,062.7126	-	0.0783
	x	Pyragas (1992)	4,195	54	14,492.0214	-	0.0449
	x	Rosenstein et al. (1993)	3,593	88	230,899.1811	0.0074	0.1149
	x	Abarbanel (1996)	3,340	51	40,424.619	-	0.0583
	x	Brandt & Pompe (2002)	2,916	39	23,261.9472	-	0.0669
x	x	Andrews & Ploberger (1994)	2,784	69 (66)	21,926 (520)	- ; (0.0016)	0.1202 (0.4637)
	x	Farmer & Sidorowich (1987)	2,674	40	31,546.742	-	0.0367
	x	Robinson (1995)	2,471	39	56,241.4555	0.0026	0.094
	x	Abarbenel et al. (1993)	2,278	161	232,010.0202	0.0057	0.3463
	x	Chen et al. (2004)	2,159	37	128,475.7873	0.0028	0.0397
	x	Casdagli (1989)	1,939	68	97,896.7212	0.0022	0.0883
	x	Chen & Dong (1998)	1,884	32	100,013.4552	0.0128	0.1567
x	x	Balke & Fomby (1997)	1,865	179 (175)	75,222.0643 (2,618.8333)	- ; (0.0087)	0.2453 (0.6525)
	x	Brock & Hommes (1998)	1,856	39	3,901.6428	0.0011	0.0145
	x	Arthur (1999)	1,635	111	-	-	0.1917
	x	Rössler (1979)	1,486	68	44,897.7349	0.0121	0.1021
x		Taylor & Allen (1992)	1,432	33	221.3333	-	0.1183

FS	TS	Publication	Cited	Degree	BC	Authority	EC
x		Abuaf & Jorion (1990)	1,283	185	-	0.0047	0.8413
	x	Pagan (1996)	1,087	65	87,326.4965	0.0021	0.1621
	x	Baptista (1998)	1,046	45	137,229.8204	0.0075	0.2016
x		Adler & Lehmann (1983)	774	49	173	0.0012	0.3567
	x	Zhang et al. (2005)	486	31	129,706.4197	-	0.0674
	x	Judd & Mees (1995)	355	48	145,363.0754	-	0.10758
	x	Abarbanel et al. (1990)	320	87	146,857.3812	0.0035	0.2473
x		Agnolucci (2009)	314	136	-	0.0015	0.5755
	x	Poincaré (1890)	263	197	-	0.0142	0.491
	x	Anishchenko et al. (1992)	242	37	57,878.7611	0.0037	0.0695
	x	Abhyankar et al. (1995)	209	88	43,766.6242	0.0023	0.1222
x		Abraham et al. (2001)	203	253	-	0.9955	0.97749
x		Aït-Sahalia & Mancini (2008)	175	141	-	0.0013	1

For the final iteration, we let the node-sizes remain at the Eigenvector Centrality and change the colours to display the communities, which remain after the degree-filter applies as shown in Figure 3 for TS and Figure 4 for FS, respectively (Vogl & Rötzel, 2021). We present the five highest-scoring communities with example references for both samples in Table 5 (Vogl & Rötzel, 2021).

Table 5: Example bridging paper out of each of the top five communities for each sample TS and FS in Figure 3 and Figure 4.

Sample	Community	#	Colour	Paper
TS	Sensitivity Analysis & Mathematical Conceptions	I	Orange	Sobol´ (1995)
	Chaos Control & Synchronisation	II	Blue	Pecora & Carroll (1990); Ott et al. (1990)
	Chaotic Dynamics & Nonlinear Analysis	III	Turquoise	Grassberger & Procaccia (1983)
	Financial Modelling	IV	Green	Abu-Mostafa et al. (2001)
	Econometric Tests & Economics	V	Red	Abuaf & Jorion (1990)
FS	Financial Chaos	I	Turquoise	Adrangi et al. (2001)
	Volatility Modelling	II	Yellow	Andersen & Bollerslev (1998)
	Economic Chaos	III	Red	Agliari et al. (2005)
	Artificial Intelligence for Finance	IV	Green	Abraham et al. (2001)
	Econometric Tests & Economics	V	Blue	Andrews & Ploberger (1994)

Regarding the respective structure of the research streams of TS and FS, several indications occur in terms of interconnectivity and dispersion of relevant research topics (e.g., financial chaos, chaos control), which we intend to further elucidate.

Beginning with TS, as stated in Figure 3, we determine a separation of the 'Sensitivity Analysis & Mathematical Conceptions' (I) from the other communities. This research stream exists solely within itself, yet serves as basis for the development of the other fields, especially 'Econometric Tests & Economics' (V) and 'Chaos Control & Synchronisation' (II). 'Chaos Control & Synchronisation' (II) and 'Chaotic Dynamics & Nonlinear Analysis' (III) tend to exist symbiotically, while mutually stimulating each other. 'Financial Modelling' (IV) and 'Econometric Tests & Economics' (V) are also in symbiosis with each other, yet just tangent the methodologies of (II) and (III) in several cases in order to broaden the respective field prospects into other domains of research. The research of (IV) and (V) are located near each other since they mostly differ in the respective choice of datasets and angles of academic vision (e.g., macroeconomic versus intra-market time series displays).

Visually, comparing TS and FS creates the impression of FS being less densely connected than TS. This is due to the fact that FS is a sub-set of TS, which consists of lesser datasets, and the higher resolution of the respective research streams within the sub-sample. FS provides a more granular view of the research area.

Elaborating further on FS stated in Figure 4, we determine a separation of the communities of 'Economic Chaos' (III) and 'Econometric Tests & Economics' (V). Whilst both tend towards the analysis of the same nature of data sets (e.g., macroeconomic data), they differ within the chosen methods for analysis. The field of 'Volatility Modelling' (II) represents a bridging research stream between all other stated communities. Regarding the streams of 'Financial Chaos' (I), we see a separation from the others, while the data basis mostly resembles those of (III), (V) or (II), thus defining another example of dispersion between research streams based upon the selection of analysis methods. With respect to 'Artificial Intelligence for Finance' (IV), a separation into a field of its own is visible, while targeting the other fields where needed.

In total, we can make the separation of research fields into their own sub-domains visible, which can be interpreted as being caused by methodological 'over-specialisations', even if the core research questions and underlying datasets vastly display high resemblances. Therefore, we hint a potential future gap between 'closely related' research streams to diverge and encapsulate themselves, building separated 'isles' of independent research areas, which may lose the academic connection towards the other streams, even if the topic of research based upon the underlying data is ultimately the same and a symbiosis would bear fruition towards more encompassing results.

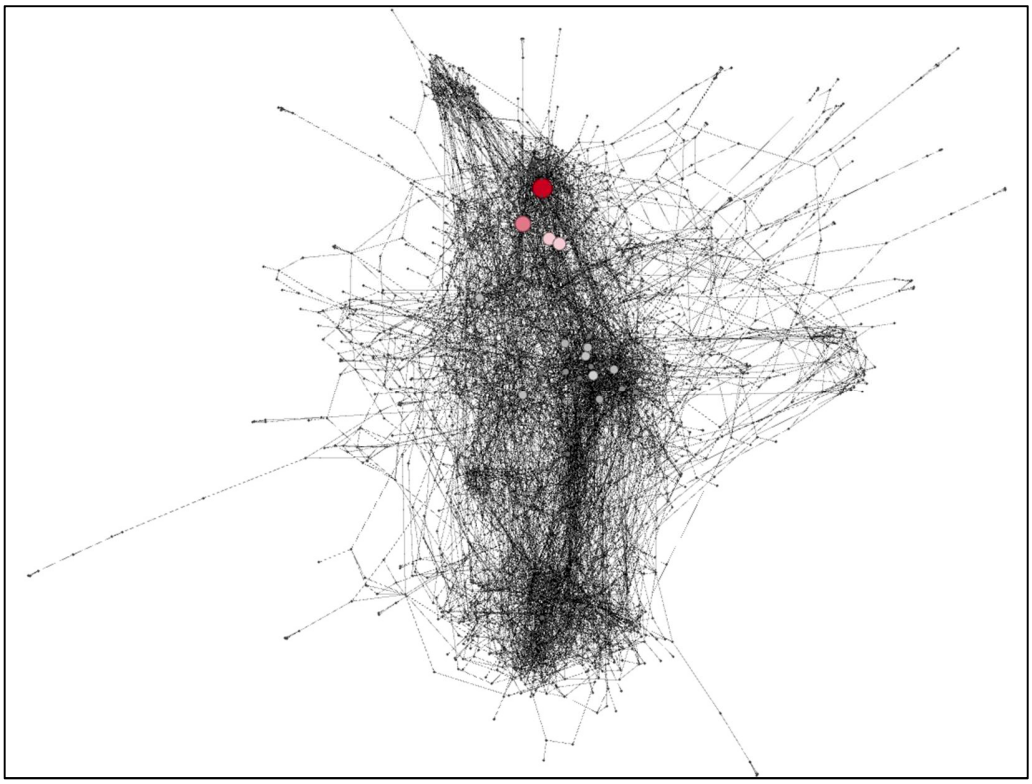

Figure 1: Citation Network TS: $\texttt{Degree} > 3$, Size and Colour equal to Betweenness Centrality (small to big; black to red).

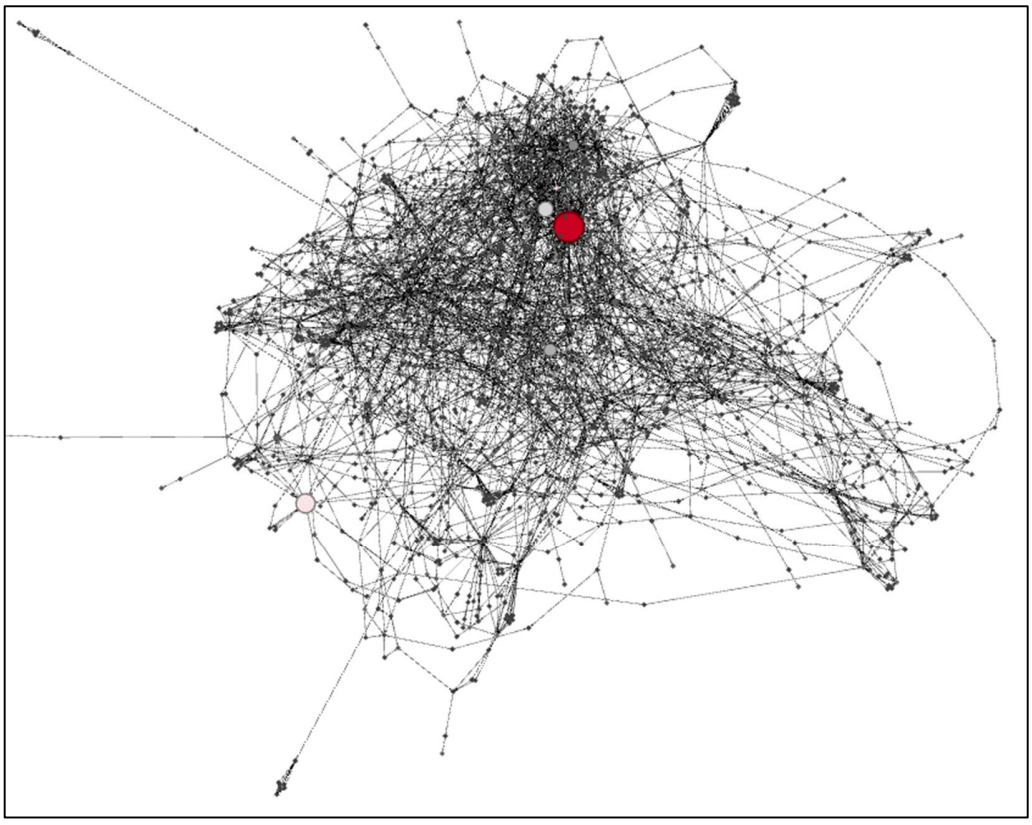

Figure 2: Citation Network FS: $\texttt{Degree} > 2$, Size and Colour equal to Betweenness Centrality (small to big; black to red).

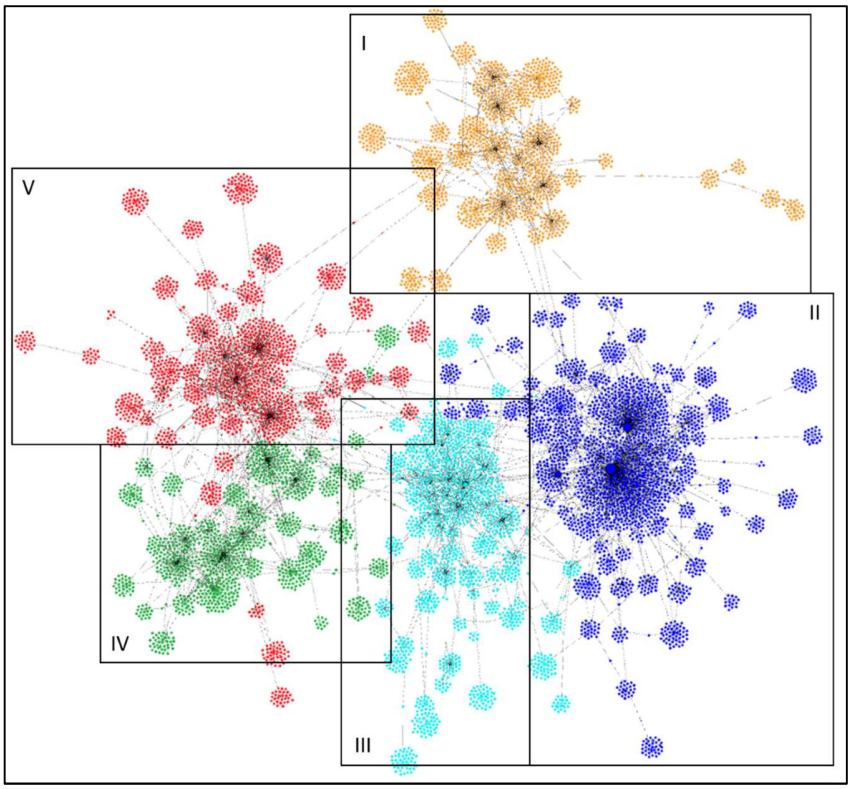

Figure 3: Citation Network: Top 5 *Communities of TS and* Degree $>$ 3 *with size equals Betweenness Centrality; for colour coding, see Table 5.*

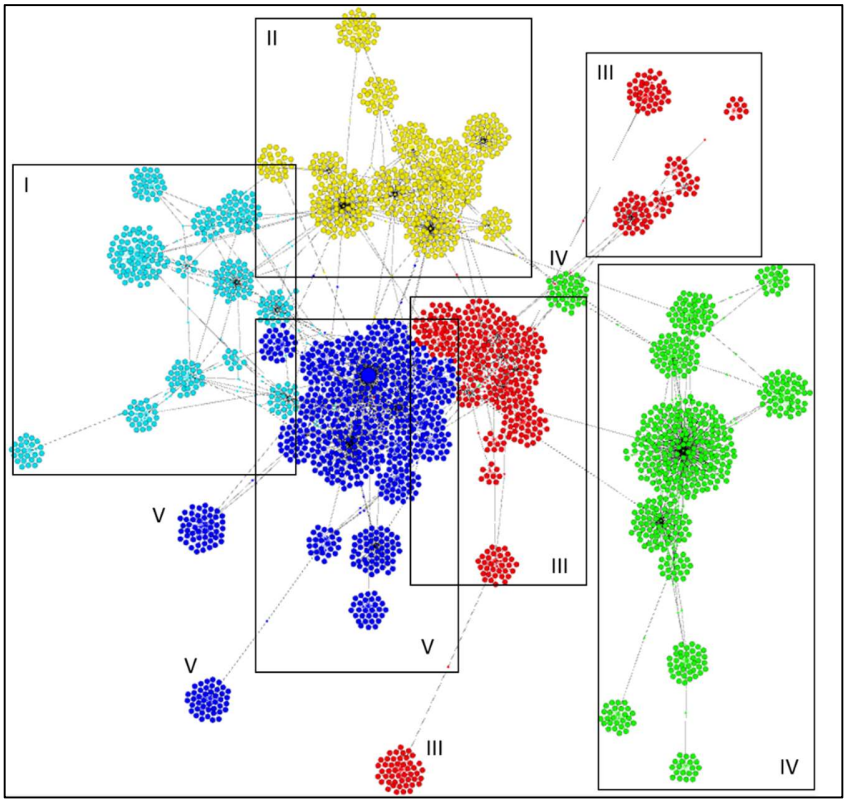

Figure 4: Citation Network: Top 5 *Communities of FS and* Degree $>$ 2 *with size equals Betweenness Centrality; for colour coding, see Table 5.*

2.3. Empirical Results Out of Literature

As indicated in the introductory part of this study, we will elaborate on the stated controversy of chaoticity versus stochasticity within the respective academic literature. Since we will develop the according theoretical background in the section hereinafter, we will begin by stating the most dominant reasons, interpretable as symbols, for the failings of tests and the inconclusiveness within the regarded empirical financial analysis of the respective literature. These are (1) small, finite data sets, which are eventually sampled at a rate that is too low (e.g., BenSaïda, 2014); (2) classical tests like the BDS-test cannot differentiate between stochasticity and chaoticity in terms of tested nonlinearities and are often misused (e.g., Matilla-García and Marín, 2010); (3) noise and measurement errors, which can render even a properly conducted analysis worthless (e.g., Aguirre and Billings, 1995); and (4) the incompleteness of analysis methodology and lack of details, which is especially mandatory within nonlinear time series analysis (e.g., Kantz and Schreiber, 2003).

In order to display the inconclusiveness as well as the controversy, we will separate the literature regarding the results, shown in Table 6, in favour of chaos or in favour of stochasticity.

Table 6: Empirical results in the academic literature about chaotic or non-chaotic financial behaviour of asset dynamics.

Paper	Result
Grandmont (1985), Brock & Hommes (1998), Park et al. (2012), Mishra et al. (2011), Çoban & Büyüklü (2009), Yousefpoor et al. (2008), Kyrtsou and Terraza (2002), Das & Das (2007), Bask M. (2002), Scarlat et al. (2007), Peters (1994), Pannas & Ninni (2000), Moshiri & Foroutan (2006), Chichilnisky et al. (1995), Iseri et al. (2008), Chiarella & He (1999), Lux (1995, 1998), Malliaris & Stein (1999), Sandubete & Escot (2020), Cai & Huang (2007), Song et al. (2016)	Chaos
BenSaïda (2014), McKennzie (2001), BenSaïda & Litimi (2013), Cecen & Erkal (1996), Agnon (1999), Barkoulas (1997, 1999), Davidson (1997), Labys (1998), Sugihara (1990, 1996), Fernandez-Rodriguez (1998), Gilbert (1997), Cromwell (2000), Barnett (1997), Serletis & Shahmoradi (2004)	No Chaos
Shwartz & Yousefi (2003), Brock & Sayers (1988), Scheinkman & LeBaron (1989), Brock & Mallaris (1989), Bajo-Rubio (1992), Frank & Stengos (1988), DeGrauwe et al. (1993), Dewachter (1993), Adrangi et al. (2001)	Inconclusive
Kyrtsou et al. (2004), Holyst & Urbanowicz (2001)	Chaoticity and Stochasticity coupled

3. Theory of Chaotic Dynamics and Methodology of the Study

Vast amounts of literature under regard for this study apply chaos tests and measures fractioned from each other, which, in total, would sum up to an implementation of a complete framework. Following Kantz and Schreiber (2003), existing research does not exert enough care while handling theoretical implications within the respective applications and interpretations. In order to build and present such a complete framework, with specialization towards application within financial analysis, we present an encompassing body of theoretical essences within this section in order to ensure transparency as well as to create an encompassing basis of comprehensibility of our empirical results presented in Section 5, which strictly follow the order of this section. In order to sum up the framework as well as the theoretical concepts, which we will present, we provide a graphical representation of the course of the empirical analysis in Figure 5.

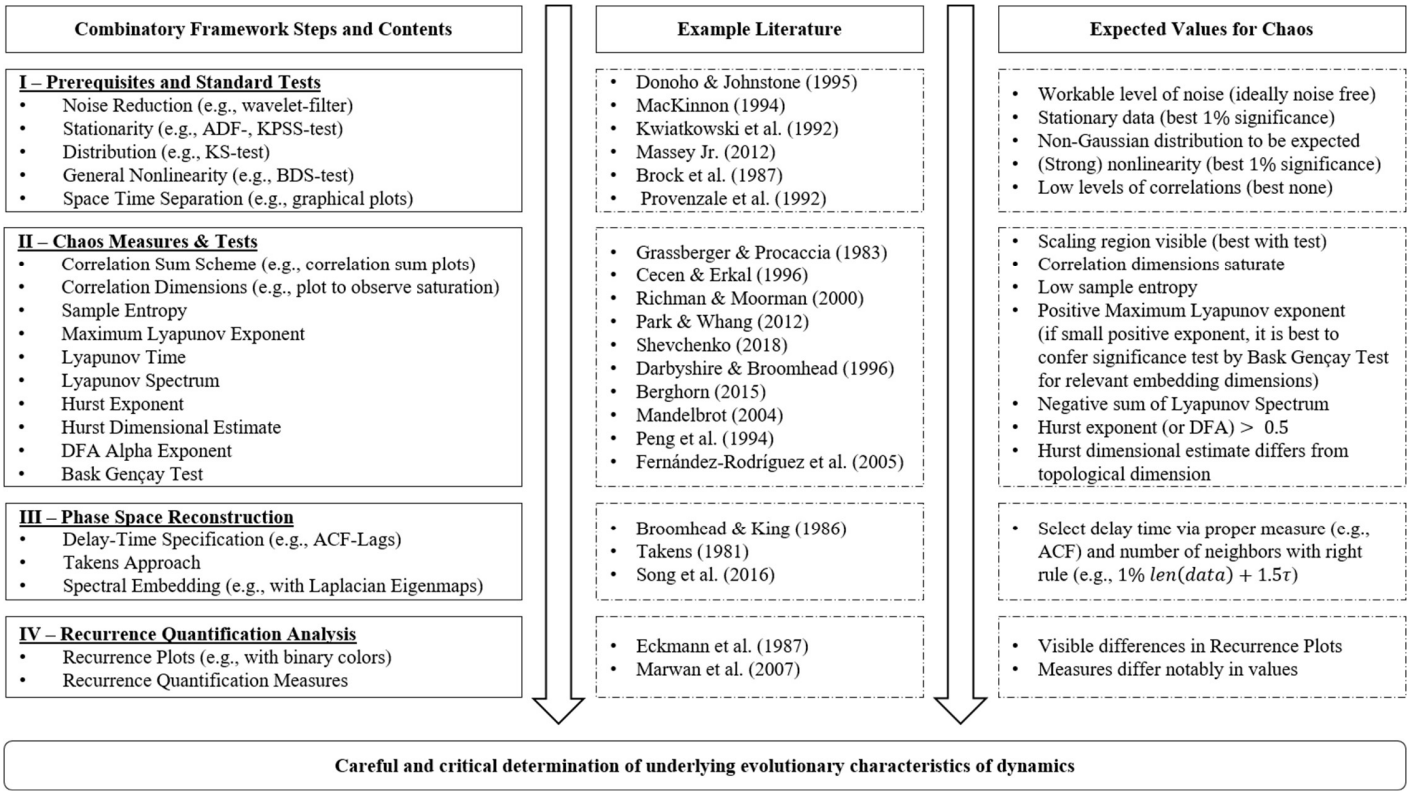

Figure 5: Novel combinatory-methodological framework to analyse nonlinear dynamics with financial data sets.

3.1. Theory of Chaotic Dynamics

3.1.1. Dynamical Systems

Before presenting the empirical analysis, we elaborate on the brief theoretical background of the research area. We will firstly discuss in a formal manner the definition of dynamical systems and related topics, which we will apply in our empirical analysis. A function present within a given system, portraying the dependence of time of a given point in a geometrical space, is called a dynamical system (Strogatz, 2014). Such a dynamical system has a state given by a tuple of real numbers (vectors) that can be depicted by a point in a phase (or state) space (mostly a geometrical manifold[15]) at any given time (Strogatz, 2014). The evolutionary rule of the dynamical system is constituted via a function[16] reflecting upon the future states, which are deducted from the current systems' states (Hasselblatt & Katok, 2003). Assuming the case that the system is solvable given an initial point (e.g., a representation by respective differential equations), the possibility arises of determining all of its possible future positions, namely, collections of points labelled as trajectories or orbits (see 3.1.2) (Hasselblatt & Katok, 2003).

Systems too complicated to be represented by one single trajectory bear fruition to a collection of difficulties, namely, (1) the system itself or its parameter setting is unknown, yielding implications in terms of the Lyapunov stability or the structural stability, (2) the type of the trajectory itself is of more prominence than the relevant realisation of the latter, (3) parameter setting variations may lead to bifurcations[17] and (4) determining the long-time behaviour of the system may differ, if considering ergodic[18] versus hyperbolic systems (Hasselblatt & Katok, 2003; Strogatz, 2014). Furthermore, alongside various other theorems as exhibited in Table 7, the Poincaré recurrence theorem indicates system states to return to a state very close to the initial state (further explicated and enhanced in the Birkhoff's ergodic theorem) (Poincaré, 1890; Hirsch, 1997; Giunti & Mazzola, 2012).

As a pathway towards a definition, a dynamical system is stated as a manifold $\mathcal{M}$, labelled the phase (or state) space endowed with a family of smooth evolutionary functions Φ^t, which, for any element $t \in T$ reflecting time, maps a point of the latter phase space back into the phase space (Giunti & Mazzola, 2012; Mazzola & Giunti, 2012). More precisely, Φ^t equals an operation of T on $\mathcal{M}$, while Φ^0 indicates the identity function and $\Phi^{s+t} = \Phi^s + \Phi^t$, thus representing a semi-group operation, which does neither require $t < 0$, nor Φ^t to be invertible (Giunti & Mazzola, 2012; Mazzola & Giunti, 2012). For a given initial condition x, the identity $\Phi^t(x) = \Phi_x(t) \equiv \Phi(t, x)$ can be derived (Giunti & Mazzola, 2012; Mazzola & Giunti, 2012).

[15] Topological space, which locally resembles Euclidean space near each point
[16] Mostly, these functions are assumed to be deterministic, but they also can reflect a stochastic system.
[17] Qualitative change in a system's dynamics due to varying parameters
[18] Ergodic theory describes the statistical properties of deterministic dynamical systems (e.g., via long-time behaviour of time averages of various functions alongside of the respective dynamical systems trajectories).

Therefore, the following formal (geometrical) definition[19] of a dynamical system can be stated as follows (Giunti & Mazzola, 2012; Mazzola & Giunti, 2012):

"A dynamical system is the tuple $\langle \mathcal{M}, \Phi^t, T \rangle$, with $\mathcal{M}$ being a manifold (locally resembling a Banach or Euclidean space), T as time domain and Φ^t as evolutionary function $t \to \Phi^t (t \in T)$ in a manner of Φ^t to be a diffeomorphism of $\mathcal{M}$ to itself."

Hence, Φ^t is regarded as a respective mapping of T into the space of diffeomorphisms (see 3.1.3) of $\mathcal{M}$ to itself, whilst Φ^t represents a diffeomorphism for every $t \in T$ (Giunti & Mazzola, 2012; Mazzola & Giunti, 2012). Furthermore, we deem it relevant to state the difference between the categorisation of a dynamical system, whether it be conservative or dissipative in nature. Conservative dynamical systems are non-singular and yield no wandering sets, which means such systems do not propose frictions or dissipative mechanisms (Danilenko & Silva, 2009). Hence, following the Liouville's theorem, results in the system´s respective phase space not to shrink over time (Danilenko & Silva, 2009). In straight contrast, a dissipative structure is characterised via anisotropy, namely, spontaneous occurrences of symmetry breaks, resulting in respective long-term correlation as well as possible chaotic structures in the dynamical system (Brogliato et al., 2007).

Table 7: Several important mathematical theorems with a short description and reference

Theorem	Short Description	Reference
Poincaré recurrence	Some systems after sufficiently long, but finite time, return to a state arbitrarily close to (continuous), or exact the same (discrete) initial states.	Poincaré (1890)
Poincaré Bendixson	Statements about long time behaviour of orbits of continuous systems on the plane, cylinder or two-sphere.	Coddington & Levinson (1955)
Ergodic/ Birkhoff's	Time averages and space averages may differ, hence, if the transformations are ergodic with an invariant measure, the time average is equal to the space average in the majority of the space.	Eckmann & Ruelle (1985)
Liouville´s	Assertion of constancy of phase space distribution, meaning, no shrinkage.	Brogliato et al. (2007)
Krylov Bogolyubov	Guarantee of the existence of invariant measures for well-behaved spaces.	Bogoliubov & Krylov (1937)
Oseledets	Multiplicative ergodic theorem provides theoretical background for computation of Lyapunov exponents in nonlinear dynamical systems.	Oseledets (1968)
Sharkovskii´s	If a discrete dynamical system on the real line has a periodic orbit of period three, then periodic orbit points of every other period must exist.	Sharkovskii (1964)
Stable Manifold	Existence of local diffeomorphism near a fixed point implies existence of a local stable centre manifold containing the said fixed point.	Hasselblatt & Katok (2003)
Takens	Delay embedding gives the conditions under which a chaotic dynamical system can be reconstructed from a sequence of observations of the state.	Takens (1981)

[19] It is also possible to deduct a measure-theoretical definition in terms of the ergodic theory, which is not regarded in this study.

3.1.2. Orbits

Orbits of a dynamical system are collections of points related by Φ^t, hence, they are subsets of the phase space concealed by the trajectories of the dynamical system, obliging a given set of initial conditions during the timely evolution of the latter system (Hasselblatt & Katok, 2003). Since each trajectory represents a unique combination of coordinates in phase space, intersections of orbits are not possible (Hasselblatt & Katok, 2003). Thus, orbits can formally be defined as follows (Hasselblatt & Katok, 2003):

"Given a dynamical system $\langle \mathcal{M}, \Phi^t, T \rangle$ with $\mathcal{M}$ being a manifold (locally resembling a Banach or Euclidean space), T as time domain and Φ^t as evolutionary function and U being a neighbourhood, one can state:

$\Phi: U \to \mathcal{M}$ *where,* $U \subset T \times \mathcal{M}$ *with* $\Phi(0, x) = x \Rightarrow \mathrm{I}(x) \equiv \{t \in T: (x, x) \in U\}$*, therefore,*

$\gamma_x \equiv \{\Phi(t, x): t \in \mathrm{I}(x)\} \subset \mathcal{M}$ *is called orbit through* x*.*

The non-constant orbit is called closed or periodic, if $t \neq 0$ *in* $I(x)$*, such that* $\Phi(t, x) = x$*."*

3.1.3. Diffeomorphisms

A diffeomorphism is an isomorphism[20] of smooth (differentiable) manifolds, which can be understood as an invertible function, mapping one differentiable manifold to another in such a manner, that the respective function as well as its according inverse are smooth and be defined as (Hirsch, 1997):

"Given two manifolds $\mathcal{M}$ and $\mathcal{N}$, a differentiable map $\Phi_f: \mathcal{M} \to \mathcal{N}$ is called a diffeomorphism, if it is a bijection and its inverse $\Phi_f^{-1}: \mathcal{N} \to \mathcal{M}$ is differentiable. If these functions are r times continuously differentiable, Φ_f is called a $\mathcal{C}^r$- diffeomorphism."

Two manifolds $\mathcal{M}$ and $\mathcal{N}$ are diffeomorphic ($\mathcal{M} \cong \mathcal{N}$), if $\Phi_f: \mathcal{M} \to \mathcal{N}$ exists (Hirsch, 1997). Additionally, following Hirsch (1997), regarding m as a subset of $\mathcal{M}$ and n as a subset of $\mathcal{N}$, a function $\Phi_f: m \to n$ is said to be smooth if for all points in m, a neighbourhood $U \subseteq \mathcal{M}$ of points exists, and a smooth function $g: U \to \mathcal{N}$ subject to $g_{|U \cap m} = \Phi_{f\,|U \cap m}$, with g as an extension of Φ_f. Therefore, Φ_f is assumed a diffeomorphism if it is bijective, smooth and its inverse is also smooth[21] (Hirsch, 1997).

3.1.4. Attractors

A set of numerical values for a general assortment of initial conditions, towards which a system tends to evolve is called the attractor of the system (Mazzola & Giunti, 2012). Realisation of system values close enough to the attractor remain close, even if subjected to small perturbations or disturbances (Strogatz, 2014).

[20] Structure-preserving mapping between two structures of the same categorisation
[21] See the Hadamard-Caccioppoli theorem.

Assuming finite-dimensional systems, the time-evolving variable[22] can be delineated algebraically as an n −dimensional vector (Mazzola & Giunti, 2012). Thus, an attractor represents a region in n −dimensional space and can depict a point, a finite set of points, a curve, a limit torus, a manifold, or an even more complicated ensemble exhibiting fractal structure, henceforth called strange attractor (Strogatz, 2014; Grassberger & Procaccia, 1983a).

Meticulously, the phase space volumes of dissipative dynamical systems are condensed by time evolution, meaning, the occupied volume of a respective attractor is generally small in comparison to the phase space (Fernández-Rodríguez et al., 2005). Further, during contraction, the length is not mandatorily contracted in all directions, yet can be stretched in one and contracted in another coordinate direction (Fernández-Rodríguez et al., 2005). This may lead to unstable motions in the final movements within the attractor, which may also be chaotic (Fernández-Rodríguez et al., 2005). These instabilities become evident in sensitive dependence on initial conditions, resulting in an exponential separation of orbits during the time evolution of the system, which were initially very close to each other on the respective attractor (Fernández-Rodríguez et al., 2005). Chaos theory can hereby provide a valid description of the respective attractors, since a trajectory of the dynamical system in the relevant attractor neglects specialised premises, except for the latter trajectory to remain on the attractor forward in time, as explicated before (Carvalho et al., 2013). To be more detailed, the subset of phase space corresponding towards the typical behaviour of a dissipative dynamical system is the said attractor itself (Carvalho et al., 2013).

Withal, invariant sets and limit sets as similar conceptions to attractors need to be elaborated on. An invariant set evolves to itself under the systems dynamics, which allows, but does not force, it to reside inside respective attractors (Milnor, 1985). Contrastingly, limit sets represent states of dynamical systems after infinite time passed, thus, reflecting upon the long-time behaviour of the referring system (Milnor, 1985). It is noteworthy that attractors are themselves limit sets, despite the fact that not all limit sets have to be attractors (Milnor, 1985; Carvalho et al., 2013). Elucidation of strange attractors reveals the evolution of two distinct points of the said strange attractor, to result in exponentially diverging trajectories (Kantz & Schreiber, 2003). Furthermore, strange (chaotic)[23] attractors include indefinitely many embedded saddle periodic orbits, which associate each saddle orbit with stable and unstable manifolds (Kostelich, 1997).

[22] If the variable is scalar, the attractor is a subset of the real number line.

[23] It can be displayed that in certain types of dynamical systems, it is possible to observe attractors that are strange but not chaotic, where 'strange' refers to the geometry or shape of the attracting set, while 'chaotic' refers to the dynamics of the orbits on the attractor (Grebogi et al., 1984). For a display of strange non-chaotic attractors, refer to Li et al. (2019), since we will not consider this scenario in this study.

An attractor in a mathematical sense can be evinced as follows (Grebogi et al., 1987; Milnor, 1985):

"An attractor is a subset $\mathcal{A}$ of the phase space, characterised by the following premises:

(1) $\mathcal{A}$ is forward invariant under Φ^t: if $a \in \mathcal{A}$, then $\Phi(t, a)\ \forall\ t > 0$ is also invariant.

(2) It exists a neighbourhood of $\mathcal{A}$, called basin of attraction of $\mathcal{A}$, labelled as $\mathcal{B}(\mathcal{A})$, which consists of all points p that enter $\mathcal{A}$ in the limit $t \to \infty$.

(3) $\mathcal{B}(\mathcal{A})$ is the set of all points in phase space with hereinafter mentioned properties:

a. For any open neighbourhood $\mathcal{N}$ of $\mathcal{A}$, there exists a positive constant $\mathcal{T}$, such that $\Phi(t, p) \in \mathcal{N}\ \forall\ t > \mathcal{T}$.

b. It exists no non-empty subset of $\mathcal{A}$, which satisfies (1) and (2).

c. Moreover, $\mathcal{A}$ is required to yield a positive measure to ensure a point not being itself an attractor."

Furthermore, regarding the Poincaré-Bendixon theorem, the inexistence of strange attractors for a phase space dimension smaller than three is constituted[24] (Coddington & Levinson, 1955).

3.1.5. Chaotic Dynamics

Following the founding father of chaos, Edward E. Lorenz (1968), chaos is 'when the present determines the future, but the approximate present does not approximately determine the future'. Hence, chaos reveals the apparent randomness of (chaotic) complex systems, yielding underlying patterns, interconnectedness, feedback loops, recurrence, self-similarity (fractality) and self-organisation capabilities (Fuh et al., 2012; Abarbenel et al., 1993; Sornette, 2004). Therefore, three characteristics are dominant for chaotic systems, namely, (1) sensitivity to initial conditions, (2) topological transitivity and (3) density of periodic orbits (Hasselblatt & Katok, 2003).

3.1.5.1. Sensitivity to initial conditions

The process of arbitrarily close points of a dynamical system separating exponentially as they evolve over time is denoted as being sensitive towards initial conditions and can be formally defined[25] as follows (Kato, 1993):

"Let $\mathcal{M}$ be the phase space for a map Φ_f^t, then Φ_f^t exhibits sensitive dependence to initial conditions if for any $x \in \mathcal{M}$ and $\delta > 0$, there exist any $y \in \mathcal{M}$ with distance $d(\cdot,\cdot)$ such that $0 < d(x, y) < \delta$ and such that $d\left(\Phi_f^t(x), \Phi_f^t(y)\right) > e^{\alpha t} d(x, y)$ for some positive α; requiring the existence of a positive Lyapunov exponent."

[24] To be very precise, it is sufficient to determine a dimension of $2 + \varepsilon$ (Kantz & Schreiber, 2003).
[25] Please note the following definition to be metrical in nature, not topological.

3.1.5.2. Topological transitivity

Following Hasselblatt and Katok (2003), topological transitivity is definable as follows[26]:

"A map $\Phi_f^t: \mathcal{M} \to \mathcal{M}$ is determined to be topological transitive if for any pair of open sets $U, V \subset \mathcal{M}$, there exists a $k > 0$ such that $\Phi_f^t(U) \cap V \neq \emptyset$, representing the weak-version of topological mixing[27]. This implies the decomposition impossibility of the system in two respective open sets."

3.1.5.3. Density of periodic orbits

Periodic orbits approach every point in the phase space arbitrarily close, which is reflected by the Sharkovskii´s theorem (Alligood et al., 2009).

3.2. Chaos Measures

3.2.1. Lyapunov Exponents

In Section 3.1.5.1, we stated the exponential divergence of nearby trajectories in chaotic dynamical systems. Overall, a slow divergence as in periodic systems is not deemed problematic, yet, exponentially fast separation is an indication of chaotic motion (Kantz & Schreiber, 2003). A proper measure of exponential divergence of neighbouring trajectories is the Lyapunov exponent, which calculates the average of exponential convergence or divergence of trajectories, which are near each other in phase space (Kantz & Schreiber, 2003). Lyapunov exponents offer information about the orbits moving apart (or closer together) on the attractor over the evolution of time (Fernández-Rodríguez et al., 2005). Additionally, it is possible to evaluate them as the rate of stretching or shrinkage of various sub-volumes of phase space, which is discussed extensively in the academic literature, wielding several methods of calculating Lyapunov exponents for unknown dynamical systems (Fernández-Rodríguez et al., 2005). Therefore, Lyapunov exponents display a measure of chaotic strength within a given dynamical system (Kantz & Schreiber, 2003).

Following Gençay and Dechert (1992, 1996) and Dechert and Gençay (2000), Lyapunov estimators derived from observed dynamics can be regarded as topological invariant, meaning a global averaged perspective over a possibly unstable or volatile system[28] (Kantz & Schreiber, 2003).In the academic literature, several publications apply Lyapunov exponents to discern chaotic dynamics in financial time series since a positive Lyapunov exponent is seen as an indication of chaos (e.g., Bajo-Rubio et al., 1992) (Fernández-Rodríguez et al., 2005).

[26] For further clarification, please refer to the Birkhoff transitivity theorem.
[27] A system evolves over time, so that any given region or open set of its phase space eventually overlaps with any other given region.
[28] We will neglect a discussion of local Lyapunov exponents in this study since interpretation of the same is difficult and ambiguous.

It is possible to define a variety of Lyapunov exponents (e.g., Lyapunov spectrum), whose count equals the dimensions of the phase space, yet, one of the most important ones is the maximum (or the largest) Lyapunov exponent, whose inverse is the Lyapunov time, which indicates the time until the system emerges into chaos (Kantz & Schreiber, 2003; Shevchenko, 2018).

3.2.1.1. Maximum Lyapunov Exponent and Lyapunov Time

The maximum Lyapunov exponent λ can be defined as follows (Kantz & Schreiber, 2003):

"Let $\mathcal{p}_1$ and $\mathcal{p}_2$ be two points in phase space with distance $d(\mathcal{p}_1, \mathcal{p}_2) = \|\mathcal{p}_1 - \mathcal{p}_2\| = \delta_0 \ll 1$. Denote by $\delta_{\Delta t}$, the time distance between two trajectories emerging from these points, namely, $d(\mathcal{p}_{1+\Delta t}, \mathcal{p}_{2+\Delta t}) = \|\mathcal{p}_{1+\Delta t} - \mathcal{p}_{2+\Delta t}\| = \delta_{\Delta t}$. Then λ is determined by $\delta_{\Delta t} \simeq \delta_0 e^{\lambda \Delta t}$ with $\delta_{\Delta t} \ll 1$ and $\Delta t \gg 1$."

Exponential divergence of close trajectories resulting in chaotic motion is indicated if $\lambda > 0$; it is noteworthy that the separation cannot exceed the extents of the respective attractor (Wolf et al., 1985). Further, if negative Lyapunov exponents are found in a dissipative system, it shows the existence of an according stable fixed point (Kantz & Schreiber, 2003). In the case of a limit cycle, $\lambda = 0$ and is labelled marginally stable, as displayed in Table 8 (Park & Whang, 2012).

Table 8: Value range of maximum Lyapunov exponents, analogue to Kantz and Schreiber (2003)

Value of λ	**Interpretation of resulting motion**
$\lambda < 0$	Stable fixed point
$\lambda = 0$	Stable limit cycle
$0 < \lambda < \infty$	Chaos
$\lambda = \infty$	Noise

Moreover, Lyapunov exponents are invariant while smooth and capable of delineation of long-term system behaviour (Abarbanel et al., 1991). Further, smooth invertible re-parametrisation of phase space can alter only the distance ratios by a finite factor (Kantz & Schreiber, 2003). As explicated, a positive Lyapunov exponent stands for a potent testimony of chaos, which raises the interest of many scholars and practitioners to apply the conceptions on empirical time series or other scalar data and measurement sets (Abraham et al., 2004). In order to follow an estimate of Lyapunov exponents from a time series, an algorithm introduced by Rosenstein et al. (1993) is mostly executed, since it directly tests the exponential divergence of close trajectories.

We will follow this algorithm in our empirical setting due to the determination of applicability as well as the assumption of the Lyapunov exponent to represent the local divergence rates over the complete time series, which is due to its invariance property (Rosenstein et al., 1993).

The procedure can be displayed as follows (Rosenstein et al., 1993; Kantz & Schreiber, 2003):

(1) Select a point $\mathcal{p}_0$ belonging to the time series under consideration, while additionally selecting relevant neighbouring points with a distance smaller than a threshold value ϵ.
(2) Determine the average over the neighbour distances to the reference part of the trajectory as a function of relative time.
(3) The logarithm of the average distance at time Δt represents an effective expansion rate over Δt.
(4) Repetition of (1) to (3) for different settings of $\mathcal{p}_0$ will diminish possible fluctuations of (3), due to averaging.
(5) Compute the equation: $S(\Delta t) = \frac{1}{T}\sum_{t=1}^{T} \ln\left(\frac{1}{|\mathcal{U}(\boldsymbol{p}_0)|}\sum_{\mathcal{p}_t \in \mathcal{U}(\boldsymbol{p}_0)} |\mathcal{p}_{0+\Delta t} - \mathcal{p}_{t+\Delta t}|\right)$, while $\boldsymbol{p}_0$ represent reference points, displayed as embedding vector, $\mathcal{U}(\boldsymbol{p}_0)$ is the respective neighbourhood of $\boldsymbol{p}_0$ and $\mathcal{p}_{t+\Delta t}$ exists outside the time span covered by $\boldsymbol{p}_0$. This is due to unknown values of the embedding dimension as well as the optimal distance ϵ.

To sum up, Rosenstein et al. (1993) assume the initial divergence to increase at the exponential rate dictated by the maximum Lyapunov exponent of the reconstructed state space of a time series (see Zeng et al., 1991), which is categorised as a direct method (Fernández-Rodríguez et al., 2005). Direct methods immediately agitate the time series data in an attempt to calculate the maximum Lyapunov estimates and are not determined ex ante, in order to distinguish dynamical effect natures (e.g., stochasticity versus chaoticity) (Damming & Mitschke, 1993). Hence, direct methods build upon the thought of chaos being capable of displaying a connection between determinism and randomness (Whang & Linton, 1999). The stated direct approach results in drawbacks in terms of financial time series analysis, since mostly nonlinear stochastic processes (e.g., GARCH) are applied instead of chaotic models (Fernández-Rodríguez et al., 2005). Contrastingly, indirect or Jacobian methods apply the data in estimates of Jacobian matrices in order to determine the conditional expectation values of the respective processes (Fernández-Rodríguez et al., 2005).

As has already been mentioned, the Lyapunov exponents[29] carry inverse time units called Lyapunov times and provide conventional time scales for the divergence or convergence of nearby trajectories, interpretable as time passing until the system diverges into chaos and is no longer predictable (Shevchenko, 2018).

[29] Following Whang and Linton (1999) and Tong (1990), Lyapunov exponents are interpretable within standard nonlinear time series analysis as measure of local stability, independent of the chaotic framework.

3.2.1.2. Lyapunov Spectrum

As stated before, the presence of close vectors in a phase space results in the diversion of two respective trajectories at exponential rate, whose time evolution is observable as linearised dynamics in a tangent space[30] and can be described as follows (Kantz & Schreiber, 2003; Sano & Sawada, 1985; Darbyshire & Broomhead, 1996):

"Assume $\boldsymbol{\vartheta}_t$ *and* $\boldsymbol{\gamma}_t$ *to be two infinitesimally close trajectories in a* $m-$*dimensional phase space and the dynamical system under consideration to reflect a map, while the time evolution of their distance is described by* $\boldsymbol{\gamma}_{t+1} - \boldsymbol{\vartheta}_{t+1} = \boldsymbol{\mathcal{F}}(\boldsymbol{\gamma}_t) - \boldsymbol{\mathcal{F}}(\boldsymbol{\vartheta}_t) = \boldsymbol{J}_t(\boldsymbol{\gamma}_t - \boldsymbol{\vartheta}_t) + O(\|\boldsymbol{\gamma}_t - \boldsymbol{\vartheta}_t\|^2)$*, where* $\boldsymbol{\mathcal{F}}(\boldsymbol{\vartheta}_t)$ *expands around* $\boldsymbol{\gamma}_t$ *and* $\boldsymbol{J}_t = \boldsymbol{J}(\boldsymbol{\vartheta}_t)$ *is the* $m \times m$ *Jacobian matrix of* $\boldsymbol{\mathcal{F}}$ *at* $\boldsymbol{\vartheta}_t$*. Further, assuming a marginal perturbation* $\delta_t = \boldsymbol{\gamma}_t - \boldsymbol{\vartheta}_t$*, the modulus one time step later is determinable. Let* $\boldsymbol{e}_i$ *be an eigenvector of* $\boldsymbol{J}$ *and assume* Λ_i *its eigenvalue.*

Decomposition of δ_t *into the before mentioned vectors with respective coefficient* β_i*, results in* $\delta_{t+1} = \sum \beta_i \Lambda_i \boldsymbol{e}_i$*. In the case of* δ_t *being parallel to one realisation of* $\boldsymbol{e}_i$*, it is either stretched or compressed by the factor* Λ_i*."*

Moreover, it is possible to deduct m unique local stretching factors and a respective decomposition of phase space into m linear subspaces. Proper averages over these different local stretching factors are insinuated via the Lyapunov exponents for each of the respective subspaces, which can be stated as follows (Kantz & Schreiber, 2003):

"The Lyapunov exponents are determined by $\lambda_i = \lim_{T\to\infty} \frac{1}{2T} \ln\left|\Lambda_i^{(T)}\right|$*, where* Λ_i *is defined as* $\Lambda_i^{(T)} \beta_i^{(T)}$*."*[31]

In order to determine whether a dynamical system is conservative or dissipative (possibly chaotic), the sum of the Lyapunov exponents has to be negative ($\sum \lambda_i < 0$) (Park et al., 2012).

3.2.2. Correlation Dimension

Strange attractors, as stated in Section 3.1.4, are specified by a fractal structure, which, after further thought, indicates the self-similarity of the strange attractor as a geometrical object (Brandstater & Swinney, 1987; Grassberger & Procaccia, 1983). Additionally, we dissected the insight of a dissipative chaotic system to deflate to the sub-volumes of its respective attractors (Fraser & Swinney, 1986). Therefore, it is a valid inclusion to state that one may apply fractal dimensionality measures to determine the dimension of a respective strange attractor, representing a dissipative chaotic nonlinear dynamical system properly (Cecen & Erkal, 1996; Altan et al., 2019).

[30] Following Lee (2009), it is possible to attach to every point of a smooth manifold a respective tangent space (a real vector space), which contains the possible directions in which one can tangentially pass through the respective point.
[31] This is a result from conducting the Oseledets theorem.

Indubitably, the application of a classical box-counting or Hausdorff-dimensional measure is a valid approach towards the delineation of the fractal dimension of a respective set; yet, in the academic literature, another widely dispensed measure has been established, namely, the correlation dimension, which is mostly determined to estimate the chaotic behaviour within simple time series datasets (Cecen & Erkal, 1996; Kostelich, 1997).

Following Grassberger and Procaccia (1983), the correlation dimension can be determined by applying a correlation sum scheme, which is defined as follows (Cecen & Erkal, 1996):

"Let $\boldsymbol{p}_n$ *be a collection of points in a given vector space as well as a fraction of possible pairs of points, which are closer than a given threshold distance* ε*, represented as a particular norm, depicted as:*

$C(\varepsilon) = \frac{2}{N(N-1)} \sum_{i=1}^{N} \sum_{J=i+1}^{N} \Theta\left(\varepsilon - \left\|\boldsymbol{p}_i - \boldsymbol{p}_j\right\|\right)$*, where* Θ *is the Heaviside step function,* $\Theta(\boldsymbol{p}) = 0$ *if* $\boldsymbol{p} \leq 0$ *and* $\Theta(\boldsymbol{p}) = 1$ *for* $\boldsymbol{p} > 0$*."*

The correlation sum merely numbers the point pairs $\left(\boldsymbol{p}_i, \boldsymbol{p}_j\right)$ with a distance smaller than the threshold ε (Kantz & Schreiber, 2003). Hence, the correlation dimension is definable as follows (Kantz & Schreiber, 2003):

"Assume the limit of an infinite set of data points $(N \to \infty)$*, while for marginal* ε*, the correlation sum* C *is expected to scale according to a respective power law, namely,* $C(\varepsilon) \propto \varepsilon^D$*, thus the correlation dimension* D *can be derived by* $d(N, \varepsilon) = \frac{\delta \ln C(N,\varepsilon)}{\delta \ln \varepsilon}$*, henceforth, stating* $D = \lim_{\varepsilon \to 0} \lim_{N \to \infty} d(N, \varepsilon)$*. It is noteworthy, that* D *is invariant, whilst* $C(\varepsilon)$ *is not."*

Following Ramsey et al. (1990), correlation dimension estimates with limited datasets reveal misleading results, notably returning artificially smaller correlation dimension estimates. Further, it is assumed that the correlation dimension for a white-noise process is infinite (Altan et al., 2019). The application of the correlation dimension is exemplified in Panas and Ninni (2000), Adrangi et al. (2001) as well as in Moshiri and Foroutan (2006), who analysed respective commodity future series.

3.2.3. Space–Time Separation

While conducting nonlinear time series analysis, the existence of non-zero autocorrelations is problematic in terms of reconstruction endeavours (e.g., estimation of correlation dimension), since trajectory vectors are closely located in the referring phase space, due to continuously evolving time known as temporal correlations (Kantz & Schreiber, 2003). In terms of determining the 'scaling region' of the correlation sums, several authors within the academic literature satisfied the analysis by fitting a straight line segment to the respective graphic representations, thus failed to notion details about the shapes of the region curves (Kantz & Schreiber, 2003).

Since the correlation sum is lacking invariance, it falls prey to effects caused by the above-mentioned temporal correlations, causing dynamical correlated time series data to violate the estimation requirements (Kantz & Schreiber, 2003). If those temporal correlations are significant in magnitude, a proper analysis is rendered invalid (Kantz & Schreiber, 2003).

Henceforth, following Provenzale et al. (1992), the detection of temporal correlations by applying estimates of correlation time t_{min} results in the display of a time separation plot. It is assumed that pairs of points in the phase space do not solely depend on ε, but on elapsed time between measurements (Provenzale et al., 1992). To render these dependencies visible, the plot displays time separation Δt versus spatial distance ε (Provenzale et al., 1992). The contour curves of the plot have to saturate, since in contrast, $1/f$ −Brownian-noise with low frequency power does not, resulting in all points in the dataset to be temporally correlated, denying a valid reconstruction of the systems attractor (Kantz & Schreiber, 2003).

3.2.4. Sample Entropy

Another measure, attributing to the determination of the self-similarity property, which is also stated for strange attractors, is the sample entropy (Richman & Moorman, 2000). The sample entropy is defined as the negative logarithm of conditional probability of two respective trajectories (sets of points) to remain similar at the next embedding point, excluding self-matches, henceforth resulting in a lower entropy value to be indicated with higher self-similarity (Richman & Moorman, 2000; Costa et al., 2005):

"Let m be an embedding dimension, r a tolerance parameter and $N = \{\mathcal{p}_1, \mathcal{p}_2, \dots, \mathcal{p}_N\}$ the amount of data points. Thus, define a template vector of length m, such that $\mathcal{P}_m(i) = \{\mathcal{p}_i, \mathcal{p}_{i+1}, \mathcal{p}_{i+2}, \dots, \mathcal{p}_{i+m-1}\}$ and $d\big(\mathcal{P}_m(i), \mathcal{P}_m(j)\big)$ with $i \neq j$ to be the Chebyshev-distance. Therefore, the sample entropy is displayed as $SampEn = -\log A/B$, with A equal to the number of template vector pairs with $d\big(\mathcal{P}_{m+1}(i), \mathcal{P}_{m+1}(j)\big) < r$ and B equal to the number of template vector pairs with $d\big(\mathcal{P}_m(i), \mathcal{P}_m(j)\big) < r$."

The sample entropy is bounded between zero and a positive value (Richman & Moorman, 2000).

3.2.5. Hurst Exponent

Dependencies within time series can also be elucidated using the Hurst exponent H, which in fractal geometry reveals long-range dependence and the existence of trends by measuring the characteristic of a data set (Hurst, 1951; Berghorn, 2015). Furthermore, the properties of the time series can be classified with $0 \leq H < 0.5$ to be mean reverting, with $H = 0.5$ to be purely random in nature and with $0.5 < H \leq 1$ to display a power law and respective persistency, resulting in fractal structures within the data (Opong et al., 1999; Berghorn, 2015).

The fractal dimension can be determined by $D = 2 - H$ (Mandelbrot, 2004). The Hurst exponent is defined as (Mandelbrot, 2004; Qian & Rasheed, 2004):

"The asymptotic patterns of the rescaled range statistic as a function of time span of a time series results in H to be displayed as: $\mathbb{E}(R(n)/S(n)) = Cn^H$ while $n \to \infty$, with $R(n)$ to be the range of the first n cumulative deviations from the mean, $S(n)$ the series (sum) of the first n standard deviations, $\mathbb{E}(\cdot)$ the expected value, n the time span of the observations and C a constant."

3.2.6. DFA

Similar to the Hurst exponent, the detrended fluctuation analysis (DFA) analyses a time series with respect to its self-affine properties, especially recommendable if the time series yields non-stationarities (Peng et al., 1994). It is related to spectral techniques (e.g., Fourier transform) and is defined as (Peng et al., 1994; Hardstone et al., 2012):

"Let x_t be a time series with length N, where $t \in \mathbb{N}$ and integrate it into an unbounded process X_t of form $X_t = \sum_{i=1}^{t}(x_i - \langle x \rangle)$, with $\langle x \rangle$ denoting the mean value. Further, X_t is divided into time windows of length n, before a local least-squares straight-line fit (local trend) is calculated by minimisation. Now let Y_t be the calculated piecewise series of straight-line fits, which results in the fluctuation $F(n) = \sqrt{1/N \sum_{t=1}^{N}(X_t - Y_t)^2}$."

To apply this procedure, the window sizes are altered and drafted by a log-log visualisation of $F(n)$ versus n (Peng et al., 1994). A straight line on this graph indicates statistical self-affinity by $F(n) \propto n^{\alpha}$, with α depicting the scaling exponent (Peng et al., 1994; Hardstone et al., 2012). The interpretation of the scaling coefficient is shown in Table 9 (Peng et al., 1994; Hardstone et al., 2012).

Table 9: Interpretation of Scaling Coefficient of the DFA

Value of Scaling Coefficient	Interpretation	Value of Scaling Coefficient	Interpretation
$\alpha < 0.5$	Anti-correlation	$\alpha \simeq 1$	$1/f$ −Noise
$\alpha \simeq 0.5$	White noise	$\alpha > 1$	Non-stationarity
$\alpha > 0.5$	Correlation	$\alpha \simeq 3/2$	Brownian Noise

3.3. Chaos Tests

3.3.1. Standard Statistics

In order to dissect the financial time series properly, we need to ensure that the previously mentioned characteristics, namely, the existence of stationarity, nonlinearity as well as freedom of noise, are guaranteed for our empirical analysis. Therefore, we will apply standardised statistical tests to validate the mentioned properties.

To test whether the financial time series is stationary, we will conduct two statistical tests, namely, the ADF (Augmented Dickey-Fuller) test with the Null hypothesis, that the variable yields a unit root and is non-stationary (e.g., MacKinnon, 1994) and the KPSS (Kwiatkowski–Phillips–Schmidt–Shin)-test, where Null hypothesis states the opposite, i.e., that the variable is stationary (e.g., Kwiatkowski et al., 1992). Furthermore, we intend to determine the distributional characteristics of the financial time series by executing the Kolmogorov–Smirnov (KS) test for a Gaussian distribution, which Null hypothesis states Gaussianity, respectively (e.g., Massey Jr., 2012).

3.3.2. BDS Test

In order to determine chaotic motion in financial markets, scholars executed the BDS test (e.g., Opong et al., 1999), however, have recognised the omnipotence of detection of nonlinearity, yet, inability to differentiate between stochastic and chaotic dynamics (BenSaïda & Litimi, 2013). The study by Yousefpoor et al. (2008) explicates inconclusive results[32] in terms of the BDS test, even if other methods should, in theory, be able to distinguish between stochasticity versus chaoticity (e.g., generalised BDS statistics of Matilla-García and Marín (2010), based on the Grassberger-Procaccia 1983s correlation integral). Nevertheless, the BDS test developed by Brock et al. (1987) and generalised by Savit and Green (1991) as well as Wu et al. (1993) is aimed exactly at the previously mentioned distinction, still, state a powerful tool for the detection of nonlinearities within a (financial) time series (Cecen & Erkal, 1996). Therefore, we will apply the BDS test only for the general detection of nonlinearities within our datasets and relinquish it in terms of differentiation of chaos versus randomness. The BDS-test is defined as follows (Cecen & Erkal, 1996):

"The BDS-statistic is based on the correlation integral (see 3.2.2) $C(\varepsilon)$, a time series $\{X_t\}$ with $t \in \{1,2,\dots,T\}$ and represents a random sample of ~iid observations with $C_n(\varepsilon) = C_1(\varepsilon)^n$. By estimation of $C_1(\varepsilon)$ and $C_n(\varepsilon)$ by sample values $C_{1,T}(\varepsilon)$ and $C_{n,T}(\varepsilon)$, the BDS-statistic can be written as $B_{n,T}(\varepsilon) = \sqrt{T}\frac{C_{n,T}(\varepsilon)-C_{1,T}(\varepsilon)}{\sigma_{n,T}(\varepsilon)}$, where $\sigma_{n,T}(\varepsilon)$ denotes the estimate of the asymptotic standard error of the numerator. The H_0 assumes the ~iid property."

Brock et al. (1987) contributed to the literature by proving that $B_{n,T}(\varepsilon) \sim N(0,1)$.

[32] For a mathematical discussion on the robustness of nonlinearity and chaos tests in terms of measurement errors, inference methods and sample size, please refer to Barnett et al. (1995).

3.3.3. Bask–Gençay Test with Bootstrapping Method

So far, we have deduced that the BDS test is not capable of determining the nature of the 'tested-for' nonlinearity, while the introduced Lyapunov exponent (see 3.2.1.1) can return positive (chaoticity-inducing) values for non-chaotic systems but yields inconclusiveness as well (Fernández-Rodríguez et al., 2005). Scholars commented on the insufficiency of the Lyapunov exponent due to the lack of a distributional theory by providing respective hypothesis testing using Lyapunov exponents[33] (Fernández-Rodríguez et al., 2005). Therefore, following Gençay (1996), a methodology to compute empirical distributions of Lyapunov exponents via blockwise bootstrap technique represents a formal test[34] of the hypothesis that the Lyapunov exponent reflects upon chaotic dynamics (Ziehmann et al., 1999). In particular, the test proposed by Gençay (1996) is applicable to Lyapunov exponents, which are slightly above zero within a small sample (Bask & Gençay, 1998).

Since we are dealing with such a dataset, we will apply this framework for our empirical analysis. The bootstrapping and test method is defined as follows (Ziehmann et al., 1999; Gençay, 1996):

"Assume a sequence of weakly dependent, stationary stochastic variables $\{X_1, X_2, \dots, X_T\}$*, and let* $\{x_1, x_2, \dots, x_T\}$ *be a realisation of this process. In order to construct the distribution of the maximum Lyapunov exponent, a moving blockwise bootstrapping method is applied. Therefore, let* $\mathfrak{B}_t^d = \{x_t, x_{t+1}, \dots, x_{t+d-1}\}$ *be a moving block of* d *consecutive observations, where* $t \leq T - d + 1$*. For a series, consisting of* T *elements, a set of blocks* $\{\mathfrak{B}_1^d, \mathfrak{B}_2^d, \dots, \mathfrak{B}_{T-d+1}^d\}$ *with length* d *is determined. For a replacement of* $k = int(T/d)$*, a bootstrap sample* $\{\mathfrak{B}_{i_1}^d, \mathfrak{B}_{i_2}^d, \dots, \mathfrak{B}_{i_k}^d\}$ *is created. For each subfamily of* k *blocks, the maximum Lyapunov exponent can be determined as stated in Section 3.2.1.1, resulting in an empirical distribution.*

In order to test for chaos, state a one-sided alternative hypothesis, such that the 97.5% confidence interval $q_{97.5\%}$ *is constructed by calculating the critical value* $\hat{\lambda}_1 - q_{97.5\%}$*, resulting from* $\mathbb{E}_q\left(P\left[\left(\hat{\lambda}_1 - \lambda_1\right) \leq q_{97.5\%}\right]\right) = 0.975$*, where* $\hat{\lambda}_1$ *is an estimate of the maximum Lyapunov exponent and* $q_{97.5\%}$ *is the quantile for the empirical distribution determined by* $\hat{\lambda}_1 - \lambda_1$*. Therefore, the Null hypothesis represents non-chaotic dynamics by* $\lambda = 0$*. If the term* $\hat{\lambda}_1 - q_{97.5\%} > 0$*, the Null hypothesis is rejected, leading to chaotic dynamics."*

[33] For a mathematical discussion, please refer to Shintani and Linton (2004).

[34] Another method is based on the Nadaraya–Watson kernel estimator of the Lyapunov exponent, following Park and Whang (2012).

3.3.4. Influence of Noise and Wavelet Filter

Before we can elaborate on the time series, it is a necessity to display the influence of noise on the intended methods with which we aim to analyse the data. Further, we want to show the methodology, namely wavelets, and its importance, with which we intend to denoise our datasets before beginning formal analysis attempts.

3.3.4.1. Influence of Noise

In terms of investigation of dynamical systems, datasets originate mostly out of physics or meteorological sciences and are purer and cleaner in nature (BenSaïda, 2014). In financial sciences (e.g., stock markets, which are complex, noisy dynamical systems with non-stationary, partly chaotic[35] data series), data is subject to measurement errors and microstructure noise (BenSaïda, 2014; Bao & Yang, 2008).

Further, following Aguirre and Billings (1995), the strong impact of noise on the identification process of chaotic dynamics is verified. In particular, if the noise level is beyond a predefined threshold value, the accurate estimation of dynamically valid models (e.g., polynomial models) renders itself almost impossible (Aguirre & Billings, 1995). This leads to the preclusion of identifications even with excellent models, which results in substantial noise reduction as best solution proposition (Aguirre & Billings, 1995).

The noise contaminating evolutionary dynamics is labelled dynamical noise, which can either be additive or multiplicative in nature, thus disrupting dynamics on different, relatively small scales (Altan et al., 2019; Çoban & Büyüklü, 2009). Chaos tests presented in existing literature require noise-free datasets, since noise (e.g., measurement errors) will cause respective test rejections (BenSaïda & Litimi, 2013). Further, noise influences the correlation dimension measure of chaotic attractors in dynamical systems, which, following the Grassberg-Procaccia algorithm, results in an increase of dimensional estimates[36] as well as of the respective systems' Lyapunov exponents (Altan et al., 2019; Argyris & Andreadis, 1998). Moreover, dynamical noise is capable of altering the dynamics of low-dimensional chaotic systems, resulting in high sensitivity towards noise intensity if chaos tests are applied (Serletis et al., 2007).

Therefore, within academic literature, a detailed empirical investigation aimed towards understanding how the addition of white and coloured noise to chaotic time series modifies the topology and structure of underlying attractors emerged (Jacob et al., 2016). Further, it is possible to identify noise levels by applying measures taken out of recurrence plot analysis[37] to the latter time series since recurrence networks measure noise with surrogate data tests (Jacob et al., 2018).

[35] See Peters (1994).
[36] See Badii & Politi (1985) and Badii et al., (1988).
[37] The noise influence can entail choosing larger thresholds in the recurrence analysis since it can distort existing structures (e.g., Mindlin & Gilmore, 1992; Koebbe & Mayer-Kress, 1992; Zbilut & Webber Jr., 1992) (Marwan, Romano, Thiel, & Kurths, 2007).

3.3.4.2. Wavelet Filter

In such noise-induced scenarios, it is advised to reduce the noise to a level that is acceptable, which can be achieved via projective filtering methodologies to remove noise contaminants (Aguirre & Billings, 1995; Çoban & Büyüklü, 2009). Noise reduction suggestions imply the implementation of non-linear filtering schemes, enabling the generation of noise-reduced datasets, which sophisticated models can then be applied to (Aguirre & Billings, 1995). The structure of filters is of secondary nature, as long as the following guidelines for the selection of filter algorithms are adhered to: (1) the filters are mandatorily unbiased and (2) the residual variance of the filters levels the noise variance accordingly[38] (Aguirre & Billings, 1995). Investigations of the dependence structure and predictability for economic systems on different time scales revealed the favourability of the wavelet multiresolution analysis[39] in the recent past (Bekiros & Marcellino, 2013; Mitra, 2006). Wavelet characteristics are appealing for the analysis of non-stationary, transient or singular signals and are suitable for denoising efforts as stated in the work by Gençay et al. (2001) (Mitra, 2006; Song et al., 2016). In contrast to the Fourier transformations' trigonometric functions, wavelets are defined over a finite domain and are localised both in time and in scale (frequency) domain[40] (Berghorn, 2015).

Analysing time scales encompasses estimates of linear, nonlinear and spectral dependencies of wavelet components combined with respective out-of-sample predictability (Bekiros & Marcellino, 2013). In terms of definition of the analytical expression, the Haar wavelet is the simplest representation of a wavelet function[41], which, therefore, represents an effective method for approximating solutions of ordinary and partial differential equations. These equations are applied to econometric relationships between money, output and price for the Indian economy by Mitra (2006) (Arbabi et al., 2017). Following Garcin and Guégan (2016), filtering wavelet coefficients enables the construction of valid estimates from noisy data, especially if the noise influence is linear as stated in Donoho and Johnstone (1995), resulting in an optimal filter design by wavelet shrinkage.

3.3.5. Surrogate Datasets

Financial systems can be reflected upon as a possible extension of nonlinear-deterministic dynamics, whose states are deterministic but return random-like computations (Çoban & Büyüklü, 2009). At times, difficulties emerge when assessing the algorithmic results in actually measuring fractal or dynamic properties of the underlying system or whether simple artificial, finite spectral properties occur in a predefined time series[42] (Kostelich, 1997).

[38] We can confirm both for our sampled datasets.
[39] For an in-depth elaboration on nonlinear evolution operators in context with wavelets, refer to Chuong (2005), while a basic guide to wavelets for economists can be found in Crowley (2007).
[40] For a mathematical discussion of wavelets, refer to Stark (2005).
[41] For new algorithms, applying Haar wavelets for the numerical solution of nonlinear systems (e.g., Fredholm and Volterro integral equations), see Aziz & Siraj-ul-Islam (2013), for the solution of a class of (partial) delay differential equations, see Aziz & Amin (2016) and for three-dimensional elliptic partial differential equations, see Aziz et al. (2017).
[42] The question is discussed in Theiler et al. (1992).

To propose a valid solution, it is advised to test for the time series to follow a linear model, which will then be tested against a predefined nonlinear observable (Kantz & Schreiber, 2003). Nevertheless, in practical cases (e.g., financial market time series), no theory for the observables distribution for linear stochastic processes is given (Kantz & Schreiber, 2003). This distribution is estimated via the method of surrogate data, stating several hypotheses to be tested upon (Kantz & Schreiber, 2003). The basic idea entails creating random datasets that preserve parts of the original properties (Kostelich, 1997; Suzuki et al., 2007). This can be achieved via random shuffles in the original time series, causing the new data sets to yield the same distribution of values as the original set, but in a different order (Kostelich, 1997).

In an ideal scenario, a clear distinction between the dimension estimates for embeddings of the randomised datasets and those of the original time series should be visible (Kostelich, 1997). Therefore, a Null hypothesis of interest considers the data originating from a stationary linear stochastic process with Gaussian inputs along with the free parameters of the mean, variance and autocorrelation functions, or equivalently, the power spectrum (Kantz & Schreiber, 2003). This can be achieved by applying different phases of the data sets' and surrogate data sets' respective Fourier transformations, holding the amplitudes constant (Kantz & Schreiber, 2003).

Fourier transformation surrogate coefficients are, therefore, characterised by the same magnitudes, but random phases, corresponding to the original series power spectrum, but without the property of determinism (Suzuki et al., 2007). We will apply these kinds of surrogates in our sample and label them as Fourier transform surrogate datasets (ft).

Nevertheless, ft is only applicable if the data follows a Gaussian distribution, but to display the output of a stationary Gaussian linear process distorted by monotonic, instantaneous, time-independent measurements functions properly, requires some adjustments (Kantz & Schreiber, 2003). Inverting and rescaling these measurement functions result in amplitude adjusted Fourier transform surrogate datasets (aaft), which can result in false rejections if strong correlations are paired with nonlinear distortion (Kantz & Schreiber, 2003). This can be solved by applying an iterative filtering scheme[43], resulting in iterative amplitude adjusted Fourier transform surrogate data sets (iaaft) (Kantz & Schreiber, 2003). Further, we will conduct our analysis with ft, aaft and iaaft surrogates.

[43] A simple implementation similar to a Wiener filter combined with another rescaling operation should suffice.

3.4. Phase Space Reconstruction

In order to apply all of the aforementioned methods in reality, it is necessary we mention that the idea of providing experimentalists with theoretical settings has already been discussed by Kosterlich (1997). In practical applications, the major challenge is the conduction of analysis on finite time series, instead of ideally theoretical noise-free infinities, which resulted in the methodology of embeddings or phase space reconstruction (Garland et al., 2016). Embedding refers to the mathematical process by which a representation of a systems attractor can be reconstructed from time series (set of scalar measurements) since its dimensional preserving (Kostelich, 1997). Common procedure is to apply time-delay reconstructions with a variety of embedding dimensions (Cao L. , 1997). In this sense, the delay time τ is defined as the time span between two respective neighbouring sample points used for the attractor reconstruction, while the embedding dimension m[44] represents the dimension of the phase space used for the reconstruction (Rüdisüli et al., 2013).

Reconstructing the trajectories of a time series in a phase space with embedding dimension m results in several issues regarding other measures, like the Lyapunov exponent, as it cannot be assumed to be invariant in terms of initial condition dependency and sample size (Fernández-Rodríguez et al., 2005). Further, relevant questions about the correct specification of the time delay τ are discussed within the literature. Following Broomhead and King (1986), the delay time can be based on the autocorrelation function, which we too will follow for our respective empirical analysis[45].

In addition, Casdagli (1991) discusses measures of distortion and noise, while Fraser and Swinney (1986) determine the time delay based on mutual information. Other potential drawbacks include the insufficient count of observations in the sample, which will increase in difficulty the higher the dimension of the reconstructed phase space, and noise has the capabilities to obscure fractal structures or render the analysis invalid, as already discussed in section 3.3.4.1 (Brandstater & Swinney, 1987). If the data is not filtered beforehand[46], one can follow Albano et al. (1988), stating the possibility of filtered embeddings to reduce noise and obtain valid dimensional estimates. Further, we will discuss two applied embedding methods, namely, Takens' time delay embedding and spectral embedding with Laplacian Eigenmaps (Takens, 1981; Song et al., 2016).

[44] We already implicitly mentioned the embedding dimension before without explicating it.

[45] The approach via autocorrelation has to be treated with care since infinite input response filters can introduce distortions, leading to deviations within the dimensional estimates, debated by Badii and Politi (1985). We decided upon wavelet-filters, since, for e.g., the application of nonlinear median-filters introduced further distortions, leading to enhanced autocorrelations, while rendering reconstructions invalid in terms of correlation dimensional estimates, even if the noise was reduced successfully.

[46] Contrary to our case

3.4.1. Takens' Time Delay Embedding Theorem

The reconstruction theorem given by Takens explicates the existence of a transformation between the original and reconstructed phase spaces with vector functions (Çoban & Büyüklü, 2009). Further, this implicates property preservation under reconstruction, meaning that the characteristics of the dynamical systems do not alter under the application of smooth coordinate changes (i.e., diffeomorphisms [see 3.1.3]), yet the preservation of original geometrical structures of phase space is not implicated either (Strogatz, 2014; Harikrishnan et al., 2017; Hirsch, 1997). Takens theorem states the following (Takens, 1981; Adachi, 1993):

"Assume the phase space of a given dynamical system to represent a $v-$*dimensional manifold* $\mathcal{M}$ *with smooth map* $\Phi_t: \mathcal{M} \to \mathcal{M}$*. Further, let the dynamics* Φ_t *yield a strange attractor* $\mathcal{A}$ *with box-counting dimension* $d_{\mathcal{A}}$*.*

Following the strong Whitney's embedding theorem, any smooth real $k-$*dimensional manifold, required to be Hausdorff- and second-countable, can be smoothly embedded in* $\mathbb{R}^{2k}$*, if* $k > 0$*. This reflects the optimal linear bound on the smallest-dimensional Euclidean space that all* $k-$*dimensional manifolds embed in, as the real projective spaces of dimension* k *cannot be embedded into real* $(2k-1)$ *space, if* m *is a power of two.*

Hence, $\mathcal{A}$ *can be embedded in a* $m-$*dimensional Euclidean space with* $m > 2d_{\mathcal{A}}$*, if there exists a diffeomorphism* $\Phi_f: \mathcal{A} \to \mathbb{R}^m$*, such that the derivative of* Φ_f *has full rank.*

Therefore, $\Phi_T(x) = \left(\alpha(x), \alpha\left(\Phi_t(x)\right), \dots, \alpha\left(\Phi_t^{m-1}(x)\right)\right)$ *is an embedding of the strange attractor* $\mathcal{A}$*. Moreover, the phase space can be reconstructed by* $\vec{x}(t) = \{x(t), x(t+\tau), \dots, x(t+(m-1)\tau\}$*."*

3.4.2. Spectral Embedding

For our dataset, we follow a novel embedding technique using manifold embedding and Laplacian Eigenmaps as proposed by Song et al. (2016) by applying a spectral embedding algorithm. Therefore, it is assumed that the strange (chaotic) attractor of financial time series to lie on a low-dimensional manifold, which is embedded into a high-dimensional Euclidean phase space (Song et al., 2016). Further, it is premised that the topological structure of the financial system in phase space can be displayed by few independent degrees of freedom embedded in a low-dimensional nonlinear manifold, visible by calculation of nonlinear dimensionality reduction algorithms (Lewandowski et al., 2014).

In order to conduct a successful mapping and extraction of the hidden strange attractor of the financial chaotic system, Laplacian Eigenmaps are determined, since in practise it is not possible to measure components of an unknown high-dimensional vector space (Belkin & Niyogi, 2003). In this study, we apply spectral embedding, which forms an affinity matrix based on a nearest neighbour algorithm and a principal component analysis given by the specified function and applies spectral decomposition to the corresponding graph Laplacian.

The resulting transformation is given by the value of the eigenvectors for each data point (Belkin & Niyogi, 2003). Nevertheless, the Laplacian Eigenmaps are determined as stated above and defined as follows (Song et al., 2016; Kim et al., 1999):

"Suppose $\mathbb{R}^D$ to be a Euclidean space and the Laplacian Eigenmaps are defined as $\mathcal{L} \overset{\Delta}{\rightarrow} \mathcal{D} - \mathcal{W}$, with $\mathcal{W}$ as adjacency matrix of the edge weights and $\mathcal{D}$ as diagonal matrix with $\mathcal{D}_{ii} = \sum_j \omega_{ij}$. The constructions are executed as follows:

(1) Construct the adjacency distance between x_i and x_j with $x_i, x_j \in \mathbb{R}^D$ through determination of $\|x_i - x_j\|^2 < \varepsilon$, with $\varepsilon \in \mathbb{R}$. Assume the norm to be Euclidean.

(2) Determine the weights of the adjacency matrix $\mathcal{W}$ by heat kernel, setting weights to $\omega_{ij} = e^{-\|x_i - x_j\|^2 / i}$.

(3) Compute Eigenmaps under the assumption that the graph is connected and conduct a mapping into a lower $d-$dimensional space with $y_1, y_2, \dots, y_k \in \mathbb{R}^d$. The embedding is provided by the $k \times d$ matrix $\Phi = \{\Phi_1, \Phi_2, \dots, \Phi_d\}$.

(4) *The objective function can be equated as $\sum_{i,j} \|\Phi^{(i)} - \Phi^{(j)}\| \omega_{ij} = (\Phi^T \mathcal{L} \Phi)^T = \mathcal{L}\Phi$, where $\Phi^{(i)}$ represents the d-dimensional indication of the $i-$th vertex."*

3.5. Recurrence Quantification Analysis

We want to achieve a full encompassing analysis of the dynamics of a financial system; therefore, we additionally employ a recurrence quantification analysis (RQA) based upon a recurrence plot analysis (RP) introduced by Eckmann et al. (1987), which originates from a topological approach in the study of nonlinear complex dynamics (Barkoulas et al., 2012). Chaos analysis based upon RQA and RP embrace the benefit of the topological approach, contrasting the metric methodologies, by preserving the time-ordering information content of the regarded data series as well as the spatial structure (Barkoulas et al., 2012).

RQA aims towards detecting fundamental characteristics of a dynamical system, namely, the recurrence of states, resulting in a potent chaos detection method, since it is robust in terms of data limitations (e.g., sample size, noise), vastly inhibited in financial data sets (Rohde et al., 2008). Therefore, we assume three main characteristics of chaotic (financial) time series, namely, (1) the existence of a low-dimensional attractor of the respective dynamical system, (2) present dependence on initial conditions (see 3.1.5.1) and (3) manifestation of recurrence property (Barkoulas et al., 2012). Additionally, applying a RP, contrasting metric-based chaos tests, the topological approach renders the degree of complexity within the system visible, since it reflects the recurrence characteristics (e.g., the fractal structure) of the respective trajectories (Barkoulas et al., 2012).

The execution of RQA and RP[47] also displays the transitions within the dynamical system of time series, respectively[48] (Marwan & Kurths, 2005). The major task of this analysis is to determine the linkage between recurrences with dynamical invariants and unstable periodic orbits, since it is assumed that recurrences[49] contain all relevant information regarding the dynamical behaviour of the system (Marwan et al., 2002). The RP can be displayed as follows (Eckmann et al., 1987; Marwan et al., 2007):

"Assume a reconstructed trajectory $\vec{x}_i \in \mathbb{R}^d$ *in phase space. Hence, the recurrence plot graphically represents the recurrence matrix, expressed by* $\mathcal{R}_{i,j}(\varepsilon) = \Theta\left(\varepsilon - \left\|\vec{x}_i - \vec{x}_j\right\|\right)$*, with* $i,j = 1,..,T$*, where* T *represents respective time steps of* $\vec{x}_i$*,* ε *a threshold value,* Θ *is the Heaviside step function,* $\Theta(x) = 0$ *if* $x \leq 0$ *and* $\Theta(x) = 1$ *for* $x > 0$ *and* $\|\cdot\|$ *is a norm*[50]*. For* ε *−recurrent states (i.e., states in* ε *−neighbourhood)* $\vec{x}_i \approx \vec{x}_j \Leftrightarrow \boldsymbol{\mathcal{R}}_{i,j} \equiv 1$*."*

The RP is obtained by graphically displaying the recurrence matrix $\boldsymbol{\mathcal{R}}_{i,j}$ in a binary colouring of choice (Rohde et al., 2008). Further, the RP is symmetric and has a line of identity as main diagonal, which, following Eckmann et al. (1987), is proportional to the maximum Lyapunov exponent (Marwan et al., 2007).

Special attention should be reserved for the choice of the parameter setting of ε, since if it is chosen too small, no recurrence points occur, whilst in the opposite case, almost every sample point is defined as a recurrence point (Marwan et al., 2007). At first, the minimum should be $\varepsilon > 5\sigma_\zeta$, where σ_ζ represents the standard deviation of the sample noise[51], while following the several indications literature has provided (Marwan et al., 2007). Following Mindlin and Gilmore (1992), a small percent of phase space diameter is sufficient, and while following Zbilut et al. (2002), we state the search for scaling regions in point density functions. Nevertheless, following Koebbe and Mayer-Kress (1992), as well as Zbilut and Webber Jr. (1992), the value of ε should not exceed 10%. Hence, for our sample we apply the standard algorithm setting of 10%.

A graphical interpretation guideline for the visualisation of the RP is provided by Marwan et al. (2007) and included within Appendix A1 of our study. Upon thoroughly investigating a RP-plot, results were obtained in a structural as a display of single-dots, diagonal lines and vertical (horizontal) lines (Rohde et al., 2008). The length of a diagonal line represents the duration of similar local evolutions of phase space trajectories, while a vertical (horizontal) line marks the time durations in which a state does not change and is trapped, and are called intermittency or laminar states (Marwan et al., 2002).

[47] The recurrence and return times with respect to their statistics have been studied by Hirata et al. (1999) and Penné et al. (1999) and linked to other fundamental characteristics of dynamical systems (e.g., Pesin's dimension by Afraimovich (1997)), point-wise local dimension by Afraimovich et al. (2000) or the Hausdorff dimension by Barreira and Saussol (2001). Further, multifractal properties have been investigated by Hadyn et al. (2002) and Saussol and Wu (2003).
[48] For an RP approach with matrix eigenvalues, see Yang and Shang (2018).
[49] Based upon the Poincaré recurrence theorem
[50] Mostly, the Euclidean $(L2)-$, $L1-$ or the $L-inf$-norm is applied.
[51] In our case $\varepsilon \approx 0.06$.

To estimate respective invariants of the system, one should exclude the identity line as well as apply the respective Theiler-windows into the computation if the data is non-stationary[52] (Theiler, 1986). We will apply the following RQA-measures, as displayed in Table 10 (Marwan et al., 2007).

Table 10: Overview of RQA-measures, with measure names, equations and short-descriptions.

RQA-Measure	Equation	Description
Recurrence Rate (RR)	$RR(\varepsilon) = \frac{1}{T^2}\sum_{i,j=1}^{T} \mathcal{R}_{i,j}(\varepsilon)$	RR is a measure of the density of recurrence points in the RP.
Measures based on diagonal lines l with minimum length l_{min} [53]		
Determinism (DET)	$DET = \frac{\sum_{l=l_{min}}^{T} l\,P(l)}{\sum_{l=1}^{T} l\,P(l)}$	DET is a measure of the predictability (determinism) of the system.
Average Diagonal Line Length (L)	$L = \frac{\sum_{l=l_{min}}^{T} l\,P(l)}{\sum_{l=l_{min}}^{T} P(l)}$	L represents the mean prediction time of the system.
Longest Diagonal Line (L_{max}) Divergence (DIV)	$L_{max} = \max(\{l_i\}_{i=1}^{T})$; $DIV = {}^{1}/_{L_{max}}$	L_{max} is the longest diagonal found in the RP.
Shannon Entropy ($ENTR$)	$ENTR = -\sum_{l=l_m}^{T} p(l)\ln p(l)$	$ENTR$ reflects the complexity of the RP, small $ENTR$ equals small complexity.
Trend ($TREND$)	$TREND = \frac{\sum_{i=1}^{\breve{N}}\left(i - \breve{N}/2\right)(RR_i - \langle RR_i\rangle)}{\sum_{i=1}^{\breve{N}}\left(i - \breve{N}/2\right)^2}$	$TREND$ provides information about non-stationarities within the RP.
Ratio ($RATIO$)	$RATIO = N^2\frac{\sum_{l=l_{min}}^{T} l\,P(l)}{(\sum_{l=1}^{T} l\,P(l))^2}$	$RATIO$ is defined as ratio between DET and RR.
Measures based on vertical lines v with minimum length v_{min}		
Laminarity (LAM)	$LAM = \frac{\sum_{v=v_{min}}^{T} v\,P(v)}{\sum_{v=1}^{T} v\,P(v)}$	LAM represents the occurrence of laminar states.
Trapped Time (TT)	$TT = \frac{\sum_{v=v_{min}}^{T} v\,P(v)}{\sum_{v=v_{min}}^{T} P(v)}$	TT indicates the average length of vertical lines; time at a state.
Longest Vertical Line (V_{max})	$V_{max} = \max(\{v_i\}_{i=1}^{T})$	V_{max} is the longest vertical found in the RP.
* $P(l)$ is a histogram; $p(l) = P(l)/T$; $\breve{N}$ the maximal number of diagonals parallel to the main diagonal.		

[52] We do not apply Theiler-windows; however, we exclude the main diagonal from the analysis.
[53] In Appendix A2, we present graphics for varying choices of l_{min} (and v_{min}).

4. Data Description

4.1. S&P 500 Returns & Surrogate Data Sets

We analyse the daily adjusted-closing prices of the S&P 500 index, extracted from Yahoo Finance for the years 2000–2020. Financial literature states that historical price-series are non-stationary, which could lead to severe problems with the applications of chaotic measures and tests. Therefore, we will compute logarithmic differences of the daily adjusted-closing prices, resulting in log-returns (BenSaïda, 2014). In order to reduce the noise level of the return series, we apply a discrete Haar wavelet cascadic filter bank with 12 levels, executing the softened wavelet-shrinkage algorithm as described in Chang et al. (2000) and as depicted in Figure 6. Furthermore, we calculate ft, aaft and iaaft surrogate data sets based on the aforementioned wavelet-filtered S&P 500 returns.

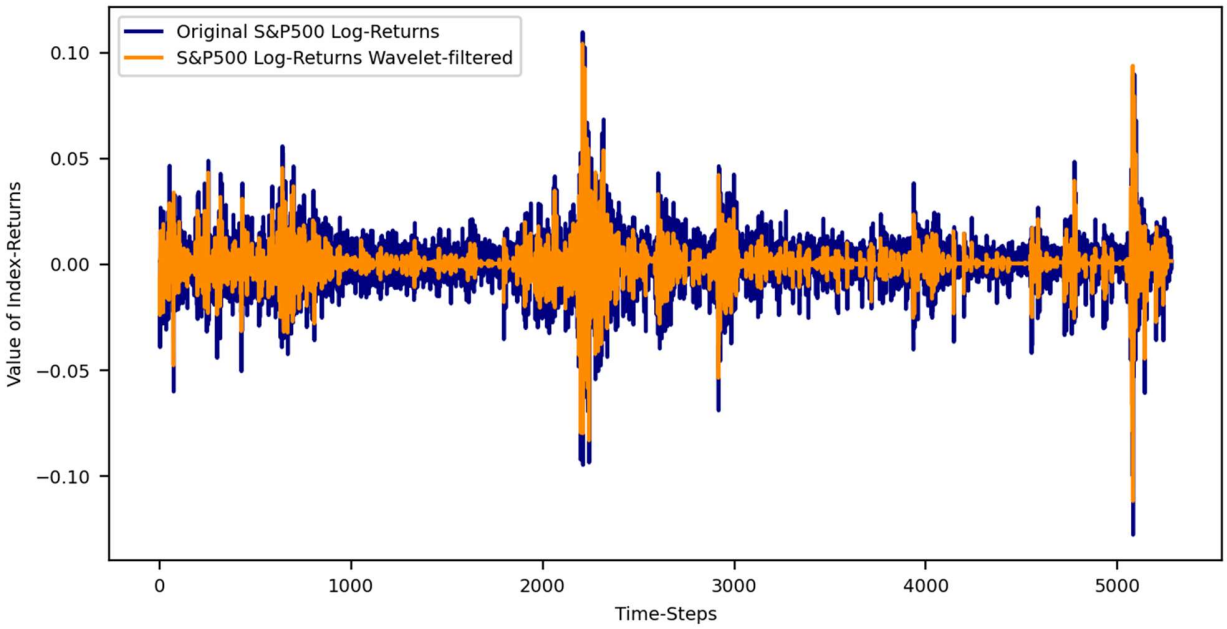

Figure 6: Daily S&P 500 logarithmic return series (blue) versus wavelet-filtered daily S&P 500 return series (orange) ranging from 2000 to 2020.

4.2. Brownian Motion Returns

Alongside the three surrogate data sets (ft, aaft and iaaft), we will apply a pure stochastic system realisation to ensure the proper specification of our S&P 500 return sample. Therefore, we will generate a realisation of a geometric Brownian motion or Wiener process S_t, whose length equals the length of our S&P 500 series (Oksendal, 2013):

(1) $S_t = \alpha e^{\left(\mu - \frac{\sigma^2}{2}\right)t + \sigma W_t}$ with $\alpha = 0.2;\ \mu = 0.4; \sigma = 0.32; t = 1$ and W_t being a Brownian Motion

For this realisation, we will compute the logarithmic return series, as stated before, to ensure comparability between the S&P 500 returns and the stochastic system-realisation change rates, as depicted in Figure 7.

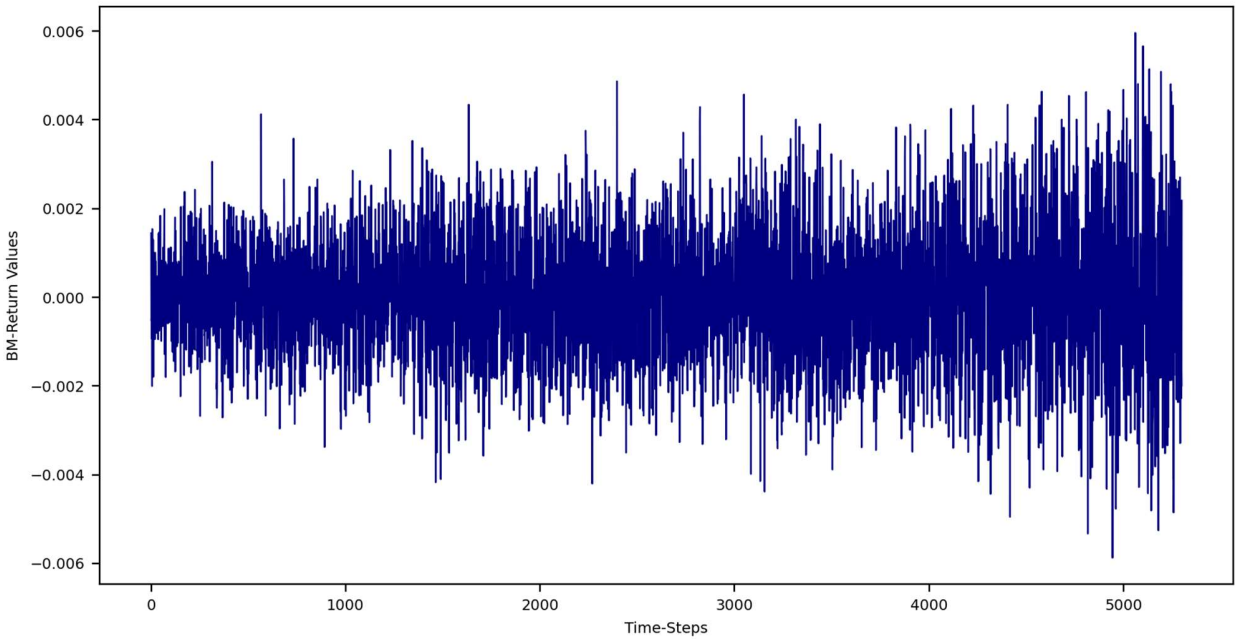

Figure 7: Realisation of Brownian Motion returns based on the S&P 500 return series length.

4.3. Lorenz System Realisation

In accordance with the pure stochastic system, we further implement a well-studied pure deterministic and chaotic system, namely the Lorenz system, with as many data points as the length of the S&P 500 series and with the following specification, as depicted in Figure 8 (Lorenz, 1963):

(2) $x_d = s(y - x)$

$y_d = rx - y - xz$ with $s = 10; r = 28;\ b = 2.667$ and $dt = 0.01$

$z_d = xy - bz$

Please note that x_d, y_d and z_d are the values of the Lorenz attractor's partial derivatives at the x, y and z points in three-dimensional space, respectively, while s, r and b are the parameters defining the Lorenz attractor.

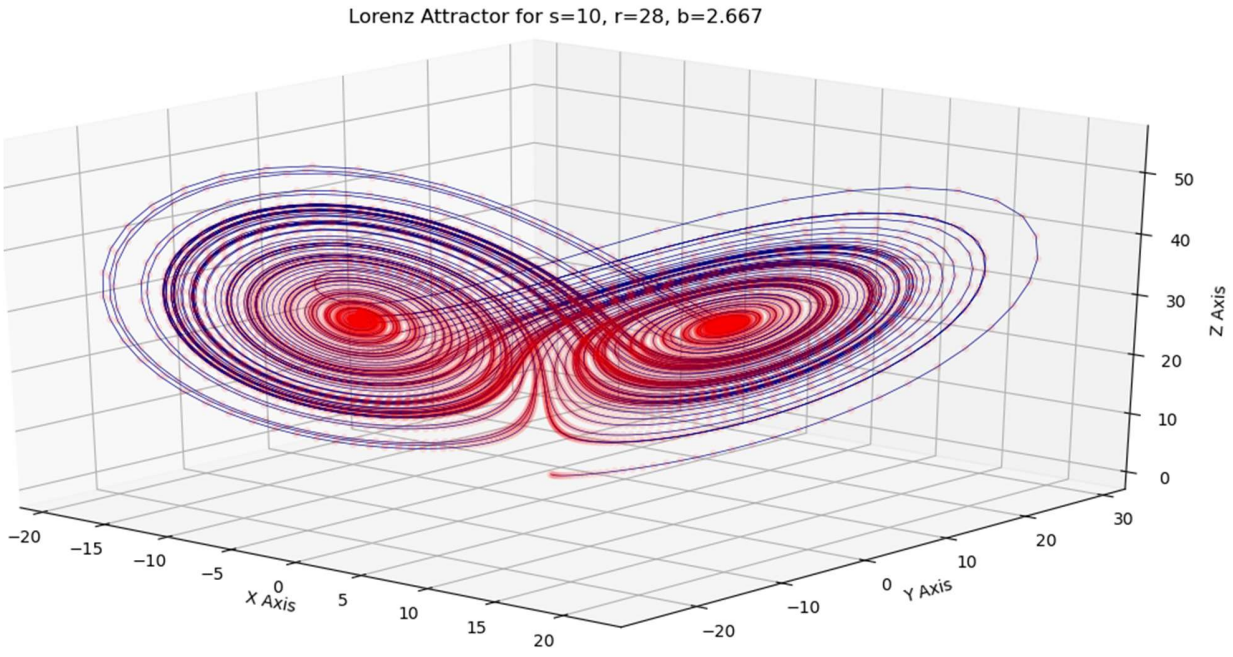

Figure 8: Lorenz System, represented by example attractor realisation for s = 10, r = 28 and b = 2.667.

5. Empirical Results

5.1. Statistical Tests

We now present the results of our empirical analysis, implementing the concepts stated in the theoretical section using self-written Python code[54]. We begin by testing the wavelet filtered S&P 500 returns, the surrogate data sets (ft, aaft and iaaft) as well as the Brownian motion realisation and the Lorenz system realisation in hindsight of stationarity by applying the ADF- and KPSS-test, as stated in Table 11. Regarding the $p-$values, we can confirm for 1% significance level, that the series are stationary, with the exception of the Lorenz system. Regarding the KPSS-test, we apply the setting "c" to test stationarity around a constant and "ct" to test for stationarity around a trend, while using two lag-algorithms, namely the "auto" as stated in Hobijn and Frances (1998) and "legacy" proposed by Schwert (1989), for each noted setting.

Furthermore, we test the distribution of the respective data series with a KS-test in terms of Gaussian distribution. Respective $p-$values, assuming a 1% significance level, indicate non-Gaussianity within the respective distributions, as displayed in Table 11. Continuing our analysis, we calculate the BDS-test for 20 different embedding dimensions, to test for nonlinearity, as stated in Table 12. Please note, as indicated in section 3.3.2, we will only interpret the results as an indication of nonlinearity and omit the consideration of the pertaining underlying nature for now. The results show nonlinearity within the S&P 500 returns and the Lorenz system.

[54] Parallel to commonly known libraries (e.g., NumPy, pandas and Matplotlib), we implemented the nonlinear dynamics packages Nolista and Nolds.

The results of the Brownian motion realisation depend on the respective embedding dimension, albeit for reasonable dimensions assumed to be linear.

Table 11: Empirical results of the S&P 500 returns, surrogate data sets (ft, aaft, iaaft), Brownian motion realisation (BM) and the Lorenz system realisation (LS) for the ADF-, KPSS- and KS-test (p –values), "-" indicates zero value.

Test	S&P 500 returns	ft	aaft	iaaft	BM	LS
ADF	-	-	-	-	-	0.0175
KPSS (c, auto)	0.0397	0.1	0.01	0.1	0.1	0.01
KPSS (c, legacy)	0.0396	0.1	0.0185	0.1	0.1	0.01
KPSS (ct, auto)	0.1	0.1	0.01	0.1	0.1	0.01
KPSS (ct, legacy)	0.1	0.1	0.01	0.1	0.1	0.01
KS	-	-	-	-	-	-

Table 12: BDS-test results (p –values) for S&P 500 returns, surrogate data sets (ft, aaft, and iaaft), Brownian motion realisation (BM) and the Lorenz system realisation (LS) for different embedding dimensions. "-" indicates zero-value.

Embedding Dimension	S&P 500 returns	ft	aaft	iaaft	BM	LS
1		0.7097	0.9472	0.6691	0.0701	
2		0.7042	0.9073	0.6186	0.0541	
3		0.7176	0.9037	0.6219	0.0425	
4		0.7378	0.9031	0.6054	0.0332	
5		0.7564	0.9152	0.5724	0.0244	
6		0.7588	0.9094	0.5424	0.0172	
7		0.7602	0.9041	0.5232	0.0112	
8		0.7597	0.8977	0.4972	0.0061	
9		0.7505	0.8827	0.4708	0.0036	
10		0.7498	0.8701	0.4553	0.0019	
11	-	0.7485	0.8625	0.4394	0.0008	-
12		0.7601	0.8632	0.4235	0.0003	
13		0.7782	0.8782	0.4035	0.0001	
14		0.7974	0.8917	0.3962		
15		0.8041	0.9041	0.3879		
16		0.8071	0.9081	0.3677		
17		0.8041	0.9102	0.3553	-	
18		0.8103	0.9066	0.3462		
19		0.8163	0.9041	0.3348		
20		0.8316	0.9013	0.3209		
Result	Nonlinear	Linear			Depending	Nonlinear

To sum up, our S&P 500 wavelet-filtered return set is noise reduced, yields stationarity characteristics, is non-Gaussian distributed and is significantly nonlinear, which concludes the prerequisites for conducting the referring of further chaotic measures. The surrogates are stationary and linear.

5.2. Chaos Measures & Chaos Tests

5.2.1. Space Time Separation

In order to deduce further chaotic tests and measures (e.g., correlation sums), we will consider the possibility of temporal correlations within our sampled data sets. We note that, with regard to the space-time separation plots displayed in Figure 9, for the S&P 500 returns, slight temporal correlations are present within the signal; nonetheless, they are not oscillating or unsettling in an analysis-destroying manner.

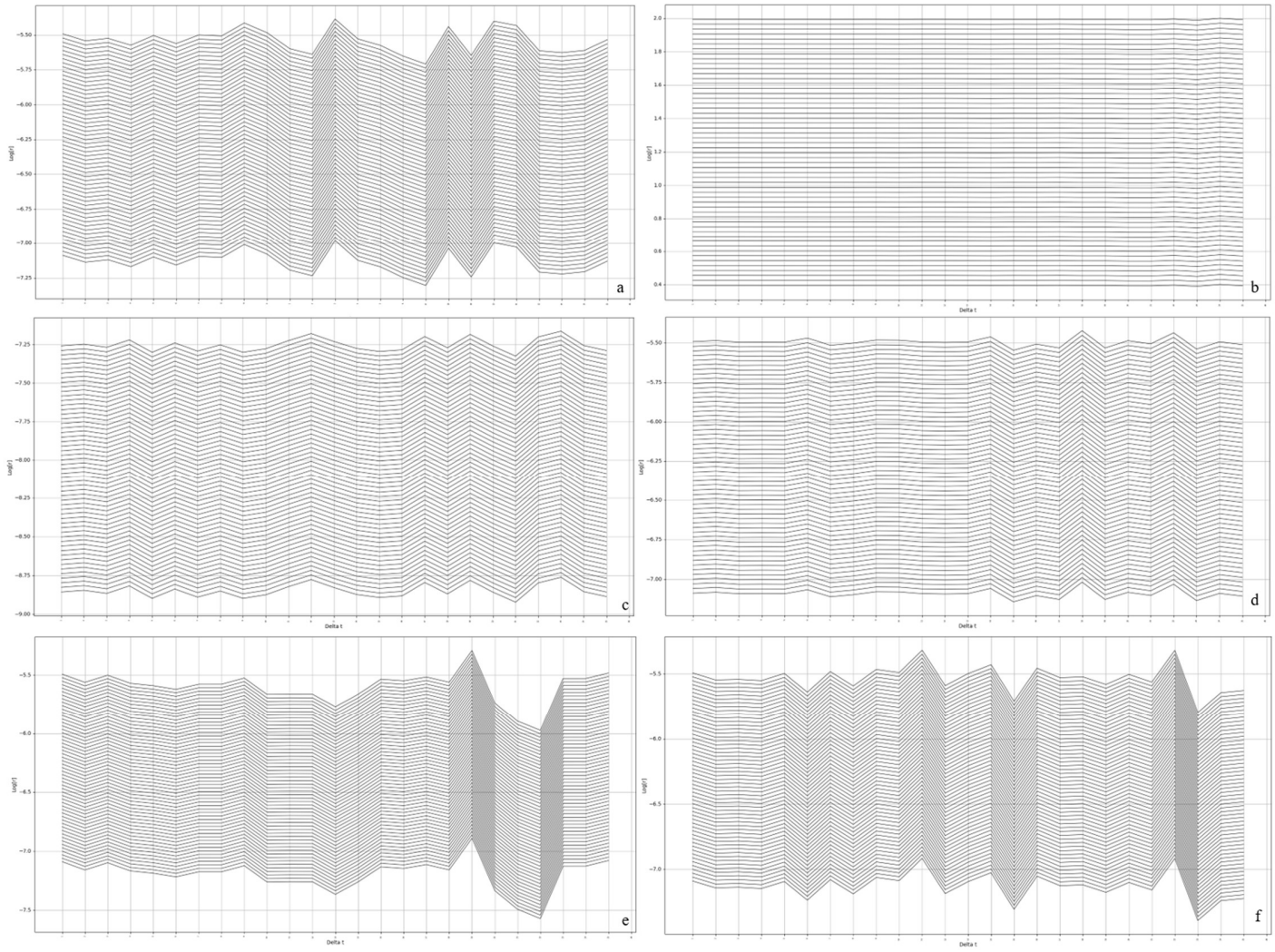

Figure 9: Space Time Separation Plots with (a) wavelet-filtered S&P 500 returns, (b) Lorenz system, (c) Brownian motion returns and (d)–(f) surrogates: (d) ft, (e) aaft and (f) iaaft. For the S&P 500 wavelet-filtered return series, the figure (a) states some low levels of temporal correlation.

5.2.2. Chaos Measures

We will continue with the empirical analysis by applying the discussed correlation sum scheme (see 3.2.2), stated in Figure 10, which is calculated for 19 respective embedding dimensions. Visually, a scaling region is determinable for the S&P 500 returns and the Lorenz system; however, we introduce a new method for quantitatively ensuring the visual impression. In order to determine a line, i.e., the scaling region in the respective correlation sum plot, we calculate the rate of changes of the correlation sums themselves and test them via a Student's t −test to be statistically different from zero, as shown in Figure 11. The results indicate the existence of a scaling region for the S&P 500 returns and the Lorenz system. Further, regarding the S&P 500 returns, it is imminent to state that five is the first minimum embedding dimension, which shows all p −values to be significant with 1% confidence, which we will therefore assume in further chaos calculations. Regarding the other data sets, no clear scaling region is detectable. The correlation dimension of the S&P 500 returns (0.8551) indicates low-dimensional fractal structures and saturates for varying embedding dimensions. The same behaviour is determinable for the Lorenz system, as stated in Figure 12. The other data sets do not show signs of saturation at a given dimensional estimate[55]. Further, regarding Figure 13, we can clearly recognise the differences between the S&P 500 return series and the respective surrogate data sets, since their respective dimensional estimates differ notably.

Moreover, we calculate the sample entropy, the Hurst exponent and the respective fractal dimensional estimate, the DFA alpha exponent, the maximum Lyapunov exponent, the Lyapunov time and the Lyapunov spectrum, as stated in Table 13.

With regard to the S&P 500 returns, the sample entropy is small (0.3213), indicating a high-level of self-similarity within the data that resembles the Lorenz system (0.1536), in contrast to the other data sets ($SampEn > 1$). This is covered by a Hurst exponent of 0.5557 for the S&P 500 returns and 0.8575 for the Lorenz system, which can be interpreted as persistent, self-similar (or fractal) behaviour, resulting in trends[56] within the data. The surrogates follow the structure of the S&P 500 returns, therefore, yielding Hurst exponents above 0.5. Further, estimating $D = 2 - H$ results in a dimensional estimate for the S&P 500 returns of 1.4443 and for the Lorenz system 1.4911. For ft (0.0641) and the Brownian motion (0.0028), a low correlation dimension is noted, while aaft (2.7402) and iaaft (2.7401) result in higher estimates, which is an artefact due to the spectral nature of the surrogates. Correlation is also testified by the DFA alpha value for the S&P 500 returns with 0.5188 and 1.5642 for the Lorenz system, yielding non-stationarity. By disregarding ft (0.4734) stating uncorrelated data, the other data sets indicate correlations ($0.5 \leq \alpha < 1$).

[55] Please note that a drop to zero for the given embedding dimensions does not represent a valid saturation.
[56] Please note that we do not refer to seasonal trends. For an in-depth discussion, refer to Berghorn (2015).

Elaborating on the S&P 500 dynamical properties, we confirm a positive maximum Lyapunov exponent of 0.0296, resulting in exponentially diverging trajectories over time evolution and a negative Lyapunov spectrum sum (-0.5182). Together, these indicate that the system is of a dissipative nature. Furthermore, we determine the Lyapunov time[57] of the S&P 500 returns to be 33.7837. Similar results occur for the Lorenz system. Hence, we can assume that the S&P 500 return system will deflate into a low-dimensional phase space sub-volume, namely an attractor, whose possible existence we will elucidate in section 5.3.

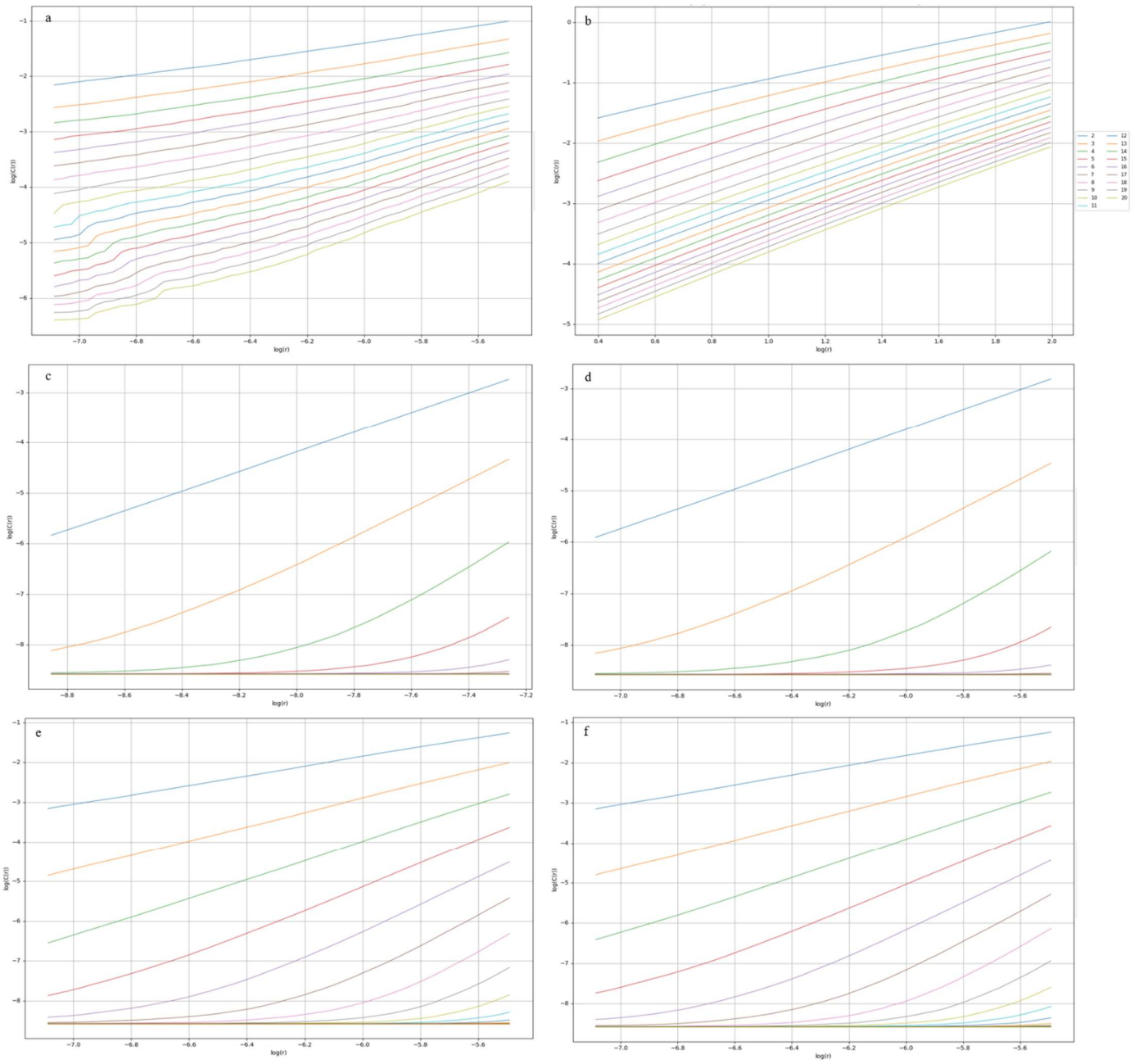

Figure 10: Log-log plot for correlation sums versus diameter for different embedding dimensions with (a) wavelet-filtered S&P 500 returns, (b) Lorenz system, (c) Brownian motion returns and (d)–(f) surrogates: (d) ft, (e) aaft and (f) iaaft.

[57] Depending on the point of view, the Lyapunov time can be seen either in standard time [s] or in the time-units of the data series.

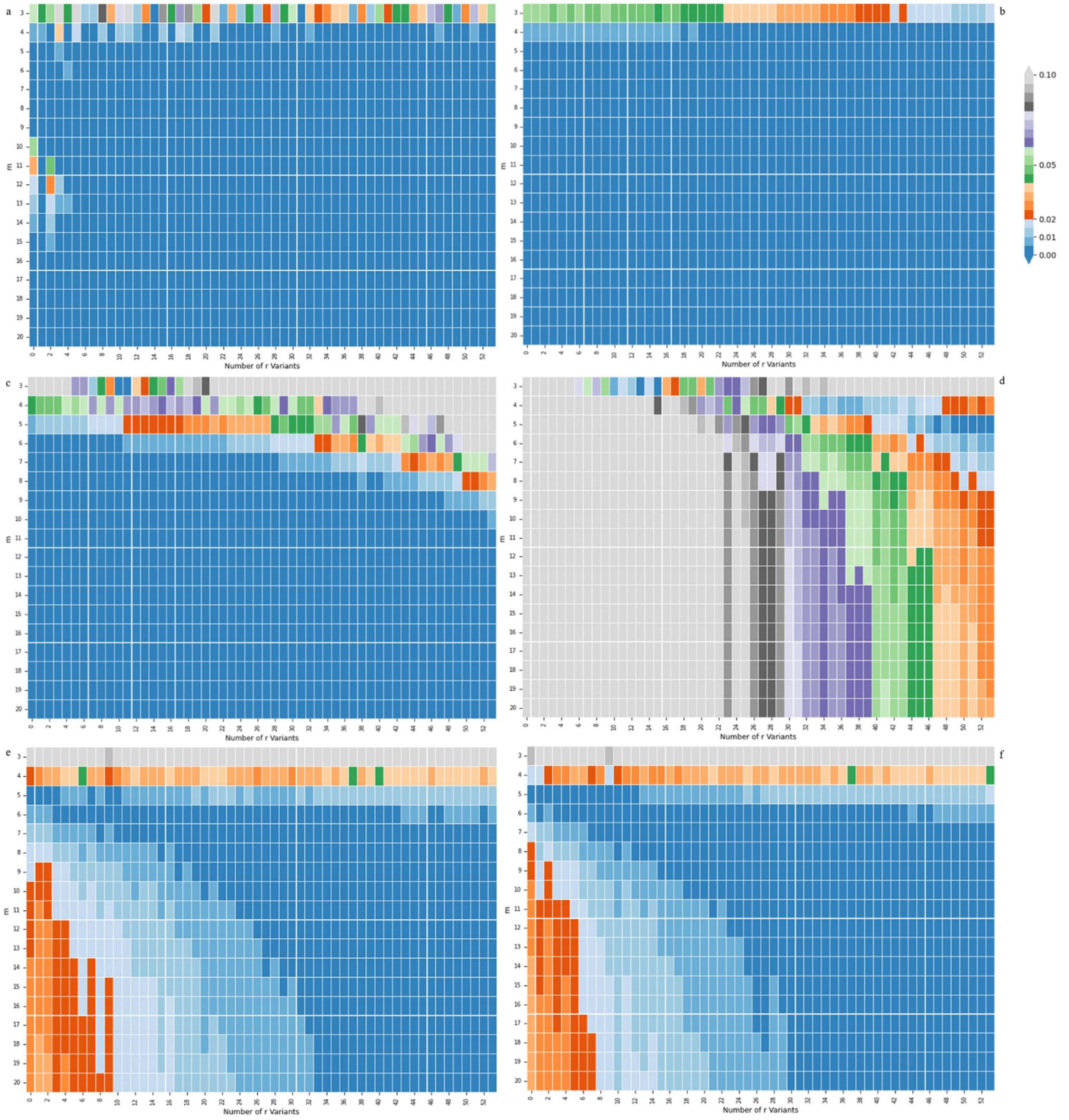

Figure 11: p −values for changes in correlation sums for different diameter (t −test for the change to be zero) for different embedding dimensions with (a) wavelet-filtered S&P 500 returns, (b) Lorenz system, (c) Brownian motion returns and (d)–(f) surrogates: (d) ft, (e) aaft and (f) iaaft.

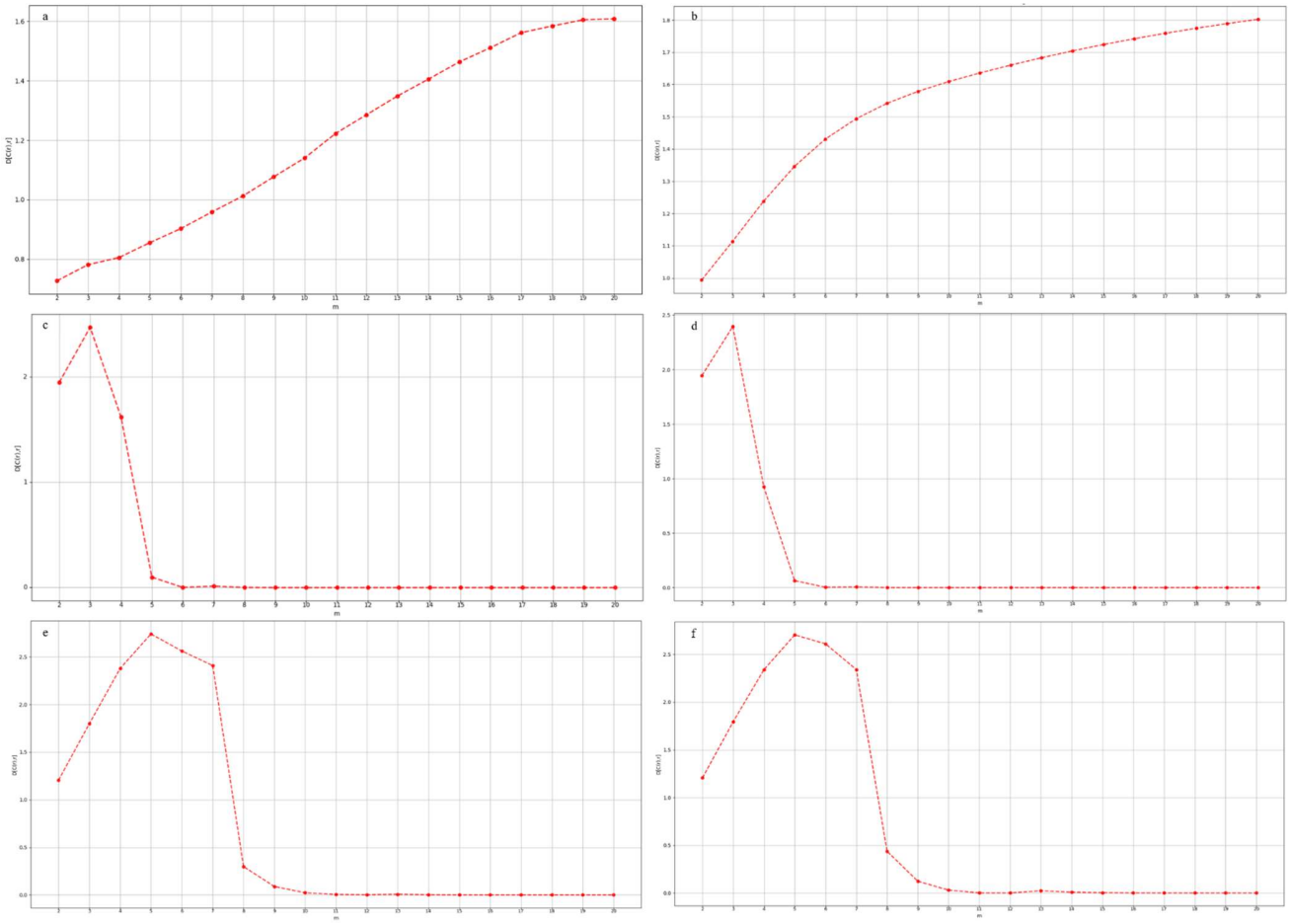

Figure 12: Correlation dimensions for different embedding dimensions with (a) wavelet-filtered S&P 500 returns, (b) Lorenz system, (c) Brownian motion returns and (d)–(f) surrogates: (d) ft, (e) aaft and (f) iaaft.

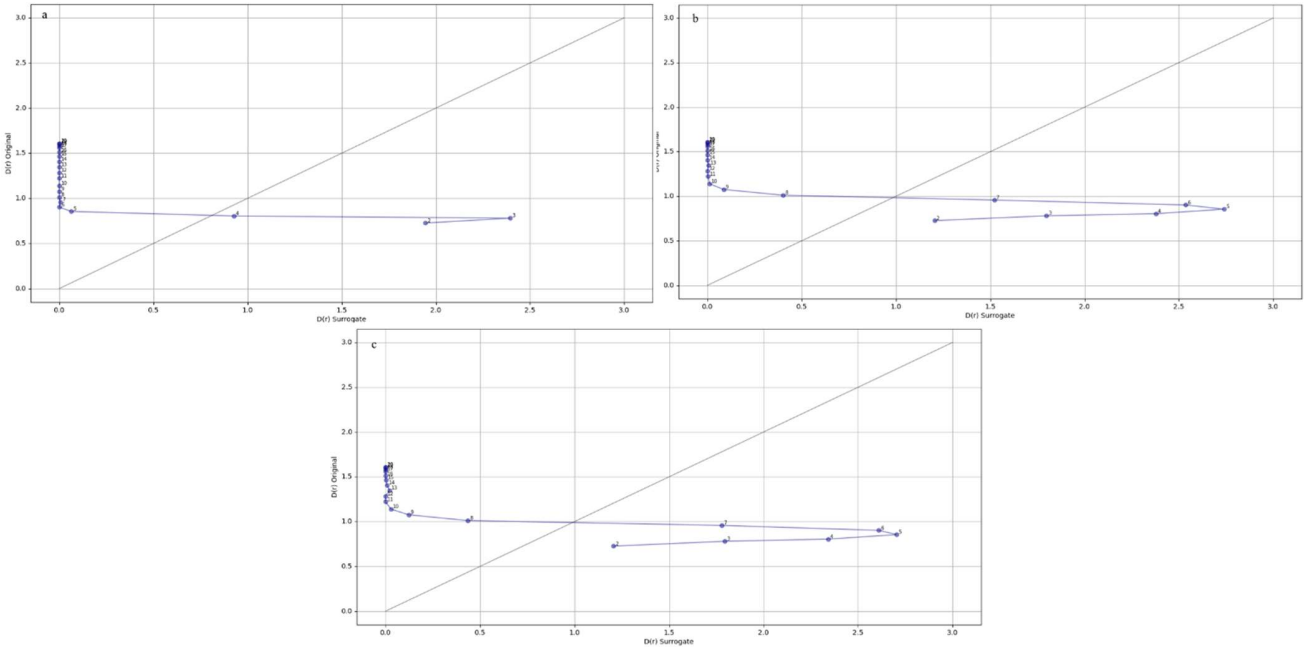

Figure 13: Correlation dimension of S&P 500 return series (y-axis) versus correlation dimensions of surrogate data (x-axis) for different embedding dimensions: (grey) diagonal indicates exact resemblance, (a) ft, (b) aaft and (c) iaaft.

Table 13: Chaos measure results for S&P 500 returns, surrogate data sets (ft, aaft, iaaft), Brownian motion realisation (BM) and the Lorenz system realisation (LS).

Chaos Measure	S&P 500	ft	aaft	iaaft	BM	LS
Sample Entropy	0.3213	2.1611	1.1126	1.0772	2.0977	0.1536
Correlation Dimension[58]	0.8551	0.0641	2.7402	2.7041	0.0821	1.4911
Maximum Lyapunov Exponent	0.0296	-0.0005	0.0006	0.0045	0.0028	0.0144
Lyapunov Time	33.7837	(2,000)	(1,666.6666)	(222.2222)	(357.1428)	69.4444
Lyapunov Spectrum	[1.7461, 0.2231,-0.2955, -0.6226, -1.5685]	[0.5663, 0.2521, 0.0339, -0.2094, -0.6767]	[0.0876, 0.31039, 0.0594, -0.1987, -0.6641]	[0.8443, 0.3195, 0.0496, -0.2027, -0.6575]	[0.5636, 0.2474, 0.0341, -0.1952, -0.6487]	[0.0177, 0.0109, -0.0037, -0.0487, -0.1176]
Lyapunov Sum	-0.5182	-0.0238	0.3836	0.3532	0.0012	-0.1413
Hurst Exponent	0.5557	0.5606	0.6833	0.5557	0.5506	0.8575
Hurst Dimensional Estimate	1.4443	1.4394	1.3167	1.4443	1.4494	1.1425
DFA Alpha Exponent	0.51883	0.4734	0.6324	0.5451	0.5286	1.5642

5.2.3. Bask-Gençay Test

Since for the S&P 500 return series, the maximum Lyapunov exponent is small above zero and the methodology suffered the critique of non-existent distributional theory in order to conduct respective hypothesis testing, we employ the Bask-Gençay test, as described in 3.3.3 by conducting the test with 50,000 bootstrapping steps for 19 respective embedding dimensions, stated in Table 14. The results of the Bask-Gençay test indicate, that for the embedding dimension of five, the Null hypothesis of $\sim iid$ properties cannot be uphold, therefore, stating chaotic dynamics for the S&P 500 returns. The Lorenz system is chaotic, up to an unrealistic assumption for the embedding dimensions. The same can be stated for the stochastic nature of the other data sets vice versa.

Table 14: Bask-Gençay test for S&P 500 returns, surrogate data sets (ft, aaft, iaaft), Brownian motion realisation (BM) and the Lorenz system realisation (LS), for different embedding dimensions and 50,000 bootstrapping steps.

Embedding Dimension	S&P 500	ft	aaft	iaaft	BM	LS
2	-0.0153	-0.0024	-0.0103	0.0011	0.0003	0.0117
3	-0.0105	-0.0024	-0.0084	-0.0005	0.0007	0.0163
4	-0.0056	-0.025	-0.0072	0.0004	-0.0002	0.0183

[58] Following Ramsey et al. (1990), correlation dimension estimates with limited data sets reveal misleading results, notably returning artificially smaller correlation dimension estimates.

Embedding Dimension	S&P 500	ft	aaft	iaaft	BM	LS
5	0.0069	-0.0031	-0.0045	-0.0005	0.0008	0.0232
6	0.0041	-0.0041	-0.0055	0.0002	0.0002	0.0218
7	0.0002	-0.0044	-0.0061	0.0022	-0.0015	0.0224
8	-0.0042	-0.0033	-0.0073	0.0021	-0.0006	0.0227
9	0.0111	-0.0036	-0.0078	0.0003	-0.0007	0.0197
10	0.0205	-0.0201	-0.0114	-0.0318	0.0017	0.0088
11	0.0321	-0.0178	-0.0165	-0.0226	-0.0401	-0.0209
12	0.0546	-0.0025	0.0271	-0.0011	-0.0297	-0.0258
13	0.0418	0.0101	0.0382	0.0094	-0.0091	-0.0241
14	0.0438	0.0178	0.0199	0.0012	-0.0044	-0.0211
15	0.0479	0.0176	0.0342	0.0006	-0.0001	-0.0238
16	0.0385	0.0163	0.0255	0.0021	-0.0011	-0.0235
17	0.0491	0.0151	0.0254	0.0004	-0.0009	-0.0251
18	0.0372	0.0134	0.0233	-0.0021	-0.0026	-0.0246
19	0.0361	0.0114	0.0223	-0.0042	-0.0043	-0.0252
20	0.0328	0.0104	0.0196	-0.0067	-0.006	-0.0266

5.3. Phase Space Reconstruction

In order to show the chaotic dynamics of the wavelet-filtered S&P 500 return series visually, we will reconstruct the strange attractor by implementing the delay-time reconstruction of Takens (1981) and display a spectral embedding as described by Song et al. (2016). As described in section 3.4.1, we will determine the delay time τ by regarding respective autocorrelation functions as stated in Figure 14. We decide upon the value $\tau = 20$ as suitable choice for our reconstruction purposes. For the spectral embedding a k −nearest neighbour algorithm is implemented, paired with a principal component analysis, before calculating Laplacian Eigenmaps for respective eigenvalues, yielding component numbers equal to the chosen embedding dimension, namely five. For the determination of k, we apply the following rule $k = 0.01T + 1.5\tau$, thus stating 83 respective neighbours.

We present the reconstructed dynamics based on Takens delay embedding in Figure 15, while the computation results of the spectral embedding are shown in Figure 16 and the Poincaré sections in Figure 17. Moreover, the attractor of the Lorenz system is already displayed in Figure 8; yet, we will propose the spectral embedding results also in Figure 16. Additionally, in order to provide a sufficient differentiation between pure chaos, pure stochastics and our financial sample, we further state in Figure 16 the spectral embedding of the Brownian motion returns[59]. We see that the financial strange attractor resembles neither sole stochastic, nor pure deterministic chaotic Lorenz system visualisations. A formal discussion of this indication is provided after the conduction of the RQA.

[59] Please note the surrogates to resemble qualitatively the Brownian motion reconstructions. Thus, we will neglect their display.

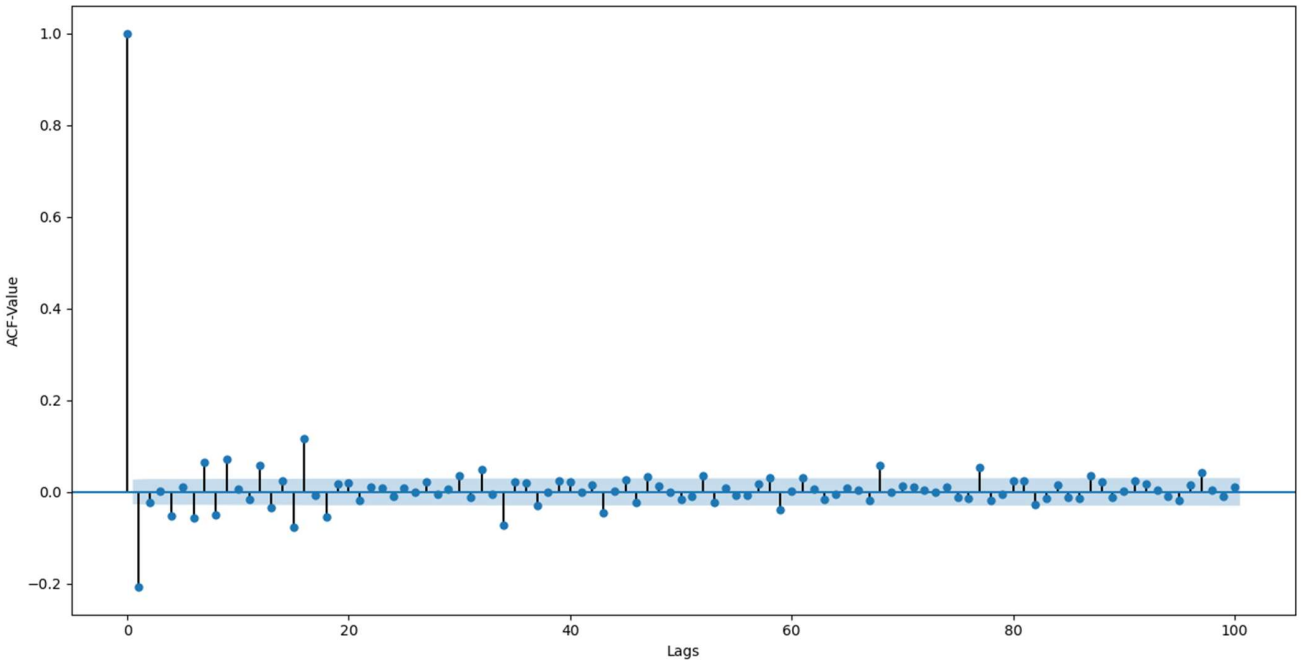

Figure 14: Autocorrelation function with 100 *lags for the wavelet-filtered S&P 500 return series.*

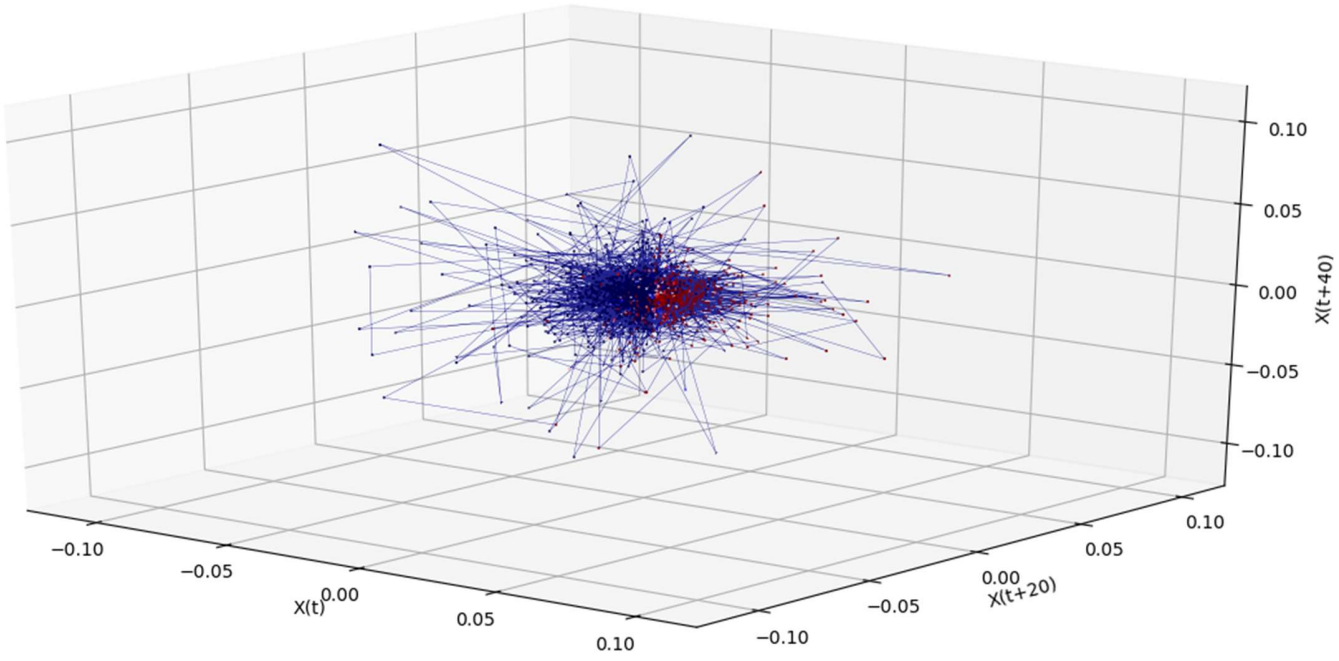

Figure 15: Takens Embedding approach with time-delay of $\tau = 20$ *for wavelet-filtered S&P 500 returns.*

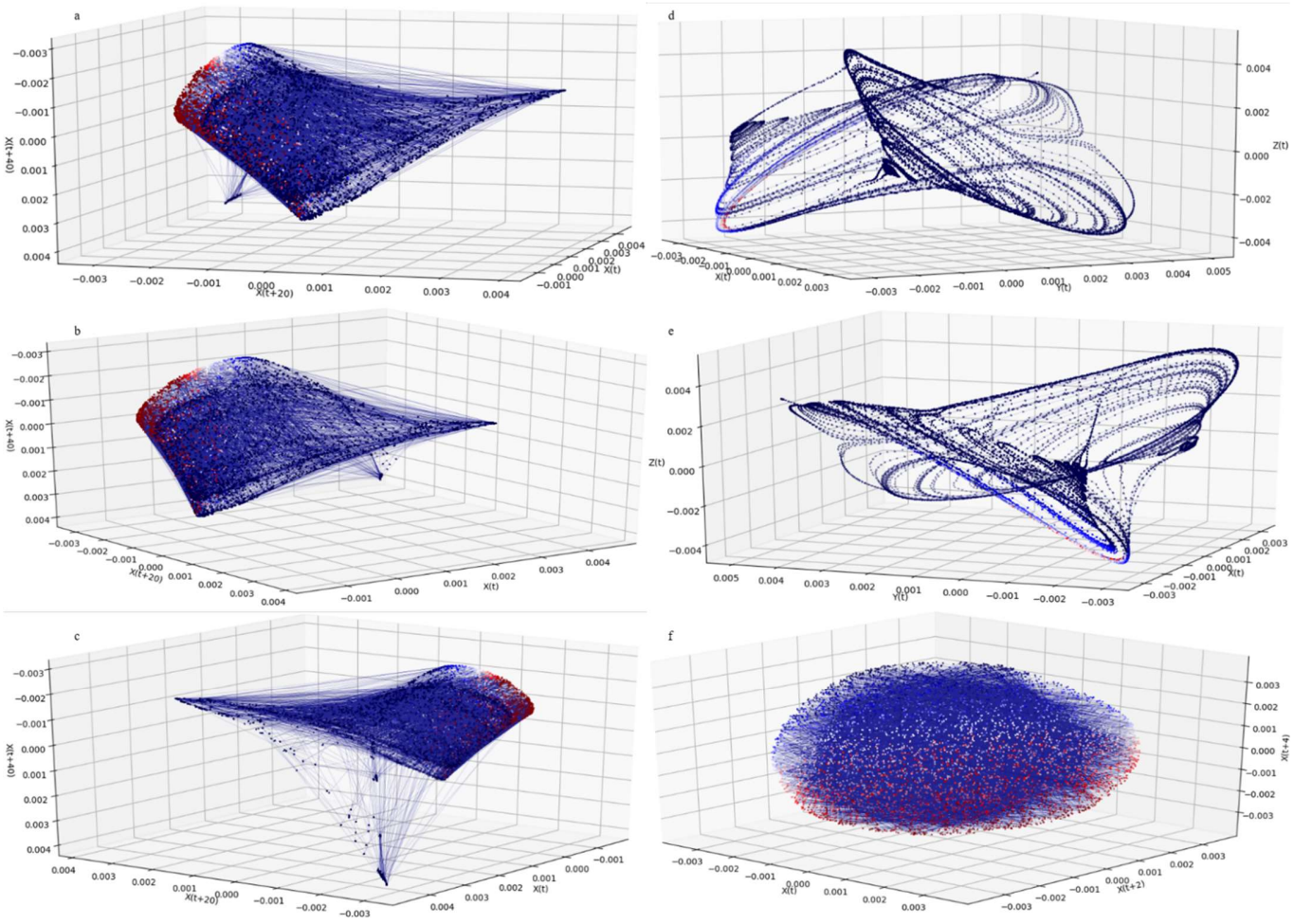

Figure 16: Graphical spectral embedding results for (a)-(c) S&P 500 wavelet-filtered returns (different angles), (d) and (e) Lorenz system (different angles) and (f) Brownian motion returns (qualitatively resembling the surrogates ft, aaft, iaaft).

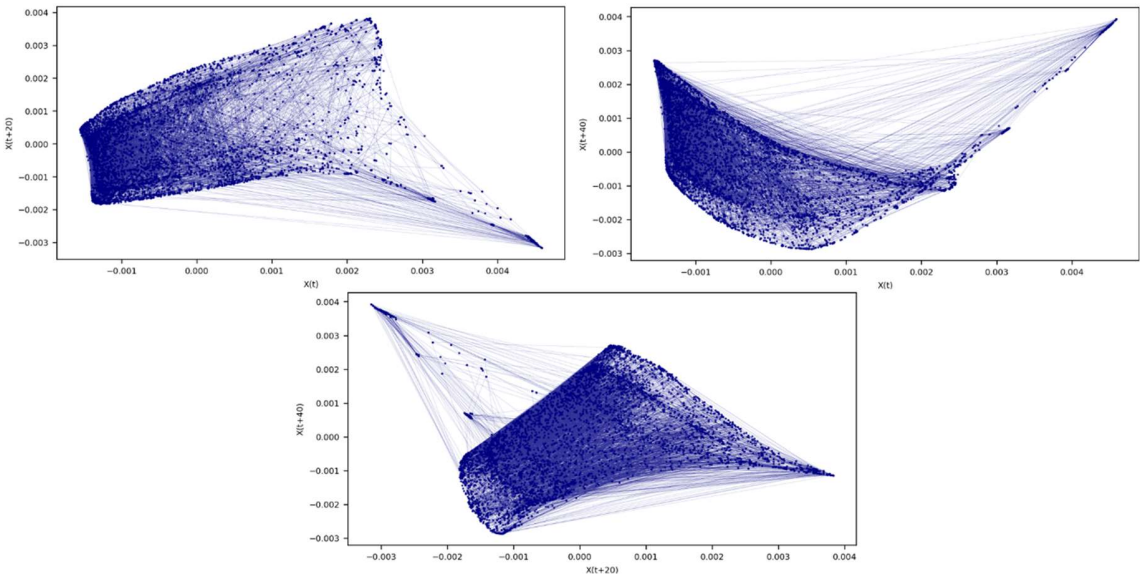

Figure 17: Poincaré sections of the spectral embedding results for the S&P 500 wavelet-filtered returns.

To sum up this section, we state that the S&P 500 wavelet-filtered daily return series is stationary, non-Gaussian distributed and nonlinear. Further, its dynamics reveal themselves to be chaotic and the system to be dissipative, following the maximum Lyapunov exponent (backed by the Bask-Gençay test) and the Lyapunov spectrum sum. Additionally, the series is hyperchaotic due to the existence of two positive Lyapunov exponents in the spectrum. Further, following the Hurst exponent, fractal trends are presents in the signal. Given saturating correlation dimensions and a scaling region in the correlation sum scheme, indicates the existence of a strange chaotic attractor, which we show by Takens approach as well as by applying spectral embedding, respectively.

5.4. Recurrence Quantification Analysis

In the previous section, we did not elaborate on the deeper nature of the dynamics, since the S&P 500 return system neither resembles a pure stochastic nor a purely deterministic system. Therefore, we will now present the results of the RQA for all data sets. The RQA is appealing due to its focus on the recurrence properties, meaning it is somewhat independent from the other analysis methods presented so far. Afterwards, we will elaborate on the respective interpretation. We begin with the visual RP analysis, as stated in section 3.5, which clearly illustrates the inherent differences between our data sets under regard visually, and is displayed in Figure 18.

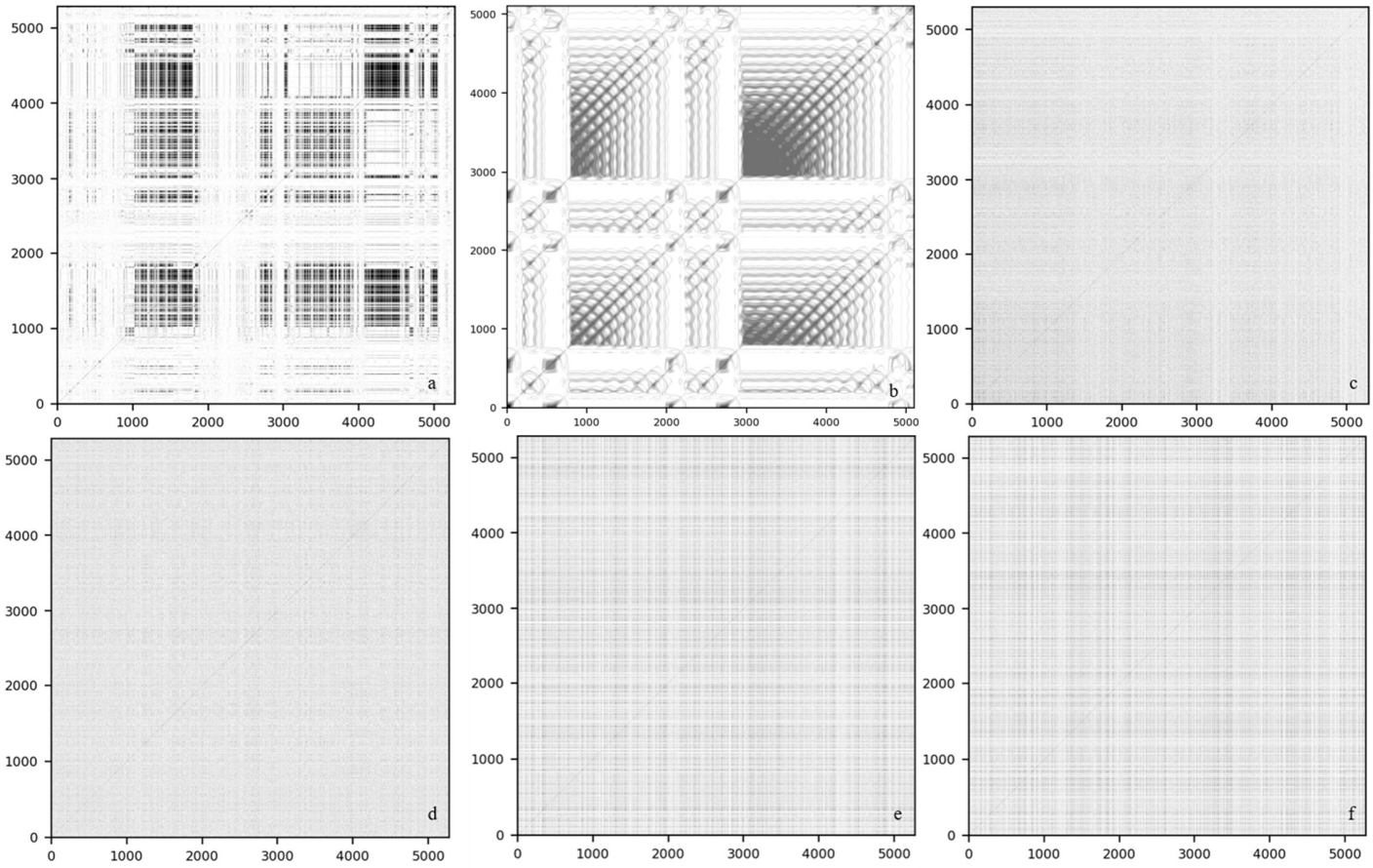

Figure 18: RPs for $\varepsilon = 0$, with (a) wavelet-filtered S&P 500 returns, (b) Lorenz system, (c) Brownian motion returns and (d)–(f) surrogates: (d) ft, (e) aaft and (f) iaaft.

We quantify these visual indications by applying the RQA measures as presented in section 3.5. Hence, we will first present single-valued measures in Table 15, which do not depend on a choice of a minimum diagonal or vertical length, before displaying for a selected length, namely $l_{min} = v_{min} = 6$, the other RQA measure results in Table 16. To be more detailed, we present the graphical developments over different choices of the minimum lengths in Appendix A2.

We focus in the following description on the differences of the S&P 500 return series versus the other data sets, respectively, to gain a deeper insight into the true underlying nature of the dynamics (ignoring the chaoticity we showed previously). In the case of single-valued RQA measures, no trend is visible (out of the Brownian motion returns with 0.0176). To elucidate further on the recurrence rate, we cannot state any notable differences between all data sets. In terms of maximum diagonal length, indicating similar local evolutions of phase space trajectories, we note two main disparities, namely (1) the S&P 500 returns show around 90% larger diagonal length maxima than the surrogate data sets and the Brownian motion return realisation and (2) the S&P 500 returns maximal diagonal length is around 95% smaller than the pure deterministic Lorenz system. With the exception of the Lorenz system, the same differences are reflected by the divergence measure.

Elaborating on the maximal vertical line length, indicating the time duration in which a state does not change and is trapped, in contrast to the diagonals, the picture changes notably with regard to the Lorenz system. As with the diagonal maxima, the vertical maxima of the surrogate data sets as well as the Brownian motion return realisation are around 90% smaller than the according S&P 500 return series. In contrast, the Lorenz system diverges from the S&P 500 returns with an approximately 38% smaller vertical maximum.

Table 15: Single-value RQA measure results for S&P 500 returns, surrogate data sets (ft, aaft, iaaft), Brownian motion realisation (BM) and the Lorenz system realisation (LS). "-" represents zero-value, while (·) states the percentage difference (in decimals) to the S&P 500 returns, if no zero-value is present.

Measure	**S&P 500 returns**	**ft**	**aaft**	**iaaft**	**BM**	**LS**
$TREND$	-	-	-	-	0.0176	-
RR	0.1998	0.1998 (-)	0.1998 (-)	0.1998 (-)	0.1998 (-)	0.1981 (0.0085)
L_{max}	104	10 (-0.9038)	11 (-0.8942)	10 (-0.9038)	11 (-0.8942)	2218 (0.9531)
DIV	0.0096	0.1 (0.904)	0.0909 (0.8943)	0.1 (0.904)	0.0909 (0.8943)	0.0004 (-0.9583)
V_{max}	108	8 (-0.9259)	11 (-0.8981)	11 (-0.8981)	12 (-0.8888)	66 (-0.3888)

Continuing the analysis, we reflect upon the RQA measures, which are dependent on the various minima choices for the referring diagonal and vertical lengths. Elaborating on the Shannon entropy, displaying the complexity of the systems being regarded, we state that the S&P 500 returns are around 93% more complex than the surrogate data sets and the Brownian motion realisation, while the Lorenz systems is over 30% more complex than the S&P 500 returns. Further, the determinism measure indicates the predictability of the data sets, stating the S&P 500 returns to be over 99% more predictable than the surrogate data sets and the Brownian motion realisation.

Moreover, we note that the S&P 500 return series also yields a predictability that is over 40% higher than the pure chaotic Lorenz system. Regarding the ratio of the systems, we only see differences with regard to the S&P 500 returns versus the Lorenz system, which displays a 99% higher ratio and indicates transitions in the Lorenz dynamics, with constant determinism as noted in Marwan and Kurths (2005). An elucidation of averaged diagonal lengths reveals that the S&P 500 returns yield around 85% longer diagonals on average than the surrogate data sets and the Brownian motion realisations, and over 92% shorter diagonals on average than the Lorenz system.

Reviewing the vertical lengths, we state the laminarity as a measure of the occurrence of laminar states in the respective systems. We see that the S&P 500 returns yield over $97 - 99\%$ more laminarity than the other data sets. Referring to the averaged vertical length, namely the trapped time indicating the time passed at one respective system state, we note the S&P 500 series to be trapped over around $90 - 97\%$ longer than the respective surrogates, while remaining at a given state around 117% longer than the Lorenz system, accordingly.

Table 16: RQA measure results with $l_{min} = v_{min} = 6$ for S&P 500 returns, surrogate data sets (ft, aaft, iaaft), Brownian motion realisation (BM) and the Lorenz system realisation (LS). "-" represents zero-value, while $(\cdot)$ states the percentage difference (in decimals) to the S&P 500 returns, if no zero-value is present.

Measure	**S&P 500 returns**	**ft**	**aaft**	**iaaft**	**BM**	**LS**
$ENTR$	17.4418	1.1925 (-0.9316)	1.2036 (-0.9309)	1.1631 (-0.9333)	1.5561 (-0.9107)	25.2621 (0.3095)
DET	0.4286	0.0017 (-0.9961)	0.0016 (-0.9962)	0.0018 (-0.9958)	0.0021 (-0.9951)	0.2497 (-0.4174)
$RATIO$	0.0008	-	-	-	-	0.2361 (0.9966)
L	8.6197	1.2268 (-0.8576)	1.3213 (-0.8467)	1.1869 (-0.8623)	1.3463 (-0.8438)	117.2926 (0.9265)
LAM	0.6146	0.0025 (-0.9959)	0.0199 (-0.9676)	0.0166 (-0.9729)	0.0028 (-0.9954)	0.0064 (-0.9895)
TT	3.2282	0.3514 (-0.8911)	0.1249 (-0.9613)	0.1046 (-0.9675)	0.0874 (-0.9729)	-0.5625 (-1.1742)

5.5. Conclusion of the Empirical Analysis

In sections 5.1–5.4, we present the empirical results of our newly proposed combinatory framework to determine the true nature of the underlying dynamics of the daily S&P 500 wavelet-filtered return series versus surrogate data sets, a Brownian motion return realisation and a Lorenz system realisation. We will now recapitulate the results before critically discussing the implications in hindsight of forecasting and chaos control. First, we ensure, via calculation of log-returns, that the S&P 500 series is stationary, while applying a level 12 cascadic Haar wavelet filter bank to secure an acceptable noise level. The stationarity is tested by implementing ADF- and KPSS-tests, which confirm stationarity for the S&P 500 returns. Furthermore, we conduct a KS-test in order to testify the distributional characteristics of the data sets, resulting in the S&P 500 returns to follow a non-Gaussian distribution. Moreover, we determine nonlinearity within the S&P 500 returns by conducting a BDS-test, as well. To prevent the impossibility of referring phase space reconstruction schemes, we elaborate on the existence of temporal correlations within the data sets, assuming the presence of light temporal correlations that we premise to be non-analysis destroying.

In order to pinpoint a suitable embedding dimension for the reconstruction schemes, we provide a respective correlation sum approach, yielding a scaling region within the S&P 500 return series that is confirmed via a change-significance test. In addition, we see for several choices of the embedding dimension that the according correlation dimension saturates at a given level. We state clear differences between the S&P 500 return series versus the surrogate data sets as well as the Brownian motion return series with regards to reconstructability. Additionally, we display the dimensional dissimilarities graphically. Moreover, we calculate several chaotic measures, namely the sample entropy, maximum Lyapunov exponent, Lyapunov time, Lyapunov spectrum, Lyapunov sum, Hurst exponent, Hurst dimensional estimate and the DFA alpha exponent to elucidate the distinctions between the data sets. The S&P 500 return series shows high-levels of self-similarity regarding the sample entropy and Hurst exponent, accompanied by correlations indicated by the DFA alpha value. This results in fractal structures, which are backed up by the fractal dimension evinced by the Hurst dimensional estimate as well as the correlation dimension itself. In addition, hyperchaotic behaviour implied by two positive Lyapunov exponents in the spectrum and a positive maximum Lyapunov exponent can be seen. Together with a negative Lyapunov sum, we identify the S&P 500 series as a dissipative system with chaotic behaviour after the very short Lyapunov time expires. To increase the credibility of the maximum Lyapunov exponent results, we determine its significance by the Bask-Gençay test with 50,000 bootstrapping steps for several embedding dimensions. We confirm significance and present the strange (chaotic) attractor for the S&P 500 returns via the Takens delay-time embedding as well as with a spectral embedding approach.

Furthermore, we exhibit the significant distinction between the S&P 500 return series and a pure stochastic, pure deterministic as well as its surrogate data series by conducting an almost independent RQA. The main indications demonstrate that the S&P 500 return series produces significantly higher deterministic properties than the surrogate as well as pure stochastic data sets. However, does not provide sufficient results to be classified as a pure deterministic system such as the Lorenz system realisation being regarded. Moreover, the S&P 500 return series manifests more laminar and trapped states than the other data sets, which reveals that its identification as a pure stochastic system is an invalid premise too.

Therefore, we follow the argumentation of Kyrtsou et al. (2004) and Holyst and Urbanowicz (2001), and we determine that the S&P 500 return series is an almost equally divided combination between stochastic and deterministic chaos.

6. Conclusion, Discussion and Implications

6.1. Concluding Summary

For the field of nonlinear dynamics, as well as the field of nonlinear financial analysis, we present an encompassing body of literature by presenting a bibliometric analysis, paired with a successive citation network analysis, displaying the respective research streams, their interconnections, vividly important publications of the field as well as a respective dispersion of related research streams. We observe the dispersion or divergence of the latter fields due to methodological choices within the referring analysis, leading to a separation of knowledge in future research attempts due to the creation of so-called research isles that are mostly independent from each other.

Further, we present and elaborate on the ongoing controversy of whether the dynamics of a financial system is stochastic or deterministic (chaotic) with regard to its underlying evolutionary process, stating the necessity of providing a sufficient framework in order to obtain clear, interpretable as well as comparable results. Moreover, in addition to the stated controversy, the publications related to financial data analysis in terms of nonlinear dynamics do not present a complete framework and the respective methods are scattered throughout the literature, rendering their unification and comparability inconclusive as well. In combination with the problems inherent within the nonlinear dynamical analysis itself, this is assumed to contribute negatively towards the solution of the aforementioned controversy.

We aim at recreating severed bridges and recombining the separated streams of research by providing a novel combinatory-methodology framework approach by combining relevant tests, measures and methods premised to achieve a conclusive analysis.

Therefore, we elaborate on the essences of theory in more detail than stated within other publications in order to create comparability and transparency in hindsight of our empirical analysis, which strictly follows the theoretical premises presented. Such a deeper elucidation of theory should also build a basis for future empirical analysis within the respective field in hindsight of financial data analysis.

Therefore, we conduct a respective analysis of the daily wavelet-filtered (denoised) S&P 500 returns (2000–2020) and compare it with respective surrogate data sets (ft, aaft and iaaft) as well as a Brownian motion return realisation and a Lorenz system realisation through the application of the aforementioned combinatory-methodology approach. Our findings indicate that the S&P 500 returns display hyperchaotic behaviour, which is almost equally divided into deterministic and stochastic chaos. Additionally, we derive a graphical representation of its strange chaotic attractor. Furthermore, we elaborate on the implications of this finding, namely that the predictability of it is only possible on short-time scales up to the expiration of the Lyapunov time, rendering financial forecasts exceeding this time-period impossible and futile. In order to forecast the time period before the S&P 500 returns descend into chaos, all initially mentioned stylised facts and other characteristics need to be accounted for, meaning that for this slight time window, all knowledge gathered in the academic literature about financial and risk modelling is relevant and applicable for respective implementations.

6.2. Limitations and Prospects of the Study

Within this study, we present a novel and powerful combinatory-methodology approach to determine chaotic dynamics in financial time series more effectively, enabling other scholars to avoid inconclusive or stained results due to misspecifications or partly missing methods, and as a reaction to Kantz & Schreiber (2003). Further, we state a vast body of literature as our reference, while, at the same time, conducting state-of-the-art analysis in order to contribute towards conclusive future results. Nevertheless, without misconduct, we also need to elaborate on potential shortcomings. At first, we want to discuss the critique of BenSaïda (2014) as well as that of Sandubete and Escot (2020), elucidating on the differences regarding sampling frequency and choice of time scale.

Even if we intentionally pick daily return series to demonstrate the possibility of conducting successful analysis with this time scale, we do not elaborate on the sub-dynamics on different time scales of the S&P 500 return series being studied. Therefore, we cannot exclude the possibility of diverging dynamics on different time scales referring to this specific system, or other time series in general. Furthermore, we neglect the development of a statistical significance test in order to determine the stated temporal correlations to be analysis destroying or acceptable. Additionally, we do not implement neural network classification, forecasting or respective chaos control algorithms ourselves in order to gain deeper insights into the time series being regarded.

Moreover, we only state the diverging streams of research without providing an in-depth analysis of the reasons and periods of this separation. In addition, we neither present the implications of the methods within each of the displayed research communities in hindsight of nonlinear dynamics nor do we analyse potential guidance for future unification of these fields. Finally, we do not elaborate deeper on possible combinations of state-of-the-art financial modelling attempts with previously determined nonlinear dynamical analysis approaches and their interaction with stated communities of research.

6.3. Theoretical Implications

Following the course of this study, we display an encompassing variety of methods to determine the true nature of the dynamics of a financial time series, i.e., the S&P 500 daily returns. In order to conduct the analysis, several mathematical prerequisites, as described in section 3, must be fulfilled. Among those requirements, we adopt a mostly[60] topological stance based on diffeomorphisms (see 3.1.3) in order to aim for a relevant reconstruction. Following Takens (1981) as well as Hirsch (1997), the computation of phase space topology of a dynamical system (e.g., a financial market) from a scalar data set (e.g., time series) prerequisites an accurate methodology in order to achieve a successful reconstruction.

Nonetheless, reconstruction processes involve a diversity of free parameters and the computation of according homology[61] for a large number of scenarios, which reveals to be demanding at the very least (Garland et al., 2016). For reconstruction by delay-embeddings (i.e., Takens's approach), a full diffeomorphic reconstruction is a mathematical underlying assumption (Garland et al., 2016). Nevertheless, following Edelsbrunner et al. (2000) and Robins (2002), the homology of data-driven underlying invariant sets contaminated by noise is resolvable by witness complexes, resulting in a respective reconstruction, even if the reconstruction dimension is below the threshold for assurance of topological conjugacy between the true and reconstructed dynamics, as specified by the embedding theorems. Following Garland et al. (2016), this insight reveals a computationally less demanding method[62], since reconstruction requirements for homology are less strict. In other words, reconstructing homology requires only homeomorphisms in contrast to the pertaining diffeomorphisms prerequisite by traditional embedding theorems, such as those we apply in this study.

Apart from the computational scarcity of the homology approach, the traditional reconstruction of a time series is very complex, since free parameter choices need to be conducted for an incomplete single trajectory of the system only represented via the latter time series (Garland et al., 2016).

[60] With the exception of some minor metrical definitions.
[61] General association of sequences of algebraic objects (e.g., groups) to other mathematical objects (e.g., topological spaces).
[62] In computational topology, the Conley-index of isolating neighbourhoods is applied to study dynamical invariants (Garland et al., 2016).

Further, it is not covered by the respective parameter decision-making guidance of traditional embedding theorems (e.g., Takens's delay-time embedding) whatsoever (Garland et al., 2016). Moreover, following Garland et al. (2016), a reduced invariant reconstruction method is sufficient in order to extract the topological structures of interest, in contrast to the delay-embedding premises of Takens (1981), Packard et al. (1980) and Sauer et al. (1991), which state equality of the reconstructed attractor and the original attractor only in the case of diffeomorphism. In addition, dimensionality of the real system, represented via a finite time series, is unknown and the determination of an according embedding dimension[63] is not without critical hindrances, as stated in section 3.4.

Following the homology approach would also render the dissection of a valid τ redundant, since important attractor-properties (e.g., transitivity, continuity, recurrence and entropy) are topological in nature and therefore extractable via homeomorphisms (Mischaikow et al., 1999). Further theoretical ambitions can be directed towards applying astrophysical conceptions on scalar time series data in order to dissect adiabatic energy diffusion for a respective financial system (Jarzynski, 1994). Following Jarzynski's (1994) elaboration on the possibility of determining the chaotic evolution and diffusion times within the respective financial system yields severe implications on forecasting and control capabilities.

From an empirical point of view, the academic literature mostly only considers one time scale (e.g., daily series) within their respective studies. This, according to Sandubete and Escot (2020), may represent a sampling interval that is too long for financial time series. This is also covered by BenSaïda (2014), who states that different dynamics apply for different time scales of financial data being regarded. Hence, an intra-day frequency data set may propose varying results than daily data sets. The choice of a sufficient sampling interval and the regard of all relevant time scales at once may render the referring loss of information less dire, as well as partly solve the inconclusiveness in the stated literature (see 2.3) (Sandubete & Escot, 2020).

6.4. Forecasting Implications

To recapitulate, Çoban and Büyüklü (2009) state that chaotic dynamics display deterministic yet unpredictable patterns. After the expiration of the Lyapunov time, no further prediction of the system is possible even if the computational capacities are increased (Shevchenko, 2018). Therefore, since we reveal sufficient empirical indications of chaoticity in the S&P 500 return series, we deem it an utmost necessity to elaborate on the implications of findings in the academic literature (see 2.3), stating financial time series to be of a chaotic nature as a result.

[63] For further details, please refer to Kennel et al. (1992).

In section 5.5, we show the existence of two positive Lyapunov exponents, indicating hyperchaotic behaviour that may result in crises and breakdowns. Following Kozłowska et al. (2016), evidence of determination of warning indicators based on catastrophic bifurcation points for unpredictable financial systems are presented. These bifurcations lead to volatility clusters under a timely evolution, displaying critical dynamics caused by small perturbations to evoke drastic consequences (Gaunersdorfer et al., 2008). Such regime shifts occur as intricate, complex occurrences caused by the aforementioned catastrophic bifurcations; hence, they represent tipping points or sudden shifts into a crisis (Kozłowska, et al., 2016). According to Matia and Yamasaki (2005), the bifurcation points are artificial and caused by the distributions of trade sizes to follow specified power laws, whose exponents originate from Lévy stable domains. Nevertheless, regarding the financial crisis of 2008, critical indications in terms of bifurcation points include the notable months ahead of the crisis's occurrence (Kozłowska, et al., 2016).

Pivoting towards the predictability of a financial system itself, nearest neighbour algorithms are stated to produce acceptable results for chaotic systems (e.g., in the case of a one-neighbour algorithm, it takes the past, whose resemblance with today's system state is the highest and assumes it for the future) (Guégan & Leroux, 2009). However, regarding the severity of chaoticity in financial systems in terms of forecasting, Matilla-García and Marín's (2010) work reveals a lack of varying testing procedures to test for complex chaotic processes. In recent years, neural network technologies due to high computational capabilities are on the rise (e.g., Tkac & Verner, 2016). However, early attempts to challenge chaotic behaviour with neural networks can be found in the work of Chapeau-Blondeau (1993). Further, implementing standard deep neural networks can be used to simulate and determine several time series, which are chaotic in nature (Boullé et al., 2020). A referring generalisation by convolutional neural networks without batch normalisation layers outperforms respective state-of-the-art neural networks for time series classifications in hindsight of chaos determination attempts (Boullé et al., 2020). A convolutional neural network with large kernel size (LKCNN) is capable of assimilating the chaotic characteristics of a dynamical system and classifying respective time series with high accuracy (Boullé et al., 2020). Furthermore, recurrent reinforcement learning (RRL) techniques, alongside staked deep dynamical recurrent reinforcement learning (SDDRRL), can be applied to control chaos in portfolio optimisations[64] (Aboussalah & Lee, 2020). For the processing of digital currencies, Altan et al. (2019) implement a hybrid solution with respect to reduction of negative eventualities. However, chaotic nature combined with measurement limitations of the initial state and sensitive dependence constitute an undeniable upper bound on the forecasting abilities for such systems, even if the respective models are sufficient as stated before, thus allowing predictions only on short time-scales (Barkoulas et al., 2012).

[64] See the rolling horizon mean-variance-optimisation (MVO), the rolling horizon risk-parity model and the uniform buy-and-hold (UBAH) index. Kolm et al. (2014) grant a sophisticated overview of portfolio optimisation literature.

Cecen and Erkal (1996) already take on the short-term predictability as well as its consequences, and state the applicability of nonlinear deterministic functions as possible solution for the assumption of low-dimensional chaos in foreign exchange markets. Exceeding the aim of so-called simple classifications, Chai and Lim (2016) propose a neural network solution with weighted fuzzy membership functions in order to predict business cycles. By empirically deducting Bayesian regression with normal as well as double-exponential priors, which are highly correlated with principal component forecasts, DeMol and Reichlin (2016) show promising results working with time series data. Lahmiri and Bekiros (2019) implement novel ideas with a cryptocurrency forecasting approach with deep learning chaotic neural networks, while chaos-based models with kernel predictors (i.e., support vector machines) to reduce prediction errors in chaotic time series are executed by Huang et al. (2010).

Another data-driven approach to challenge the predictability of chaos is exhibited in Guo et al.'s (2008) work as they bring up chaos-evolutionary-programming algorithms (CEPA), merging a modified chaotic optimisation algorithm (COA) with a modified evolutionary- programming algorithm (EPA). Procedures that are considered to be more exotic exploit chaotic particle swarm optimisations for data clustering, as presented in Chuang et al. (2011), while a more basic attempt by identifying intrinsic characteristics of high-dimensional financial data with kernel entropy manifold learning can be seen in Huang and Kou (2014, 2017). Another powerful method of determination of chaotic time series is called power spectral analysis. Following Brandstater and Swinney (1987), chaotic time series are characterised by broadband spectra and, according to Fenstermacher et al. (1979), these spectra are intrinsic for either chaotic or stochastic time series, accordingly Therefore, Cao et al. (1995) go on to state the superiority of wavelet neural networks (WNNs) to forecast chaotic time series, which is enhanced by ensemble empirical mode decomposition (EEMD) into WNNs with random time (WNNRT) in the hybrid prediction model for commodity and energy prices by Yang and Wang (2021). A sophisticated overview of econophysically concepts can be found in Chakraborti et al. (2011).

6.5. Chaos Control

Parallel to the thought of accepting chaoticity and aiming towards classifications and so-called before-chaos predictions as stated in the previous section, following Grebogi and Lai (1997), early impactful reviews about the idea of controlling chaotic dynamics exist. We state examples of control algorithms and schemes in Table 17. Since chaotic responses increase uncertainty in financial systems, control schemes, synchronisation models[65] or suppression algorithms applied to hyperchaotic economical systems[66] may yield the respective resolutions (Jahanshahi et al., 2019, 2019a, 2019b).

[65] See Zaho et al. (2011).
[66] For more on multifractals and their scaling laws, refer to Paladin and Vulpiani (1987).

We will not elaborate further on this subject due to the scope of this study, yet we state that the field of chaos control for financial markets is still under-represented and can produce interesting future prospects.

Table 17: Overview of chaos control possibilities.

Author	Short Description
Hajiiloon et al. (2018)	Chaos control algorithm for unknown discrete time chaotic system employed to reconstruct delayed phase space.
Tirandaz et al. (2018); Fuh et al. (2012)	Feedback linearisation.
Shukla & Sharma (2017); Yu et al. (2017)	Backstepping method.
Jahanshahi et al. (2019a); Mahmoodabadi & Jahanshahi (2016)	Intelligent control.
Jahanshahi et al. (2019b); Jahanshahi (2018)	Adaptive control.
Tsai et al. (2018); Jahanshahi et al. (2018a)	Nonlinear sliding mode control.
Holyst & Urbanowicz (2000); Vargas et al. (2015); Jararmi et al. (2017); Dadras & Momeni (2010); Wang et al. (2012)	Behavioural control of hyperchaotic financial systems.
Khan & Bhat (2017)	Control input limitations and external disturbances.
Du et al. (2010)	Chaos stabilisation by phase space compression.

6.6. Frontiers and Future Remarks

During the literature analysis, as well as during the empirical determination of our results, we recognise several frontiers of research in terms of financial nonlinear dynamical analysis and chaos research. To mention a few, we would like to note potential possibilities of enhancement in the academic literature in terms of testing the "micro-foundations of across scale-causal heterogeneity" as the basis for trader behaviour, as stated in Bekiros and Marcellino (2013). Further, we see potential in the application of wavelet neural network solutions (e.g., Lahmiri & Bekiros, 2019) as well as in the implementation of neural networks for the determination of embedding dimensions, as presented in Maus and Sprott (2011). Moreover, regarding other fields of research, namely quantum finance, which extends the formalism of quantum mathematics into the regime of quantitative (financial) modelling, we see promising implications (e.g., representing financial instruments by non-normalisable state vectors, which are elements of time dependent Hilbert spaces), as presented in Baaquie and Belal (2013).

We will leave the determination of sub-dynamics on differing time scales, the deduction of methodology for the application of adiabatic and diffusion chaos measures for time series data and elaborations on the stability dynamics of the chaos measures themselves to future research and hint at interests in the potential impacts of our findings on financial reports and banking regulation.

References

Abarbanel, H. (1996). *Analysis of Observed Chaotic Data.* New York: Springer.

Abarbanel, H., Brown, R., & Kadtke, J. (1990). Prediction in chaotic nonlinear systems: methods for time series with boadband Fourier spectra. *Physical Review A*, (41): 1782.

Abarbanel, H., Brown, R., & Kennel, M. (1991). Lyapunov exponents in chaotic systems: their importance and their evaluation using observed data. *International Journal of Modern Physics B*, (5)(9): 1347-1375.

Abarbenel, H., Brown, R., Sidorowich, J., & Tsimring, L. (1993). The analysis of observed chaotic data in physical systems. *Reviews of Modern Physics*, (65): 1331.

Abhyankar, A., Copeland, L., & Wong, W. (1995). Nonlinear Dynamics in Real-Time Equity Market Indices: Evidence from the United Kingdom. *Economic Journal*, (105)(431): 864-80.

Aboussalah, A. M., & Lee, C.-G. (2020). Continuous control with Stacked Deep Dynamic Reccurent Reinforcement Learning for portfolio optimization. *Expert Systems with Applications*, (140): 112891.

Abraham, A., Nath, B., & Mahanti, P. (2001). Hybrid intelligent systems for stock market analysis. *Computational Science, ICSS*, 337-345.

Abraham, C., Biau, G., & Carde, B. (2004). On Lyapunov exponent and sensitivity. *Journal of Mathematical Analysis and Applications*, (290): 395-404.

Abuaf, N., & Jorion, P. (1990). Purchasing power parity in the long run. *Journal of Finance*, (45): 157-174.

Abu-Mostafa, Y., Atiya, A., Magdon-Ismail, M., & White, H. (2001). Introduction to the special issue on neural networks in financial engineering. *IEEE Transactions on Neural Networks*, (12): 653-655.

Adachi, M. (1993). *Embeddings and Immersions.* American Mathematical Society.

Adler, M., & Lehmann, B. (1983). Deviations from purchasing power parity in the long run. *Journal of Finance*, (38): 1471-1487.

Adrangi, B., Chatrath, A., Dhanda, K., & Raffiee, K. (2001). Chaos in futures prices? Evidence from futures markets. *Energy Economics*, (23): 405-425.

Afraimovich, V. (1997). Pesin's dimension for Poincaré recurrences. *Chaos*, (7)(1): 12-20.

Afraimovich, V., Chazottes, J.-R., & Saussol, B. (2000). Local dimensions for Poincaré recurrences. *Electronic Research Announcements*, (6): 64-74.

Agliari, A., Gardini, L., & Puu, T. (2005). Some global bifurcations related to the appearance of closed invariant curves. *Mathematics and Computers in Simulation*, (68): 201-219.

Agnolucci, P. (2009). Volatility in crude oil futures: a comparison of the predictive ability of GARCH and implied volatility models. *Energy Economics*, (31): 316-321.

Aguilar-Rivera, R., Valenzuela-Rendón, M., & Rodríguez-Ortiz, J. (2015). Genetic algorithms and Darwinian approaches in financial applications: A survey. *Expert Systems with Applications*(42), 7684-7697.

Aguirre, L. A., & Billings, S. (1995). Identification of models for chaotic systems from noisy data: implications for performance and nonlinear filtering. *Physica D*, (85): 239-258.

Aït-Sahalia, Y., & Mancini, L. (2008). Out of Sample Forecasts of Quadratic Variation. *Journal of Econometrics*, (147): 17-33.

Albano, A., Muench, J., Schwartz, C., Mees, A., & Rapp, P. (1988). Singular value decomposition and the Grassberger-Procaccia algorithm. *Physical Review A*, (38): 3017-3026.

Alligood, K., Yorke, J., & Sauer, T. (2009). *Chaos: An Introduction to Dynamical Systems.* New York: Springer.

Altan, A., Karasu, S., & Bekiros, S. (2019). Digital currency forecasting with chaotic meta-heuristic bio-inspired signal processing techniques. *Chaos, Solitons and Fractals*, (126): 325-336.

Andersen, T., & Bollerslev, T. (1998). Answering the skeptics: Yes, standard volatility models do provide accurate forecasts. *International Economic Review*, (39): 885-905.

Andrews, D. (1991). Heteroskedasticity and autocorrelation consistent covariance matrix estimation. *Econometrica*, (59): 817-858.

Andrews, D., & Ploberger, W. (1994). Optimal Tests when a Nuisance Parameter is Present Only Under the Alternative. *Econometrica*, (62): 1383-1414.

Anishchenko, V., Vadivasova, T., Postnov, D., & Safonova, M. (1992). Synchronization of chaos. *International Journal of Bifurcation and Chaos*, (2): 633.

Arbabi, S., Nazari, A., & Darvishi, M. T. (2017). A two-dimensional Haar wavelets method for solving systems of PDEs. *Applied Mathematics and Computation*, (292): 33-46.

Argyris, J., & Andreadis, I. (1998). The influence of noise on the correlation dimension of chaotic attractors. *Chaos, Solitons and Fractals*, (9)(3): 343-361.

Arthur, W. (1999). Complexity and the economy. *Science*, (284): 107-109.

Aziz, I., & Amin, R. (2016). Numerical solution of a class of delay differential and delay partial differential equations via Haar wavelet. *Applied Mathematical Modelling*, (0): 1-14.

Aziz, I., & Siraj-ul-Islam. (2013). New algorithms for the numerical solution of nonlinear Fredholm and Volterra integral equations using Haar wavelets. *Journal of Computational and Applied Mathematics*, (239): 333-345.

Aziz, I., Siraj-ul-Islam, & Asif, M. (2017). Haar wavelet collocation method for three-dimensional elliptic partial differential equations. *Computers and Mathematics with Applications*, (73)(9): 2023-2034.

Baaquie, B. E. (2013). Financial modeling and quantum mathematics. *Computers and Mathematics with Applications*, (65)(10): 1665-1673.

Badii, R., & Politi, A. (1985). Statistical description of chaotic attractors: The dimension function. *Journal of Statistical Physics*, (40): 725-750.

Badii, R., Broggi, G., Derighetti, B., Ravani, M., Ciliberto, S., Politi, A., & Rubio, M. (1988). Dimension increase in filtered chaotic signals. *Physical Review Letters*, (60): 979-982.

Bajo-Rubio, O., F., F.-R., & Sosvilla-Riverio, S. (1992). Chaotic behaviour in exchange-rate series: first results for the Peseta-U.S. Dollar case. *Economics Letters*, (39): 207-211.

Balke, N., & Fomby, T. (1997). Threshold cointegration. *International Economic Review*, (38): 627-645.

Bao, D., & Yang, Z. (2008). Intelligent stock trading system by turning point confirming and probabilistic reasoning. *Expert Systems with Applications*, (34): 620-627.

Baptista, M. (1998). Cryptography with chaos. *Physics Letters A*, (240): 50-54.

Barberis, N., Shleifer, A., & Vishny, R. (1998). A model of investor sentiment. *Journal of Financial Economics*, (49): 307-343.

Barkoulas, J. T., Chakraborty, A., & Ouandlous, A. (2012). A metric and topological analysis of determinism in the crude oil spot market. *Energy Economics*, (34): 584-591.

Barnett, W. A., Gallant, A. R., Hinich, M. J., Jungeilges, J. A., Kaplan, D. T., & Jensen, M. J. (1995). Robustness of nonlinearity and chaos tests to measurement error, inference method, and sample size. *Journal of Economic Behavior & Organization*, (27): 301-320.

Barnett, W. A., Gallant, R. A., Hinich, M. J., Jungeilges, J. A., Kaplan, D. T., Kaplan, D. T., & Jensen, M. J. (1997). A single-blind controlled competition among tests for nonlinearity and chaos. *Journal of Econometrics*, (82): 157-192.

Barnett, W., Gallant, A., Hinich, M., Jungeilges, J., Kaplan, D., & Jensen, M. (1997). A single-blind controlled competition among tests for nonlinearity and chaos. *Journal of Econometrics*, (82): 157-192.

Barreira, L., & Saussol, B. (2001). Hausdorff dimension of measures via Poincaré recurrence. *Communications in Mathematical Physics*, (219)(2): 443-463.

Bask, M. (2002). A positive Lyapunov exponent in Swedish exchange rates? *Chaos, Solitons and Fractals*, (14): 1295-1304.

Bask, M., & Gençay, R. (1998). Testing chaotic dynamics via Lyapunov exponents. *Physica D*, (114): 1-2.

Bekiros, S., & Marcellino, M. (2013). The multiscale causal dynamics of foreign exchange markets. *Journal of International Money and Finance*, (33): 282-305.

Belkin, M., & Niyogi, P. (2003). Laplacian eigenmaps for dimensionality reduction and data representation. *Neural Computation*, (15)(6): 1373-1396.

Beltratti, A., & Stulz, R. M. (2019). Why is contagion asymmetric during the European sovereign crisis? *Journal of International Money and Finance*(99-C).

BenSaïda. (2014). Noisy chaos in intraday financial data: Evidence from the American index. *Applied Mathematics and Computation*, (226): 258-265.

BenSaïda, A. (2012). Are financial markets stochastic: a test for noisy chaos. *American International Journal of Contemporary Research*, (2)(8): 57-68.

BenSaïda, A., & Litimi, H. (2013). High level chaos in the exchange and index markets. *Chaos, Solitons and Fractals*, (54): 90-95.

Berghorn, W. (2015). Trend Momentum. *Quantitative Finance*(15), 261-284.

Biernacki, P., & Waldorf, D. (1981). Snowball sampling: Problems and techniques of chain referral sampling. *Sociological Methods and Research*(10), 141-163.

Black, F., & Scholes, M. (1973). The pricing of options and corporate liabilities. *Journal of Political Economy*, (59): 817-858.

Blondel, V. D., Guillaume, J.-L., Lambiotte, R., & Lefebvre, E. (2008). Fast unfolding of communities in large networks. *Journal of Statistical Mechanics in : Theory and Experiment (10)*, 1000.

Bodnar, T., & Hautsch, N. (2016). Dynamic conditional correlation multiplicative error process. *Journal of Empirical Finance*(36), 41-67.

Bogoliubov, N., & Krylov, N. (1937). La theorie generalie de la mesure dans son application a l'etude de systemes dynamiques de la mecanique-non-lineaire. *Annals of Mathematics Second Series (in French)*, (38)(1): 65-113.

Boullé, N., Dallas, V., Nakatsukasa, Y., & Samaddar, D. (2020). Classification of chaotic time series with deep learning. *Physica D: Nonlinear Phenomena*, (403): 132261.

Bradley, E., & Kantz, H. (2015). Nonlinear time-series analysis revisited. *Chaos*, (25): 097610.

Brandstater, A., & Swinney, H. (1987). Strange attractors in weakly turbulent Couette-Taylor flow. *Physical Review A*, (35): 2207-2220.

Brandt, C., & Pompe, B. (2002). Permutation entropy: a natural complexity measure for time series. *Physical Review Letters*, (88): 174102.

Briner, R. B., & Deyner, D. (2012). Systematic Review and Evidence Synthesis as a Practice and Scholarship Tool. In: Denise M. Rousseau (Hg.): The Oxford handbook of evidence-based management. *Oxford Univ. Press*, 112-129.

Brock, W., & Hommes, C. (1997). A rational route to randomness. *Econometrica*, (65): 1059-1095.

Brock, W., & Hommes, C. (1998). Heterogeneous beliefs and routes to chaos in a simple asset pricing model. *Journal of Economics Dynamics and Control*, (22): 1235-1274.

Brock, W., & Malliaris, A. (1989). *Differential Equations, Stability and Chaos in Dynamic Economics.* Amsterdam: Elsevier.

Brock, W., & Sayers, C. (1988). Is the business cycle characterized by deterministic chaos? *Journal of Monetary Economics*, (22): 71-90.

Brock, W., Dechert, W., Scheinkman, J., & LeBaron, B. (1996). A test for independence based on the correlation dimension. *Econometric Reviews*, (15): 197-235.

Brogliato, B., Lozano, R., Maschke, B., & Egeland, O. (2007). *Dissipative Systems Analysis and Control. Theory and Applications.* London: Springer.

Broomhead, D., & King, G. (1986). Extracting qualitative dynamics from experimental data. *Physica D*, (20): 217-236.

Cai, G., & Huang, J. (2007). A New Finance Chaotic Attractor. *International Journal of Nonlinear Science*, (3)(3): 213-220.

Cao, L. (1997). Practical method for determining the minimum embedding dimension of a scalar time series. *Physica D*, (110)(1-2): 43-50.

Cao, L., Hong, Y., Fang, H., & He, G. (1995). Predicting chaotic time series with wavelet networks. *Physica D*, (85): 225-238.

Carvalho, A., Langa, J., & Robinson, J. (2013). *Attractors for infinite-dimensional non-autonomous dynamical systems.* New York: Springer.

Casdagli, M. (1989). Nonlinear prediction of chaotic time series. *Physica D*, (35): 256-335.

Casdagli, M. (1992). Chaos and deterministic versus stochastic nonlinear modeling. *Journal of the Royal Statistical Society*, (54)(2): 303-328.

Casdagli, M., Eubank, S., Farmer, J., & Gibson, J. (1991). State space reconstruction in the presence of noise. *Physica D*, (51)(1-3): 52-98.

Cecen, A. A., & Erkal, C. (1996). Distinguishing between stochastic and deterministic behavior in high frequency foreign exchange rate returns: Can non-linear dynamics help forecasting? *International Journal of Forecasting*, (12): 465-473.

Celeste, V., Corbet, S., & Gurdgiev, C. (2019). Fractal dynamics and wavelet analysis: Deep volatility and return properties of Bitcoin, Ethereum and Ripple. *The Quarterly Review of Economics and Finance*.

Cencini, M., Cecconi, E., & Vulpiani, A. (2010). Chaos from Simple Models to Complex Systems. *World Scientific*, (17).

Chai, S. H., & Lim, J. S. (2016). Forecasting business cycle with chaotic time series based on neural network with weighted fuzzy membership functions. *Chaos, Solitons and Fractals*, (0): 1-9.

Chakraborti, A., Toke, I. M., Patriarca, M., & Abergel, F. (2011). Econophysics review: I. Empirical facts. *Quantitative Finance*, (11): 991-1012.

Chakraborti, A., Toke, I. M., Patriarca, M., & Abergel, F. (2011). Econophysics review: II. Agent-based models. *Quantitative Finance*, (11): 1013-1041.

Chang, S., Grace, S., Yu, B., & Vetterli, M. (2000). Adaptive wavelet thresholding for image denoising and compression. *IEEE Transactions*, 1532-1546.

Chapeau-Blondeau, F. (1993). Analysis of Neural Network with Chaotic Dynamics. *Chaos, Solitons and Fractals*, (3)(2): 133-139.

Charfeddine, L. (2014). True or spurious long memory in volatility: Further evidence on the energy futures markets. *Energy Policy*(71-C), 76–93.

Chen, G., & Dong, X. (1998). From chaos to order: methodologies, perspectives and applications. *World Scientific Series on Nonlinear Science Series A*.

Chen, G., Mao, Y., & Chui, C. (2004). A symmetric image encryption scheme based on 3D chaotic cat maps. *Chaos, Solitons and Fractals*, (12): 749-761.

Chiarella, C., & He, X.-Z. (1999). Heterogeneous beliefs, risk and learning in a simple asset price model. *Research Paper 18, Quantitative Finance Research Group, University of Technology, Sydney*.

Chichilnisky, G., Heal, G., & Lin, Y. (1995). Chaotic price dynamics, increasing returns and the Phillips curve. *Journal of Economic Behavior and Organization*, (27): 279-291.

Chuang, L.-Y., Hsiao, C.-J., & Yang, C.-H. (2011). Chaotic particle swarm optimization for data clustering. *Expert Systems with Applications*, (38): 14555-14563.

Chuong, N. M. (2005). Nonlinear evolution operators and wavelets. *Nonlinear Analysis*, (63): e65- e75.

Çoban, G., & Büyüklü, A. H. (2009). Deterministic flow in phase space of exchange rates: evidence of chaos in filtered series of Turkish Lira-Dollar daily growth rates. *Chaos, Solitons and Fractals*, (42)(2): 1062-1067.

Coddington, E., & Levinson, N. (1955). *The Poincaré-Bendixson Theory of Two-Dimensional Autonomous Systems - Theory of Ordinary Differential Equations.* New York: McGraw-Hill.

Costa, M., Goldberger, A., & Peng, C.-K. (2005). Multiscale entropy analysis of biological signals. *Physical Review E*, (71)(2): 021906.

Crowley, P. M. (2007). A Guide to Wavelets for Economists. *Journal of Economic Surveys*, (21)(2): 207-267.

Dadras, S., & Momeni, H. (2010). Control of a fractional-order economical system via sliding mode. *Physica A*, (389): 2434-42.

Damming, M., & Mitschke, F. (1993). Estimation of Lyapunov exponents from time series: The stochastic case. *Physics Letters A*, (178): 385-394.

Danilenko, A., & Silva, C. (2009). *Ergodic Theory: Non-singular Transformations. In: Meyers R. (eds) Encyclopedia of Complexity and Systems Science.* New York: Springer.

Darbyshire, A., & Broomhead, D. (1996). Robust estimation of tangent maps and Lyapunov spectra. *Physica D*, (89): 287.

Das, A., & Das, P. (2007). Chaotic analysis of the foreign exchange rates. *Applied Mathematics and Computation*, (185)(1): 388-396.

De Luca, G., Dominique, G., & Giorgia, R. (2019). Assessing tail risk for nonlinear dependence of MSCI sector indices: A copula three-stage approach. *Finance Research Letters*, (30): 327-333.

De Mol, C., & Reichlin, L. (2008). Forecasting using a large number of predictors: Is Bayesian shrinkage a valid alternative to principal components? *Journal of Econometrics*, (146): 318-328.

Dechert, W. D., & Gençay. (1996). The topological invariance of Lyapunov exponents in embedded dynamics. *Physica D*, (90): 40-55.

Dechert, W., & Gençay, R. (1992). Lyapunov exponents as a nonparametric diagnostic for stability analysis. *Journal of Applied Econometrics*, (7): 41-60.

Dechert, W., & Gençay, R. (2000). Is the largest Lyapunov exponent preserved in embedded dynamics? *Physics Letters A*, (276): 59-64.

DeGrauwe, P., & Dewachter, H. (1993). A chaotic model of the exchange rate: The role of fundamentalists and chartists. *Open Economics Review*, (4): 351-379.

DeGrauwe, P., Dewachter, H., & Embrechts, M. (1993). *Exchange Rate Theory: Chaotic Models of Foreign Exchange Markets.* London: Blackwell.

Devaney, R. (1989). *An introduction to chaotic dynamical systems.* Cambridge: Addison Wesley.

Ding, M., Grebogi, C., Ott, E., Sauer, T., & Yorke, J. A. (1993). Estimating correlation dimension from a chaotic time series: when does plateau onset occur? *Physica D*, (69): 404-424.

Donoho, D., & Johnstone, I. (1994). Ideal spatial adaption by wavelet shrinkage. *Biometrika*, (81)(3): 425-455.

Donoho, D., & Johnstone, J. (1995). Adapting to unknown smoothness via wavelet shrinkage. *Journal of the American Statistical Association*, (90)(432): 1200-1244.

Du, J., Huang, T., Sheng, Z., & Zhang, H. (2010). A new method to control chaos in an economic system. *Applied Mathematics and Computation*, (217): 2370-2380.

Dzieliński, M., Rieger, M. O., Tonn, & Talpsepp. (2018). Asymmetric attention and volatility asymmetry. *Journal of Empirical Finance*, (45): 59-67.

Eckman, J., Kamphorst, S., Ruelle, D., & Ciliberto, S. (1986). Lyapunov exponents from time series. *European Economic Review*, (50): 1-33.

Eckmann, J., & Ruelle, D. (1985). Ergodic theory of chaos and strange attractors. *Reviews of Modern Physics*, (57)(3): 617-656.

Eckmann, J.-P., Kamphorst, S., & Ruelle, D. (1987). Recurrence plots of dynamical systems. *Europhysics Letters*, (5): 973-977.

Edelsbrunner, H., Letscher, D., & Zomorodian, A. (2000). Topological persistence and simplification. *IEEE Symposium on Foundations of Computer Science*, 454-463.

Eubank, J., Farmer, D., & Jen, E. (. (1990). *An Introduction to Chaos and Randomness.* USA: 1989 Lectures in Complex Systems, SFI Studies in the Sciences of Complexity, Vol. II, Jen E (ed.). Addison-Wesley.

Faggini, M. (2014). Chaotic time series analysis in economics: balance and perspectives. *Chaos*, (24)(4).

Farmer, J., & Sidorowich, J. (1987). Predicting chaotic time series. *Physical Review Letters*, (59): 845.

Feller, W. (1949). Fluctuation theory of recurrent events. *Transactions of the American Mathematical Society*, (67): 98-119.

Fenstermacher, P., Swinney, H., & Gollub, J. (1979). Dynamical instabilities and the transaction to chaotic Taylor vortex flow. *Journal of fluid Mechanics*, (94): 103-128.

Fernández-Rodríguez, F., Sosvilla-Rivero, S., & Andrada-Félix, J. (2005, March 31). Testing chaotic dynamics via Lyapunov exponents. *Journal of Applied Econometrics*, (20): 911-930.

Frank, M., & Stengos, T. (1988). Some evidence concerning macroeconomic chaos. *Journal of Monetary Economics*, (22): 423-438.

Fraser, A., & Swinney, H. (1986). Independent coordinates for strange attractors from mutual information. *Physical Review A*, (33)(2): 1134-1140.

Fuh, C.-C., Tsai, H.-H., & Yao, W.-H. (2012). Combining a feedback linearization controller with a disturbance observer to control a chaotic system under external excitation. *Communications in Nonlinear Science and Numerical Simulation*, (17): 1423-9.

Gao, Q., & Ma, J. (2009). Chaos and Hopf bifurcation of a finance system. *Nonlinear Dynamics*, (58): 209.

Garcin, M., & Guégan, D. (2014). Probability density of the empirical wavelet coefficients of a noisy chaos. *Physica D*, (276): 28-47.

Garcin, M., & Guégan, D. (2016). Wavelet shrinkage of a noisy dynamical system with non-linear noise impact. *Physica D*, (325): 126-145.

Garfield, E. (1979). Is citation analysis a legitimate evaluation tool? *Scientometrics*, 1(4): 359-375.

Garland, J., Bradley, E., & Meiss, D. J. (2016). Exploring the topology of dynamical reconstructions. *Physica D*, (334): 49-59.

Gaunersdorfer, A., Hommes, C. H., & Wagener, F. O. (2008). Bifurcation routes to volatility clustering under evolutionary learning. *Journal of Economic Behavior & Organization*, (67): 27-47.

Gençay, R. (1996). A statistical framework for testing chaotic dynamics via Lyapunov exponents. *Physica D*, (89): 423-438.

Gençay, R., & Dechert, W. (1992). An algorithm for the n Lyapunov exponents of an n-dimensional unknown dynamical system. *Physica D*, (59): 142-157.

Gençay, R., & Dechert, W. (1996). The identification of spurious Lyapunov exponents in Jacobian algorithms. *Studies in Nonlinear Dynamics and Econometrics*, (1): 145-154.

Gençay, R., Selçuk, F., & Whitcher, B. (2001). *An Introduction to Wavelets and Other Filtering Methods in Finance and Economics.* New York, USA: Academic Press.

Giunti, M., & Mazzola, C. (2012). Dynamical systems on monoids: Toward a general theory of deterministic systems and motion. *In Mintai G., Abram M., Pessa E. (eds.), Methods, models, simulations and approaches towards a general theory of change, Singapore: World Scientific*, 173-185.

Gong, & Xu, L. B. (2018). The incremental information content of investor fear gauge for volatility forecasting in the crude oil futures market. *Energy Economics*, (74): 370-386.

Grandmont, J. (1985). On endogenous competitive business cycles. *Econometrica*, (5): 995-1045.

Grassberger, P., & Procaccia, I. (1983). Measuring the strangeness of strange attractors. *Physica 9D*, 189-208.

Grassberger, P., & Procaccia, I. (1983a). Characterization of strange attractors. *Physica Review Letters*, (50): 346-394.

Grebogi, C., & Lai, Y.-C. (1997). Controlling chaotic dynamical systems. *Systems & Control Letters*, (31): 307-312.

Grebogi, C., Ott, E., & Yorke, J. (1987). Chaos, Strange Attractors, and Fractal Basin Boundaries in Nonlinear Dynamics. *Science*, (238)(4827): 632-638.

Grebogi, C., Ott, E., Pelikan, S., & Yorke, J. (1984). Strange attractors that are not chaotic. *Physica 13D*, 261-268.

Guckenheimer, J., & Holmes, P. (1983). *Nonlinear Oscillations, Dynamical Systems, and Bifurcations of Vector Fields.* New York: Springer.

Guégan, D., & Leroux, J. (2009). Forecasting chaotic systems: The role of local Lyapunov exponents. *Chaos, Solitons and Fractals*, (41): 2401-2404.

Guo, S., Liu, K., Tsai, J., & Shieh, L. (2008). An observer-based tracker for hybrid interval chaotic systems with saturating inputs: The chaos-evolutionary-programming approach. *Computers and Mathematics with Applications*, (55): 1225-1249.

Hadyn, N., Luevano, J., Mantica, G., & Vaienti, S. (2002). Multifractal properties of return time statistics. *Physical Review Letters*, (88)(22): 224502.

Hajiiloo, R., Salarieh, H., & Alasty, A. (2018). Chaos control in delayed phase space constructed by the Takens embedding theory. *Communications in Nonlinear Science and Numerical Simulation*, (54): 453-465.

Hajipour, M., Jajarmi, A., & Baleanu, D. (2018). An efficient nonstandard finite difference scheme for a class of fractional chaotic systems. *Journal of Computational Nonlinear Dynamics*, (13): 021013.

Hardstone, R., Poil, S.-S., Schiavone, G., Jansen, R., Nikulin, V., Mansvelder, H., & Linkenkaer-Hansen, K. (2012). Detrended fluctuation analysis: A scale-free view on neuronal oscillations. *Frontiers in Physiology*, (30).

Harikrishnan, K., Misra, R., & Ambika, G. (2017). Is a hyperchaotic attractor superposition of two multifractals? *Chaos, Solitons and Fractals*, (103): 450-459.

Harzing, A.-W. (2019, Juni 30). *https://harzing.com/*. Retrieved from https://harzing.com/resources/journal-quality-list

Hasselblatt, B., & Katok, A. (2003). *A First Course in Dynamics: With a Panorama of Recent Developments.* Cambridge: Cambridge University Press.

Hirata, M., Saussol, B., & Vaienti, S. (1999). Statistics of return times: a general framework and new applications. *Communications in Mathematical Physics*, (206)(1): 33-55.

Hirsch, M. (1997). *Differential Topology.* Berlin, New York: Springer.

Hobijn, B., & Frances, B. (1998). Increasing seasonal variation; unit roots versus shifts in mean and trend. *Applied Stochastic Models and Data Analysis*, (14)(3): 255-261.

Holyst, J., & Urbanowicz, K. (2000). Chaos control in economical model by time-delayed feedback method. *Physica A*, (287): 587-98.

Holyst, J., & Urbanowicz, K. (2001). Observations of deterministic chaos in financial time series by recurrence plots, can one control chaotic economy? *The European Physical Journal B*, (20): 531-535.

Hommes, C., & Manzan, S. (2005). Testing for nonlinear structure and chaos in economic time series: a comment. *Journal of Macroeconomics*, (62): 311-337.

Hsieh, D. (1991). Chaos and nonlinear dynamics: application to financial markets. *Journal of Finance*, (46)(5): 1839-1877.

Huang, S.-C., Chaung, P.-J., Wu, C.-F., & Lai, H.-J. (2010). Chaos-based support vector regressions for exchange rate forecasting. *Expert Systems with Applications*, (37): 8690-8598.

Huang, Y., & Kou, G. (2014). A kernel entropy manifold learning approach for financial data analysis. *Decision Support Systems*, (64): 31-42.

Huang, Y., & Kou, G. (2017). Nonlinear manifold learning for early warnings in financial markets. *European Journal of Operational Research*, (258)(2): 692-702.

Hurst, H. (1951). Long-term storage capacity of reservoirs. *Transactions of the American Society of Civil Engineers*, (116):770.

Iseri, M., Caglar, H., & Caglar, N. (2008). A model proposal for the chaotic structure of Istanbul stock exchange. *Chaos, Solitons and Fractals*, (36): 1392-1398.

Iwaszczuk, N., & Kavalets, I. (2013). Delayed feedback control method for generalized Cournot-Puu oligopoly model/in. *In: Iwaszczuk, N., editor. Selected Economic and Technological Aspects of Management ed. Krakow*, 108-23.

Jacob, R., Harikrishnan, K., Misra, R., & Ambika, G. (2016). Characterization of chaotic attractors under noise: A recurrence network perspective. *Communications in Nonlinear Science and Numerical Simulation*, (41): 32-47.

Jacob, R., Harikrishnan, K., Misra, R., & Ambrika, G. (2018). Recurrence network measures for hypothesis testing using surrogate data: Application to black hole light curves. *Communications in Nonlinear Science and Numerical Simulation*, (54): 84-99.

Jahanshahi, H. (2018). Smooth control of HIV/AIDS infection using a robust adaptive scheme with decoupled sliding mode supervision. *The European Physical Journal - Special Topics*, (227): 707-18.

Jahanshahi, H., Jafarzadeh, M., Sari, N., Pham, V.-T. H., & Nguyen, X. (2019). Robot Motion Planning in an Unknown Environment with Danger Space. *Electronics*, (8): 201.

Jahanshahi, H., Rajagopal, K., Akgul, A., Sari, N., Namazi, H., & Jafari, S. (2018a). Complete analysis and engineering applications of a megastable nonlinear oscillator. *International Journal of Non-Linear Mechanics*, (107): 126-36.

Jahanshahi, H., Shahriari-Kahkeshi, M., Alcaraz, R., Wang, X., Singh, V., & Pham, V.-T. (2019b). Entropy Analysis and Neural Network-based Adaptive Control of a Non-Equilibrium Four-Dimensional Chaotic System with Hidden Attractors. *Entropy*, (21): 156.

Jahanshahi, H., Yousefpour, A., Wei, Z., Alcaraz, R., & Bekiros, S. (2019a). A financial hyperchaotic system with coexisting attractors: Dynamic investigation, entropy analysis, control and synchronization. *Chaos, Solitons and Fractals*, (126): 66-77.

Jajarmi, A., Hajipour, M., & Baleanu, D. (2017). New aspects of the adaptive synchronization and hyperchaos suppression of a financial model. *Chaos, Solitons and Fractals*, (99): 285-96.

Jarzynski, C. (1994). Chaotic adiabatic energy diffusion and the Fermi mechanism. *Physica D*, (77): 276-288.

Judd, K., & Mees, A. (1995). On selecting models for nonlinear time series. *Physica D*, (82): 426-444.

Jung, R., & Maderitsch, R. (2014). Structural breaks in volatility spillovers between international financial markets: Contagion or mere interdependence? *Journal of Banking & Finance*, (47): 331-342.

Kaffashi, F., Foglyano, R., Wilson, C. G., & Loparo, K. A. (2008). The effect of time delay on Approximate & Sample Entropy calculations. *Physica D*, (237): 3069-3074.

Kantz, H., & Schreiber, T. (2003). *Nonlinear Time Series Analysis.* Cambridge: Cambridge University Press.

Kato, H. (1993). Continuum-wise expansive homeomorphisms. *Canadian Journal of Mathematics*, (45)(3): 576-598.

Katok, A., & Hasselblatt, B. (1995). *Introduction to the Modern Theory of Dynamical Systems.* Cambridge: Cambridge University Press.

Kennedy, J., & Eberhart, R. (1995). Particle Swarm Optimization. *Proceedings of ICNN'95 - International Conference on Neural Networks, Perth, WA, Australia*, (4): 1942-1948.

Kennel, M., Brown, R., & Abarbanel, H. (1992). Determining minimum embedding dimension using a geometrical construction. *Physical Review A*, (45): 3403-3411.

Khan, A., & Bhat, M. (2017). Hyper-chaotic analysis and adaptive multi-switching synchronization of a novel asymmetric non-linear dynamical system. *International Journal of Dynamics and Control*, (5): 1211-21.

Kim, H., Eykholt, R., & Salas, J. (1999). Nonlinear dynamics, delay times, and embedding windows. *Physica D: Nonlinear Phenomena*, (127)(1-2): 48-60.

Kleinberg, J. M. (1999). Authoritative sources in a hyperlinked environment. *Journal of the ACM*, 604–632.

Koebbe, M., & Mayer-Kress, G. (1992). Use of recurrence plots in the analysis of time-series data . *in: M. Casdagli, S. Eubank (Eds.), Proceedings of SFI Studies in the Science of Complexity, vol. XXI, Redwood City, 1992, Addison-Wesley, Reading, MA*, 361-378.

Kolm, P. N., Tütüncü, R., & Fabozzi, F. J. (2014). 60 years of portfolio optimization: Practical challenges and current trends. *European Journal of Operational Research*, (234)(2): 356-371.

Kostelich, E. J. (1997). The analysis of chaotic time-series data. *Systems & Control Letters*, (31): 313-319.

Kozłowska, M., Denys, M., Wiliński, M., Link, G., Gubiec, T., Werner, T., & Kutner, R. (2016). Dynamic bifurcations on financial markets. *Chaos, Solitons and Fractals*, (0):1-14.

Kwiatkowski, D., Phillips, P., Schmidt, P., & Shin, Y. (1992). Testing the null hypothesis of stationary against the alternative of a unit root. *Journal of Econometrics*, (54): 159-178.

Kyrtsou, C., & Terraza, M. (2002). Stochastic chaos or ARCH effects in stock series? A comparative study. *International Review of Financial Analysis*, (11)(4): 407-431.

Kyrtsou, C., Labys, W. C., & Terraza, M. (2004). Noisy chaotic dynamics in commodity markets. *Empirical Economics*, (29): 489-502.

Lahmiri, S., & Bekiros, S. (2019). Cryptocurrency forecasting with deep learning chaotic neural networks. *Chaos, Solitons and Fractals*, (118): 35-40.

Lee, J. M. (2009). Manifolds and Differentia Geometry. *Graduate Studies in Mathematics: Providence: American Mathematical Society*, (107).

Lee, K., & Seo, B. K. (2017). Marked Hawkes process modeling of price dynamics and volatility estimation. *Journal of Empirical Finance*, 174–200.

Lewandowski, M., Makris, D., Velastin, S., & Nebel, J.-C. (2014). Structural Laplacian Eigenmaps for modeling sets of multivariate sequences. *IEEE Transactions on Cybernetics*, (44)(6): 936-949.

Li, G., Yue, Y. X., & Grebogi, C. (2019). Strange nonchaotic attractors in a nonsmooth dynamical system. *Communications in Nonlinear Science and Numerical Simulation*, (78): 104858.

Lorenz, E. (1963). Deterministic nonperiodic flow. *Journal of the Atmospheric Sciences*, (20): 130-141.

Lux, T. (1995). Herd behaviour, bubbles and crashes. *Economic Journal*, (105): 881-896.

Lux, T. (1998). The socio-economic dynamics of speculative markets: interacting agents, chaos, and the fat tails of returns distribution. *Journal of Economic Behavior and Organization*, (33): 143-165.

Ma, C., & Wang, X. (2012). Hopf bifurcation and topological horseshoe of a novel finance chaotic system. *Communications in Nonlinear Science and Numerical Simulation*, (17): 721-30.

Ma, F., Wahab, M., Huang, H. D., & Xu, W. (2017). Forecasting the realized volatility of the oil futures market: A regime switching approach. *Energy Economics*, (67): 136-145.

MacKinnon, J. (1994). Approximate asymptotic distribution functions for unit-root and cointegration tests. *Journal of Business and Economic Statistics*, (12): 167-76.

Mahmoodabadi, M., & Jahanshahi, H. (2016). Multi-objective optimized fuzzy-PID controllers for fourth order nonlinear systems. *Engineering Science and Technology*, (19): 1084-98.

Malliaris, A., & Stein, J. (1999). Methodological issues in asset pricing: random walk or chaotic dynamics. *Journal of Banking and Finance*, (23): 1605-1635.

Mandelbrot, B. (2004). *Fractals and Chaos.* New York: Springer.

Marwan, N., & Kurths, J. (2005). Line structures in recurrence plots. *Physical Letters A*, (336)(4-5): 349-357.

Marwan, N., Romano, M. C., Thiel, M., & Kurths, J. (2007). Recurrence plots for the analysis of complex systems. *Physics Reports*, (438): 237-329.

Marwan, N., Wessel, N., Meyerfeldt, A., Schirdewan, A., & Kurths, J. (2002). Recurrence plot based measures of complexity and its application to heart rate variability data. *Physical Reviews E*, (66)(2): 026702.

Massey Jr., F. J. (2012). The Kolmogorov-Smirnov Test for Goodness of Fit. *Journal of the American Statistical Association*, (46)(253): 68-78.

Matia, K., & Yamasaki, K. (2005). Statistical properties of demand fluctuation in the financial market. *Quantitative Finance*, (5)(6): 513-17.

Matilla-García, M., & Marín, M. R. (2010). A new test for chaos and determinism based on symbolic dynamics. *Journal of Economic Behavior & Organization*, (76): 600-614.

Matilla-García, M., Queralt, R., Sanz, P., & Vázquez, F. (2004). A generalized BDS statistic. *Computational Economics*, (24): 277-300.

Maus, A., & Sprott, J. (2011). Neural network method for determining embedding dimension of a time series. *Communications in Nonlinear Science and Numerical Simulation*, (16): 3294-3302.

May, R. (1976). Simple mathematical models with very complicated dynamics. *Nature*, (261): 459-467.

Mazzola, C., & Giunti, M. (2012). Reversible dynamics and the directionality of time. *Mintai G., Abram M., Pessa E. (eds), Methods, models, simulations and approaches towards a general theory of change, Singapore: World Scientific*, 161-171.

McKenzie, M. (2001). Chaotic behaviour in national stock market indices: new evidence from the close return test. *Global Finance Journal*, (12)(1): 35-53.

Milnor, J. (1985). On the concept of attractor. *Communications in Mathematical Physics*, (99)(2): 177-195.

Mindlin, G., & Gilmore, R. (1992). Topological analysis and synthesis of chaotic time series. *Physica D*, (58)(1-4): 229-242.

Mischaikow, K., Mrozek, M., Reiss, J., & Szymczak, A. (1999). Construction of symbolic dynamics from experimental time series. *Physical Review Letters*, (82): 1144-1147.

Mishra, R., Sehgal, S., & Bhanumurthy, N. (2011). A search for long-range dependence and chaotic structure in Indian stock market. *Review of Financial Economics*, (20)(2): 96-104.

Mitra, S. (2006). A wavelet filtering based analysis of macroeconomic indicators: the Indian evidence. *Applied Mathematics and Computation*, (175): 1055-1079.

Moshiri, S., & Foroutan, F. (2006). Forecasting nonlinear crude oil futures prices. *The Energy Journal*, (27): 81-96.

Nawrocki, D., & Vaga, T. (2014). A bifurcation model of market returns. *Quantitative Finance*, (14)(3): 509-28.

Newman, M. (2010). Networks. An Introduction. *Oxford University Press, Oxford*.

Nychka, D., Ellner, S., & Bailey, B. (1997). Chaos with confidence: asymptotics and application of local Lyapunov exponents. *American Mathematical Society*, 115-33.

Oksendal, B. (2013). *Stochastic Differential Equations - An Introduction with Applications.* Springer.

Opong, K., Mulholland, G., Fox, A., & Farahmand, K. (1999). The behaviour of some UK equity indices: an application of Hurst and BDS tests. *Journal of Empirical Finance*, (6)(3): 267-282.

Oseledets, V. (1968). A multiplicative ergodic theorem. Lyapunov characteristic numbers for dynamical systems. *Transactions of the Moscow Mathematical Society*, (19): 197-221.

Ott, E. (2002). *Chaos in Dynamical Systems.* Cambridge: Cambridge University Press.

Ott, E., Grebogi, C., & Yorke, J. (1990). Controlling chaos. *Physical Review Letters*, (64): 1196-1199.

Packard, N., Crutchfield, J., Farmer, J., & Shaw, R. (1980). Geometry from a time series. *Physical Review Letters*, (45)(9): 712-716.

Pagan, A. (1996). The econometrics of financial markets. *Journal of Empirical Finance*, (3): 15-102.

Paladin, G., & Vulpiani, A. (1987). Anomalous scaling laws in multifractal objects. *Physics reports*, (156): 147-225.

Panas, E., & Ninni, V. (2000). Are oil markets chaotic? A nonlinear dynamic analysis. *Energy Economics*, (22): 549-568.

Park, J. Y., & Whang, Y.-J. (2012). Random walk or chaos: A formal test on the Lyapunov exponent. *Journal of Econometrics*, (169): 61-74.

Pecora, L., & Carroll, T. (1990). Synchronization in chaotic systems. *Physical Review Letters*, (64): 821.

Peng, C.-K., Buldyrev, S., Havlin, S., Simons, M., Stanley, H., & Goldberger, L. (1994). Mosaic organization of DNA nucleotides. *Physical Review E*, (49)(2).

Penné, V., Saussol, B., & Vaienti, S. (1999). Dimensions for recurrence times: topological and dynamical properties. *Discrete and Continuous Dynamical Systems A*, (4)(4): 783-798.

Peters, E. E. (1994). *Fractal market analysis: applying chaos theory to investment and economics.* New York: Wiley & Sons, Inc.

Poincaré, H. (1890). Sur la probleme des trois corps et les équations de la dynamique. *Acta Mathematica*, (13): 1-271.

Poon, S.-H., & Granger, C. W. (2003). Forecasting Volatility in Financial Markets: A Review. *Journal of Economic Literature*, 478-539.

Provenzale, A., Smith, L., Vio, R., & Murante, G. (1992). Distinguishing between low-dimensional dynamics and randomness in measured time series. *Physica D*, (58): 31-49.

Pyragas, K. (1992). Continuous control to chaos by self-controlling feedback. *Physics Letters A*, (170): 421-428.

Qian, B., & Rasheed, K. (2004). Hurst exponent and financial market predictability. *IASTED conference on Financial Engineering and Applications (FEA)*, 203-209.

Ramiah, V., Xu, X., & Moosa, I. A. (2015). Neoclassical finance, behavioural finance and noise traders: A review and assessment of the literature. *International Review of Financial Analysis*, (41): 89-100.

Ramsey, J., Sayers, C., & Rothman, P. (1990). The statistical properties of dimension calculations using small data sets: Some economic applications. *International Economic Review*, (4): 991-1020.

Richman, J., & Moorman, J. (2000). Physiological time-series analysis using approximate entropy and sample entropy. *American Journal of Physiology - Heart and Circulatory Physiology*, (278)(6): H2039-H2049.

Robins, V. (2002). Computational topology for point data: Betti numbers of α-shapes. *in K. Mecke. D. Stoyan (Eds.). Morphology of Condensed Matter, in: Lect. Notes in Physics vol. 600, Springer, Berlin, Heidelberg*, 261-274.

Robinson, C. (1995). *Dynamical Systems.* New York: CRC Press.

Rohde, G. K., Nichols, J. M., Dissinger, B. M., & Bucholtz, F. (2008). Stochastic analysis of recurrence plots with applications to the detection of deterministic signals. *Physica D*, (237): 619-629.

Rosenstein, M., Collins, J., & De Luca, C. (1993). A practical method for calculating largest Lyapunov exponents from small data sets. *Physica D*, (65): 117-134.

Rössler, O. (1979). An equation for hyperchaos. *Physics Letters A*, (71): 155-7.

Rötzel, P. G. (2019). Information Overload in the Information Age: A Review of the Literature from Business Administration, Business Psychology, and Related Disciplines With Bibliometric Approach and Framework Development. *Business Research*.

Rüdisüli, M., Schildhauer, T., Biollaz, S., & Van Ommen, J. (2013). Measurement, monitoring and control of fluidized bed combustion and gasification. In F. Scala, *Fluidized Bed Technologies for Near-Zero Emission Combustion and Gasification* (pp. 813-864). Woodhead Publishing.

Sandubete, J. E., & Escot, L. (2020). Chaotic signals inside some tick-by-tick financial time series. *Chaos, Solitons and Fractals*, (137): 109852.

Sano, M., & Sawada, Y. (1985). Measurement of the Lyapunov spectrum from a chaotic time series. *Physical Review Letters*, (55): 1082.

Sauer, T., Yorke, J., & Casdagli, M. (1991). Embedology. *Journal of Statistical Physics*, (65): 95-116.

Saussol, B., & Wu, J. (2003). Recurrence spectrum in smooth dynamical systems. *Nonlinearity*, (16)(6): 1991-2001.

Savit, R., & Green, M. (1991). Time series dependent variables. *Physica D*, (50): 95-116.

Scarlat, E., Stan, C., & Cristescu, C. (2007). Chaotic features in Romanian transition economy as reflected onto currency exchange rate. *Chaos, Solitons and Fractals*, (33)(2): 396-404.

Scheinkman, J., & LeBaron, B. (1989). Nonlinear Dynamics and Stock Returns. *The Journal of Business*, (62)(3): 311-37.

Schreiber, T., & Kantz, H. (1995). Noise in chaotic data: diagnostics and treatment. *Chaos*, (5): 133-142.

Schuster, H. (1989). Deterministic Chaos: An Introduction. *VCH-Verlag: Weinheim*, 2nd ed.

Schwert, G. (1989). Tests for unit roots: A Monte Carlo investigation. *Journal of Business & Economic Statistics*, (7): 147-159.

Scimago Lab. (2021, 01 04). *SJR* . Retrieved from Scimago Journal & Country Rank: https://www.scimagojr.com/journalrank.php

Serletis, A., & Shahmoradi, A. (2004). Absence of chaos and 1/f spectra, but evidence for TAR nonlinearities, in the Canadian exchange rate. *Macroeconomic Dynamics*, (8): 543-551.

Serletis, A., Shahmoradi, A., & Serletis, D. (2007). Effect of noise on estimation of Lyapunov exponents from a time series. *Chaos, Solitons and Fractals*, (32): 883-887.

Sharkovskii, A. (1964). Co-existence of cycles of a continuous mapping of the line into itself. *Ukrainian Mathematical Journal*, (16): 61-71.

Shevchenko, I. I. (2018). Lyapunov and diffusion timescales in the solar neighborhood. *Working Paper with arXiv-ID: 1012.3606v2*, 1-22.

Shintani, M., & Linton, O. (2004). Nonparametric neural network estimation of Lyapunov exponents and a direct test for chaos. *Journal of Econometrics*, (120): 1-33.

Shukla, M., & Sharma, B. (2017). Stabilization of a class of fractional order chaotic systems via backstepping approach. *Chaos, Solitons and Fractals*, (98): 56-62.

Shwartz, B., & Yousefi, S. (2003). On complex behaviour and exchange rate dynamics. *Chaos, Solitons and Fractals*, (18)(3): 503-523.

Small, H. (1978). Co-citation context analysis and the structure of paradigms. *J Doc*, 36(3): 183-196.

Smith, L. (1992). Identification and prediction of low dimensional dynamics. *Physica D*, (58)(1-4): 50-76.

Sobol′, I. (1995). Sensitivity estimates for nonlinear mathematical model. *Mathematical models and computer experiments*, (7): 16-28.

Song, X., Niu, D., & Zhang, Y. (2016). The Chaotic Attractor Analysis of DJIA Based on Manifold Embedding and Laplacian Eigenmaps. *Mathematical Problems in Engineering*, (4): 1-10.

Sornette, D. (2004). *Critical Phenomena in Natural Sciences: Chaos, Fractals, Selforganization and Disorder: Concepts and Tools.* Heidelberg: Springer Verlag.

Stark, H.-G. (2005). *Wavelets and Signal Processing. An Application-Based Introduction.* Berlin, Heidelberg: Springer.

Strogatz, S. (2014). *Nonlinear Dynamics and Chaos.* Colorado: Westview Press.

Suzuki, T., Ikeguchi, T., & Suzuki, M. (2007). Algorithms for generating surrogate data for sparsely quantized time series. *Physica D*, (231): 108-115.

Takala, K., & Virén, M. (1996). Chaos and nonlinear dynamics in financial and nonfinancial time series: evidence from Finland. *European Journal of Operational Research*, (93)(1): 155-172.

Takens, F. (1981). Detecting strange attractors in fluid turbulence. *in: D. Rand. L.-S. Young (Eds.). Dynamical Systems and Turbulence. Springer Berlin*, 366-381.

Taylor, M., & Allen, H. (1992). the use of technical analysis in the foreign exchange market. *Journal of International Money and Finance*, (11): 304-314.

Taylor, M., & Lehmann, B. (1992). Deviations from purchasing power parity in the long run. *Journal of International Money and Finance*, (11): 304-314.

Theiler, J. (1986). Spurious dimension from correlation algorithms applied to limited time-series data. *Physical Reviews A*, (34)(3): 2427-2432.

Theiler, J., Eubank, S., Longtin, A., Galdrikian, B., & Farmer, J. (1992). Testing for nonlinearity in time series: the method of surrogate data. *Physica D*, (58): 77-94.

Tirandaz, H., Aminabadi, S., & Tavakoli, H. (2018). Chaos synchronization and parameter identification of a finance chaotic system with unknown parameters, a linear feedback controller. *Alexandria Engineering Journal*, (57): 1519-24.

Tkac, M., & Verner, R. (2016). Artificial neural networks in business: Two decades of research. *Applied Soft Computing*, (38): 788-804.

Tong, H. (1990). Non-linear Time Series, a Dynamical System Approach. *Oxford University Press: New York*.

Trulla, L., Giuliani, A., Zbilut, J., & Webber Jr., C. (1996). Recurrence quantification analysis of the logistic equation with transients. *Physical Letters A*, (223)(4): 255-260.

Tsai, J.-H., Fang, J.-S., Yan, J.-J., Dai, M.-C., Guo, S.-M., & Shieh, L.-S. (2018). Hybrid robust discrete sliding mode control for generalized continuous chaotic systems subject to external disturbances. *Nonlinear Analysis*, (29): 74-84.

Vargas, J., Grzeidak, E., & Hemerly, E. (2015). Robust adaptive synchronization of hyperchaotic finance system. *Nonlinear Dynamics*, (80): 239-48.

Vogl, M., & Rötzel, P. G. (2021). Insights, Trends and Frontiers - A Literature Review on Financial and Risk Modelling in the Information Age (2008-2019). *Working paper under review*, https://papers.ssrn.com/sol3/papers.cfm?abstract_id=3764570.

Wang, Z., Huang, X., & Shen, H. (2012). Control of an uncertain fractional order economic system via adaptive sliding mode. *Neurocomputing*, (83): 83-8.

Webber Jr., C., & Zbilut, J. (1994). Dynamical assessment of physiological systems and states using recurrence plot strategies. *Journal of Applied Physiology*, (76)(2): 965-973.

Weron, R. (2002). Estimating long-range dependence: finite sample properties and confidence intervals. *Physica A: Statistical Mechanics and its Applications*, (312)(1): 285-299.

Whang, Y., & Linton, O. (1999). The asymptotic distribution of nonparametric estimates of the Lyapunov exponent for stochastic time series. *Journal of Econometrics*, (91): 1-42.

Wolf, A., Swift, J., Swinney, H., & Vastano, J. (1985). Determining Lyapunov exponents from a time series. *Physica D*, (16)(3): 285-317.

Wolff, R., Yao, Q., & Tong, H. (2004). Statistical tests for Lyapunov exponents of deterministic systems. *Studies Nonlinear Dynamics & Econometrics*, (8)(2).

Yang, P., & Shang, P. (2018). Recurrence quantity analysis based on matrix eigenvalues. *Communications in Nonlinear Science and Numerical Simulation*, (59): 15-29.

Yang, Y., & Wang, J. (2021). Forecasting wavelet neural hybrid network with financial ensemble empirical mode decomposition and MCID evaluation. *Expert Systems with Applications*, (166): 114097.

Yousefpoor, P., Esfahani, M., & Nojumi, H. (2008). Looking for systematic approach to select chaos tests. *Applied Mathematics and Computation*, (198)(1): 73-91.

Yu, H., Cai, G., & Li, Y. (2012). Dynamic analysis and control of a new hyperchaotic finance system. *Nonlinear Dynamics*, (67): 2171-82.

Yu, J., Lei, J., & Wang, L. (2017). Backstepping synchronization of chaos system based on equivalent transfer function method. *Optik*, (130): 900-13.

Zbilut, J., & Webber Jr., C. (1992). Embeddings and delays as derived from quantification of recurrence plots. *Physics Letters A*, (171)(3-4): 199-203.

Zbilut, J., Zaldívar-Comenges, J.-M., & Strozzi, F. (2002). Recurrence quantification based Liapunov exponents for monitoring divergence in experimental data. *Physical Letters A*, (297)(3-4): 173-181.

Zeng, X., Eykholt, R., & Pielke, R. (1991). Estimating the Lyapunov exponent spectrum from short time series of low precision. *Physical Review Letters*, (66): 3229-3232.

Zhang, L., Liao, X., & Wang, X. (2005). An image encryption approach based on chaotic maps. *Chaos, Solitons and Fractals*, (243): 759-765.

Zhao, X., Li, Z., & Li, S. (2011). Synchronization of a chaotic finance system. *Applied Mathematics and Computation*, (217): 6031-6039.

Ziehmann, C., Smith, L. A., & Kurths, J. (1999). The bootstrap and Lyapunov exponents in deterministic chaos. *Physica D*, (126): 49-59.

Appendix

A1. Interpretation of RP structures

Table 18: Typical patterns in RPs and their meanings. Taken from Marwan et al., (2007, p.251).

Pattern	Meaning
Homogeneity	The process is stationary
Fading to the upper left and lower right corners	Non-stationary data; the process contains a trend or a drift
Disruptions (white bands)	Non-stationary data; some states are rare or far from the normal; transitions may have occurred
Periodic/quasi-periodic patterns	Cyclicities in the process; the distance between periodic patterns (e.g. lines) corresponds to the period; different distances between long diagonal lines reveal quasi-periodic processes
Single isolated points	Strong fluctuation in the process; if only single isolated points occur, the process may be an uncorrelated random or even anti-correlated process
Diagonal lines (parallel to the LOI)	The evolution of states is similar at different epochs; the process could be deterministic; if these diagonal lines occur beside single isolated points, the process could be chaotic (if these diagonal lines are periodic, unstable periodic orbits can be observed)
Diagonal lines (orthogonal to the LOI)	The evolution of states is similar at different times but with reverse time; sometimes this is an indication for an insufficient embedding
Vertical and horizontal lines/clusters	Some states do not change or change slowly for some time; indication for laminar states
Long bowed line structures	The evolution of states is similar at different epochs but with different velocity; the dynamics of the system could be changing

A2. Graphical results for different RQA measures depending on minimal length selections

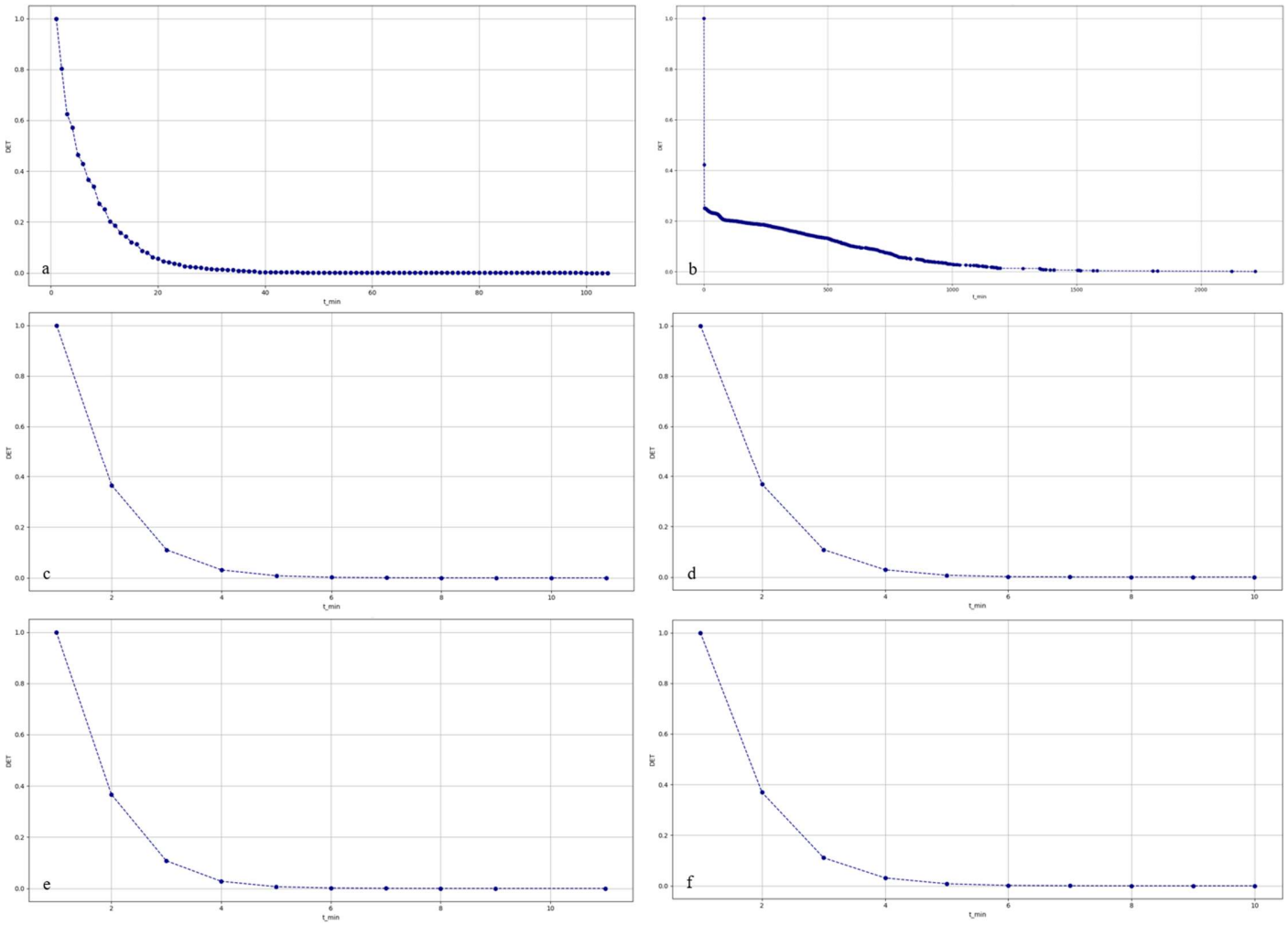

Figure 19: Determinism for different minimum lengths with (a) S&P 500 returns, (b) Lorenz system, (c) Brownian motion returns and (d)–(f) surrogate data sets: (d) ft, (e) aaft and (f) iaaft.

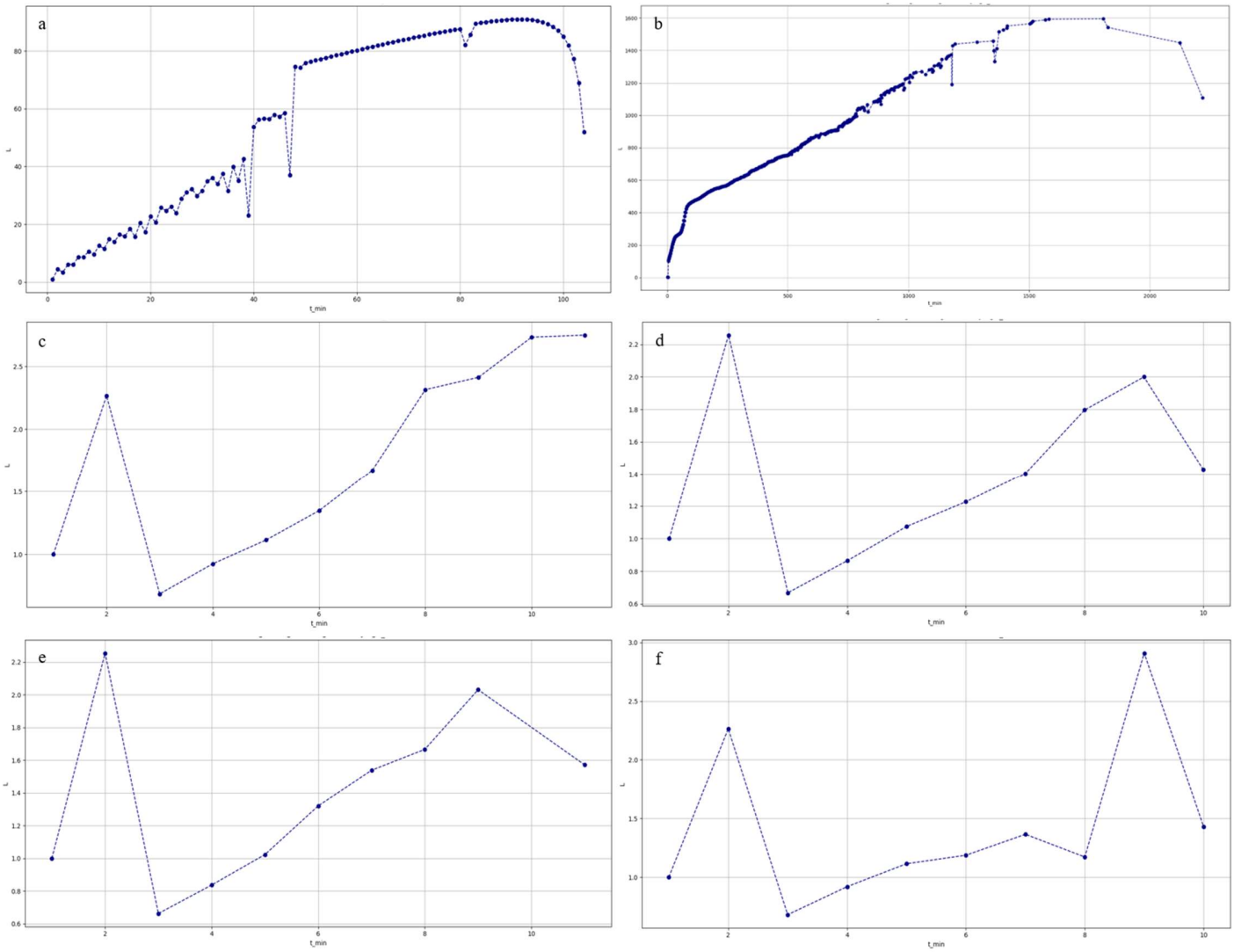

Figure 20: Averaged Diagonal Length for different minimum lengths with (a) S&P 500 returns, (b) Lorenz system, (c) Brownian motion returns and (d)–(f) surrogate data sets: (d) ft, (e) aaft and (f) iaaft.

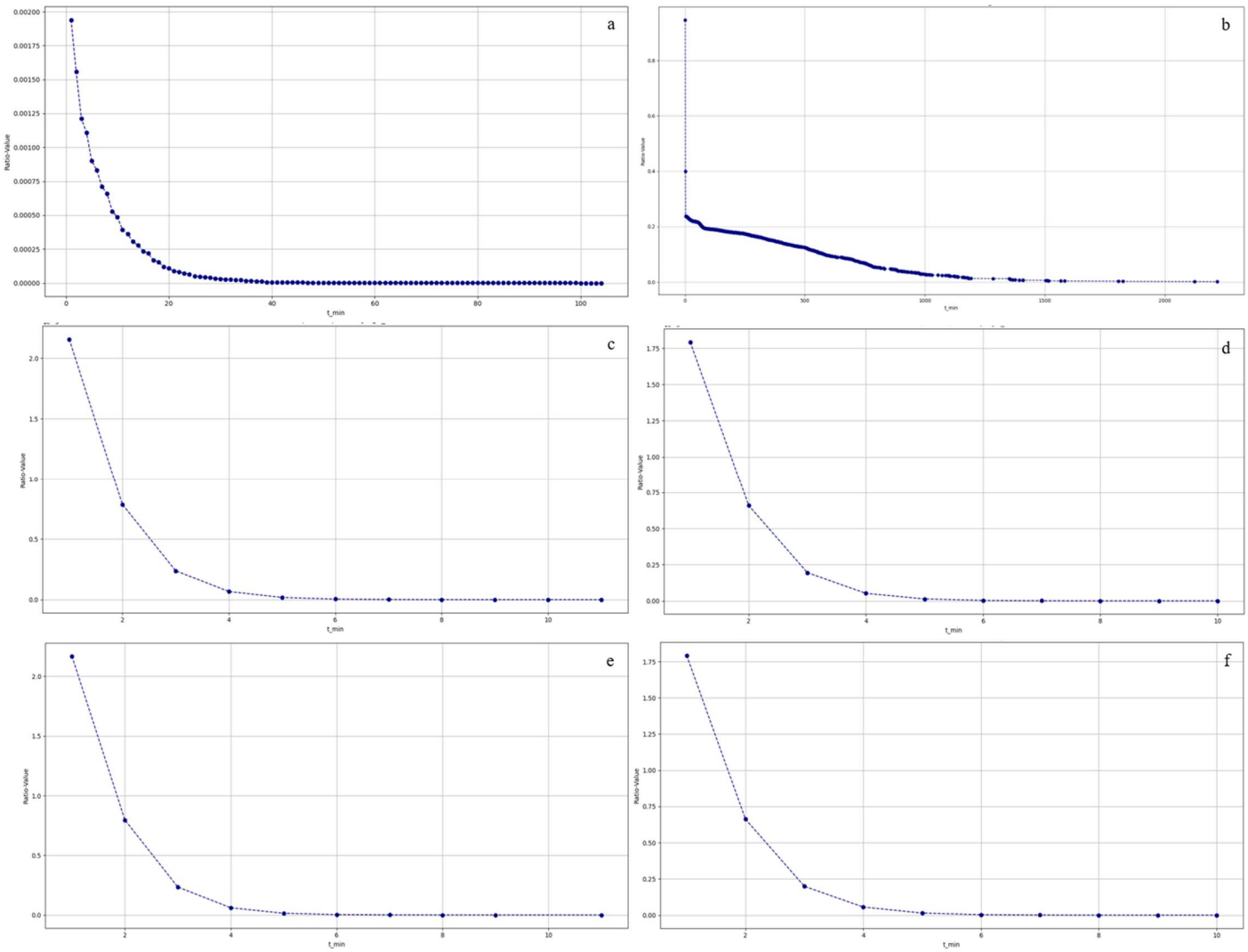

Figure 21: Ratio for different minimum lengths with (a) S&P 500 returns, (b) Lorenz system, (c) Brownian motion returns and (d)–(f) surrogate data sets: (d) ft, (e) aaft and (f) iaaft.

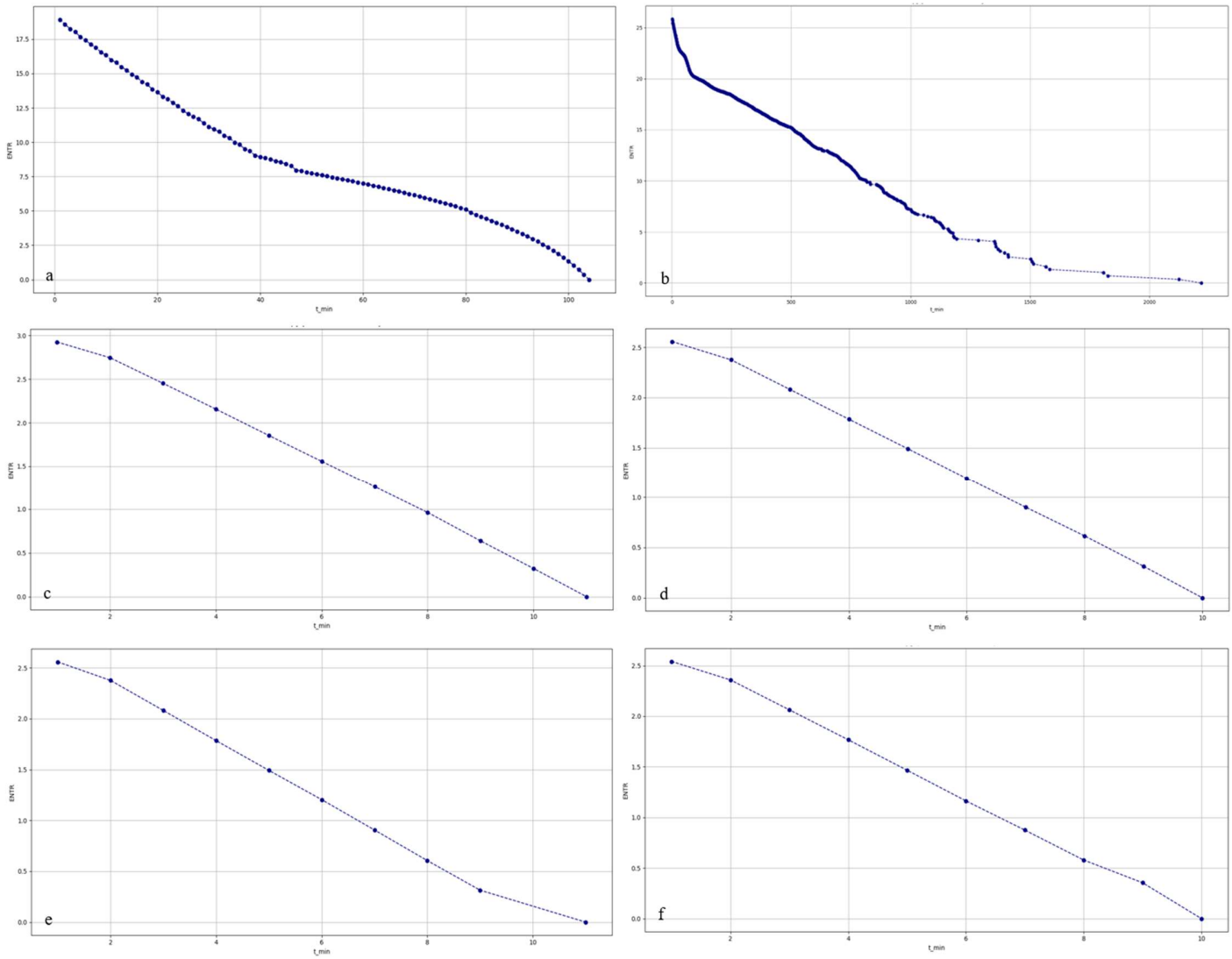

Figure 22: Shannon entropy for different minimum lengths with (a) S&P 500 returns, (b) Lorenz system, (c) Brownian motion returns and (d)–(f) surrogate data sets: (d) ft, (e) aaft and (f) iaaft.

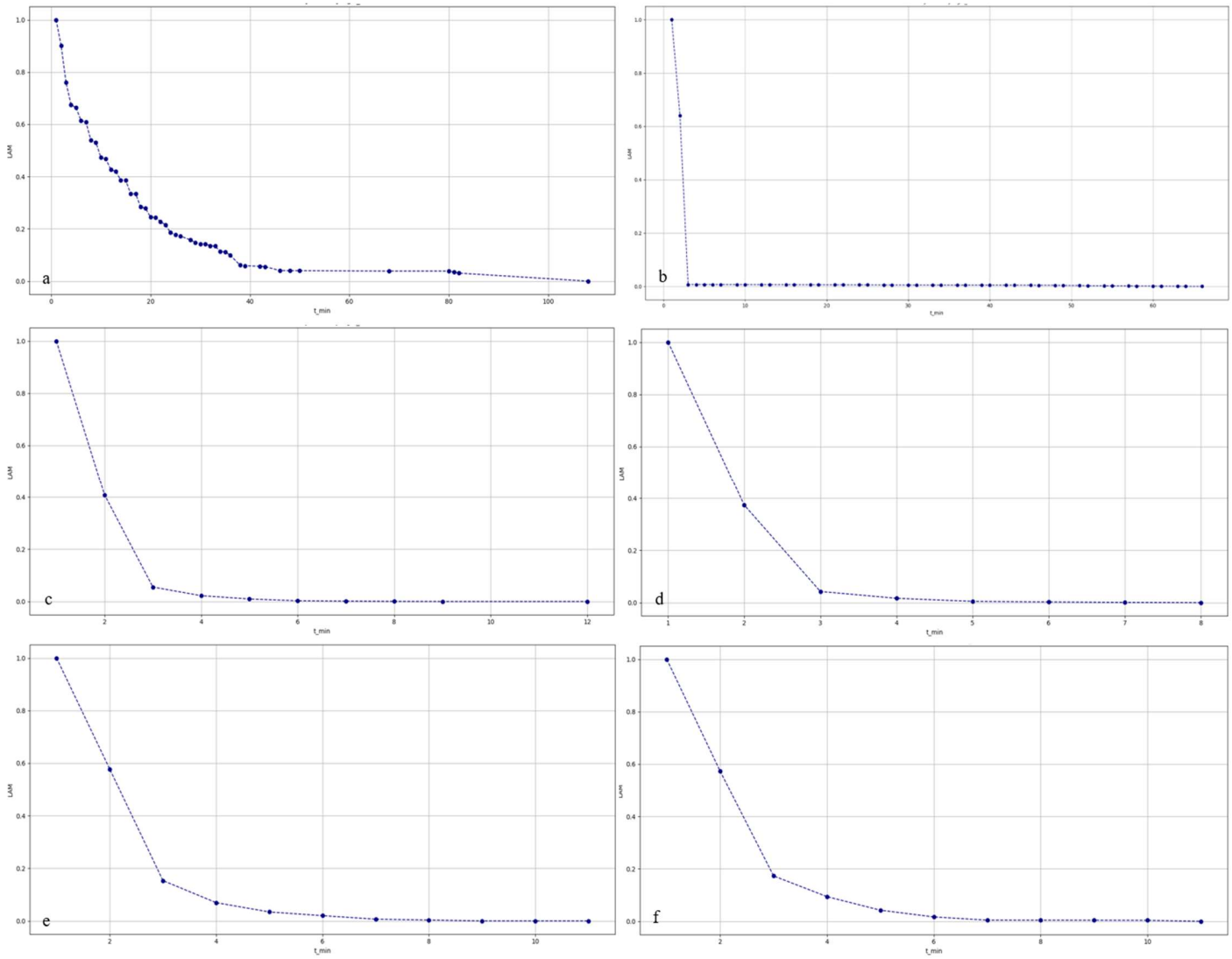

Figure 23: Laminarity for different minimum lengths with (a) S&P 500 returns, (b) Lorenz system, (c) Brownian motion returns and (d)-(f) surrogate data sets: (d) ft, (e) aaft and (f) iaaft.

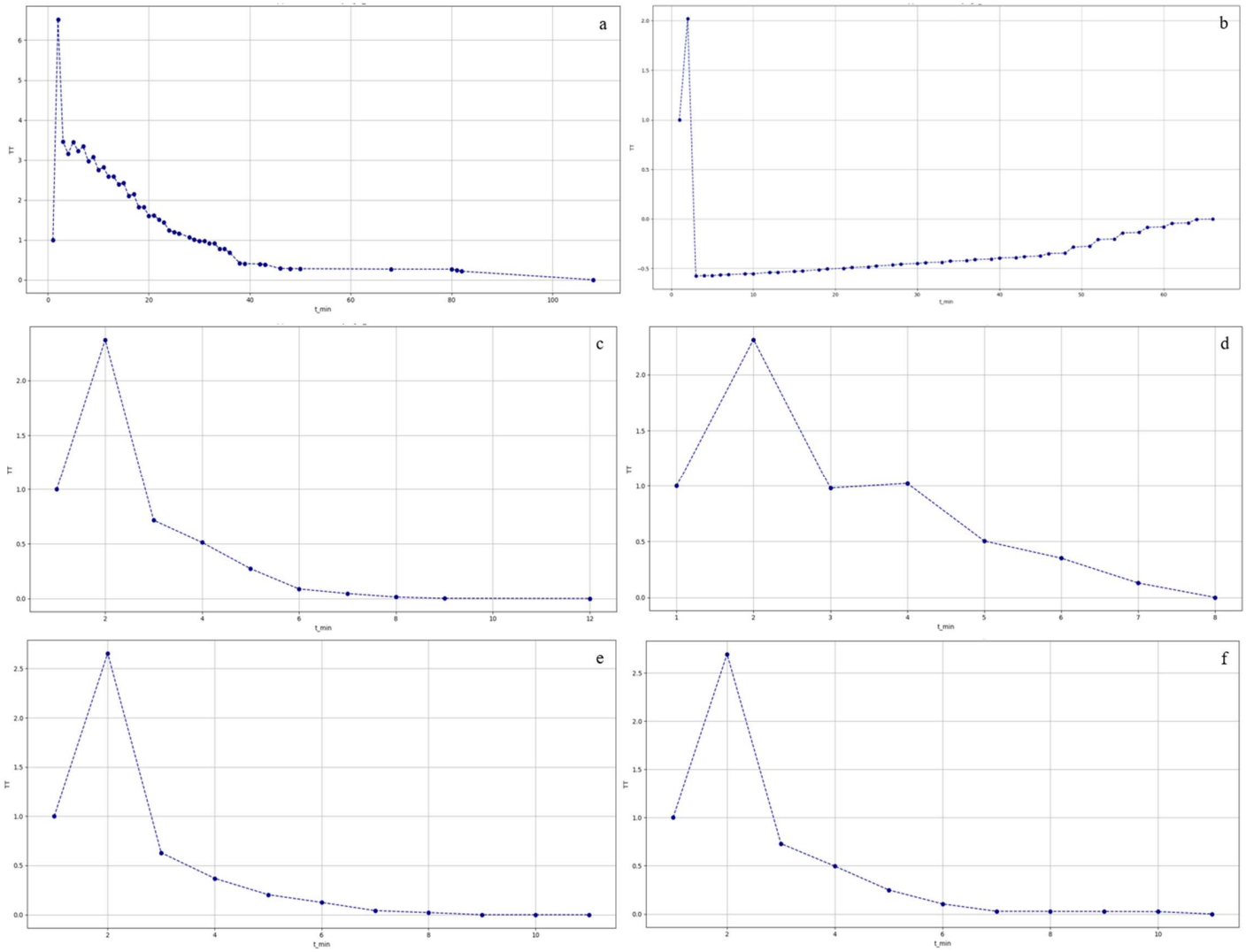

Figure 24: Trapped Time for different minimum lengths with (a) S&P 500 returns, (b) Lorenz system, (c) Brownian motion returns and (d)-(f) surrogate data sets: (d) ft, (e) aaft and (f) iaaft.